

**VOLUME I
PERFORMANCE FLIGHT TESTING**

**CHAPTER 6
SUPERSONIC AERODYNAMICS**

DTIC QUALITY INSPECTED 2

19970116 085

JANUARY 1991

**USAF TEST PILOT SCHOOL
EDWARDS AIR FORCE BASE, CALIFORNIA
AIR FORCE MATERIAL COMMAND**

DISTRIBUTION STATEMENT A
Approved for public release;
Distribution Unlimited

TABLE OF CONTENTS

6.1	INTRODUCTION	6.1
6.2	TYPES OF GASES	6.1
6.3	COMPRESSIBLE, ELASTIC, NON-VISCOUS FLOW	6.2
	6.3.1 ONE-DIMENSIONAL FLOW	
	APPROXIMATION	6.3
6.4	COMPRESSIBLE FLOW EQUATIONS	6.4
6.5	TOTAL (STAGNATION) PROPERTIES	6.5
	6.5.1 TOTAL TEMPERATURE	6.5
	6.5.2 TOTAL PRESSURE	6.7
	6.5.3 TOTAL DENSITY	6.7
	6.5.4 MATHEMATICAL	
	RELATIONSHIPS FOR TOTAL	
	PROPERTIES	6.8
6.6	SPEED OF SOUND	6.8
6.7	MACH	6.12
6.8	CLASSIFICATION OF SPEED RANGES	6.13
6.9	TWO-DIMENSIONAL PROPAGATION OF SOUND WAVES	6.13
	6.9.1 MACH ANGLES	6.15
	6.9.2 ACTIVITY ENVELOPE	6.16
6.10	ISENTROPIC FLOW	6.16
6.11	FLOW IN CONVERGENT-DIVERGENT STREAMTUBES	6.21
	6.11.1 COMPRESSIBLE	
	STREAMTUBE FLOW	6.23
	6.11.2 AREA CHANGES	6.24
	6.11.3 FLOW AT THE THROAT	6.26
	6.11.4 MASS FLOW IN A CHOKED	
	STREAMTUBE	6.29
	6.11.5 LOCAL SONIC CONDITIONS	6.30
	6.11.6 M^*	6.32
	6.11.7 AREA RATIO	6.33
6.12	NORMAL SHOCK WAVES	6.34
	6.12.1 NORMAL SHOCK	
	EQUATIONS	6.35
	6.12.2 NORMAL SHOCK SUMMARY	6.36
6.13	SUPERSONIC PITOT TUBE	6.37

6.14	OBLIQUE SHOCK WAVES	6.39
	6.14.1 OBLIQUE SHOCK RELATIONS	6.43
	6.14.2 MINIMUM AND MAXIMUM WAVE ANGLES	6.45
	6.14.3 RELATION BETWEEN θ AND δ	6.46
	6.14.4 MACH LINES	6.49
6.15	ISENTROPIC COMPRESSION	6.50
6.16	ISENTROPIC COMPRESSION	6.52
	6.16.1 SUPERSONIC INITIAL CONDITIONS	6.57
	6.16.2 MAXIMUM TURNING ANGLE	6.57
6.17	INTERACTION OF WAVE FORMS	6.59
6.18	TWO-DIMENSIONAL SUPERSONIC AIRFOILS	6.63
6.19	PRESSURE COEFFICIENT FOR TWO-DIMENSIONAL SUPERSONIC AIRFOILS AND INFINITE WINGS	6.65
6.20	THIN WING THEORY	6.67
6.21	SUPERSONIC FLOW IN THREE DIMENSIONS	6.70
6.22	THREE-DIMENSIONAL SUPERSONIC WINGS	6.73
6.23	TRANSONIC FLOW REGIME	6.75
	6.23.1 THICKNESS	6.77
	6.23.2 SUPERCRITICAL AIRFOILS	6.80
	6.23.3 WING SWEEP	6.81
	6.23.4 FUSELAGE SHAPE AND AREA RULE	6.84
	6.23.5 TRANSONIC AND SUPERSONIC CONTROL SURFACES	6.88
6.24	SUMMARY	6.90

6.1 INTRODUCTION

Some basic concepts of Aerodynamics and Thermodynamics have previously been covered. These related to determination of fluid flow around various shapes and the resultant forces acting upon these shapes. Fluids previously studied were assumed to be incompressible. This assumption, among others, reduced the number of variables involved and allowed relatively simple solutions to previously complex sets of equations. Making assumptions to eliminate some variables is an everyday activity of the engineer, but care needs to be taken to ensure assumptions made to provide an idealized solution to a given physical system are still valid if the idealized solution is applied to a related, but different, physical system.

Historically, for an aircraft system performing in low speed air the idealized incompressible flow solution was good enough to achieve accurate design results. This was the case for all aerodynamics consideration up to the late 1930s. Although as aircraft speeds increased toward the speed of sound, so did requirements for new idealized solutions to physical systems using different and better assumptions. In this chapter, the assumption of incompressible flow for aerodynamic analysis will be dropped, and flow fields will be considered compressible. Results obtained from the study of compressible fluids will then be applied to high speed flow situations.

6.2 TYPES OF GASES

A real gas, such as air, is a compressible, viscous, elastic, nonhomogeneous, and chemically active fluid (any gas is also a fluid). The physical principles governing its behavior are not understood completely enough to permit the exact mathematical formulation of a general flow problem. Even if it were possible, the resulting equations would defy simple solution. Using reasonable assumptions which can be verified by experiment, specific physical systems can be described by simpler equations, and the necessary properties determined.

The use of three different characteristic fluids has been found acceptable for solving most fluid dynamics problems involving subsonic, transonic, and supersonic flows. In each of the three cases the characteristic fluid is assumed to be homogeneous and non-chemically reacting. Using the assumption of a homogeneous fluid is acceptable until the mean free path between gas molecules becomes a significant fraction of the size of the object being studied, such as Near Space. The assumption of a nonchemically reacting gas is good up to fairly significant temperatures, well above those encountered by the SR-71.

The three characteristic fluids are:

1. An ideal fluid; one which is incompressible, inelastic, and non-viscous. The ideal fluid assumption gives reasonable results when analyzing slow-speed flow outside of a boundary layer. More rigorously, thermally perfect or calorically perfect gases are those whose internal energy is a function of temperature only (thermally perfect) or a linear function of temperature (calorically perfect--hence a calorically perfect gas is also thermally perfect). More broadly, an ideal or perfect fluid is simply one which obeys the thermal equation of state. For low densities, all gases follow this relation.

2. An incompressible, inelastic, viscous fluid, which differs from an ideal fluid because of viscosity. This fluid assumption gives reasonable results for low-speed flow inside a boundary layer and in vortex wakes behind an object.

3. A compressible, elastic, nonviscous fluid, which will be used in this chapter. This fluid assumption provides reasonable results for flow outside of the boundary layer up to hypersonic speeds (five times the speed of sound). Elasticity in a fluid is closely related to compressibility and is characterized by the finite amount of time it takes to affect the change in fluid pressure per unit change in specific volume. This property accounts for the finite propagation of a sound wave, as opposed to instantaneous propagation that is modeled in an inelastic fluid.

Analysis of a viscous, compressible fluid would be very complex and rely heavily on experimental evidence for confirmation of the associated theory. Hypersonic flow requires the consideration of a viscous, compressible, nonhomogeneous, dissociated, and chemically active fluid. It should easily be seen that the complexity of hypersonic analysis is much greater than subsonic and supersonic flow analysis.

6.3 COMPRESSIBLE, ELASTIC, NON-VISCOUS FLOW

All aerodynamics is concerned with changes in pressure that occur over bodies of various sizes and shapes and the causes and effects of these changes (lift and drag). A large part of early aerodynamic research was based on the assumption of a nonviscous, inelastic, incompressible (ideal) fluid. The assumption of ideal flow was acceptable at low speeds where a small change in pressure caused virtually no change in the density of the fluid. The assumption of a nonviscous fluid was acceptable as long as the viscous effects were considered limited to the vicinity of the surface (in the boundary layer). With the advent of high speed flight, these assumptions had to be

reconsidered.

The inelastic flow assumption implies that pressure variations are instantaneously felt everywhere in the fluid. In reality, they are transmitted at a finite speed, the speed of sound. As the velocity of an aircraft approaches some sizeable fraction of the speed of sound (one half or more), the results obtained from incompressible flow relations are found to be in error due to the effects of compressibility. Viscous effects can be omitted from this discussion by studying flow on an object outside of the boundary layer. Boundary layer effects are a very small percentage of the total flow effects.

Compressible flow exists when a change in pressure is accompanied by a change in density. The amount of compressibility depends on the velocity of the fluid flow. All gaseous flow is compressible, and even the so-called incompressible (low speed) flow experiences some degree of compression. In the incompressible case, the velocity is so low that the change in density is insignificant compared to the change in pressure.

The introduction of the new variable, density (as a function of velocity), in aerodynamic problems requires the introduction of an equation of state and other thermodynamic relations to describe the changes in pressure, density, and temperature. The study of compressible flow combines the science of fluid mechanics and thermodynamics.

The general solution of a compressible flow problem consists of finding three unknown velocity components and three density and pressure changes with respect to the spatial coordinates x , y , and z . The mathematical complexity of this three-dimensional solution obscures many of the fundamental concepts of compressible flow that are quite clear when the flow is analyzed in one or, in some cases, two dimensions. In this chapter, fluid flow equations will be developed for one-dimensional flow. The modifications necessary to use the equations for two-dimensional flow will be discussed later in the chapter. Lastly, three-dimensional flow will be discussed qualitatively.

6.3.1 ONE-DIMENSIONAL FLOW APPROXIMATION

One-dimensional flow generally implies straight line or linear motion; however, it need not be this restrictive. The equations of "one-dimensional" fluid flow can apply to flow through a passage in which the cross-sectional area varies slowly such that components of velocity normal to the primary direction of flow are minor compared to the primary direction flow components and can be considered negligible. For instance, flow in a curved channel can be considered one-dimensional as long as the turning of

the flow is small compared to the length of the segment of channel that is under consideration. The channel need not be constant in area as long as the divergence or convergence is small compared with the distance along the channel. The channel may either be bounded by physical boundaries such as the walls of a pipe or wind tunnel or by streamlines such as those surrounding an airfoil in flight.

6.4 COMPRESSIBLE FLOW EQUATIONS

The compressible flow equations which relate the flow velocity to the pressure, temperature, and density are obtained from three fundamental conservation principles and the equation of state for the particular fluid in question. These are:

1. Conservation of Mass
2. Conservation of Momentum
3. Conservation of Energy
4. Equation of State

The assumptions that are made when first developing the compressible flow relations (equations) are that: the flow is steady, one-dimensional, nonviscous, adiabatic, and the fluid conforms to the equation of state for a perfect (or ideal) gas. As restrictive as these assumptions may seem, they do not seriously limit the validity of the resulting equations.

For steady flow it is assumed flow properties upstream do not change with time. The one-dimensional assumption can be extended to other than linear motion with certain restrictions. Viscosity can be ignored when flow is examined outside of a boundary layer. The adiabatic assumption can be justified by the fact that the temperature gradients, which are the driving potential for the transfer of heat in a flow, are small, causing the heat transfer, dq , to be small or negligible. The perfect gas assumption is good for air up to moderately high temperatures.

Under these assumptions, the conservation equations and equation of state may be written:

1. Conservation of Mass: (Continuity Equation)

$$\dot{m} = \rho VA = \text{constant} \quad (6.1)$$

Applying the product rule of differentials and dividing by ρVA gives

$$(6.2)$$

$$\frac{d\rho}{\rho} = \frac{dV}{V} + \frac{dA}{A} = 0$$

2. Conservation of Momentum: (Momentum Equation)

$$dP + \rho V dV = 0 \quad (6.3)$$

3. Conservation of Energy: (First Law of Thermodynamics)

$$dq - dw = de \quad (6.4)$$

4. Equation of State: (Ideal Gas)

$$P = \rho R T \quad (6.5)$$

Before deriving the compressible flow equations, the concepts of total properties, speed of sound, Mach, speed ranges, and sound wave propagation must be studied in detail.

6.5 TOTAL (STAGNATION) PROPERTIES

Temperature, density, and pressure are normally thought of as static properties of a gas. Since we will be dealing entirely with a flowing gas, it becomes convenient to define a new temperature, density, and pressure to include a velocity component. We will find that not only does it simplify calculation, but, under certain conditions, it is more convenient to measure the total values of temperature, density, and pressure than the static values and velocities.

6.5.1 TOTAL TEMPERATURE

Consider the restricted steady flow energy equation from Derivation F.4 in App. F.

$$h + \frac{V^2}{2} = \text{constant}$$

(F.4)

The constant, resulting from the kinetic energy term combined with static enthalpy, forms a new term, total enthalpy, h_T

$$\text{constant} = h_r = h + \frac{V^2}{2} \quad (6.6)$$

Now, consider a calorically perfect gas (constant specific heat values), where $h = C_p T$, then

$$h_r = C_p T + \frac{V^2}{2} = C_p \left[T + \frac{V^2}{2C_p} \right]$$

$$h_r = C_p T_r \quad (6.8)$$

where $T_r = T + V^2/2C_p$ and is called the Total or Stagnation Temperature. Thus the Total Temperature at a given point in a flow is that temperature that would exist if the flow were slowed down adiabatically (without external heat transfer) to zero velocity. Physically this means in a flowing gas the molecules have superimposed on their random motion the directed motion of the flow. Recall, static temperature is just a measure of the amount of random molecular motion in a gas. The kinetic energy of the directed motion is the cause of the difference between static and total temperature. If, in some manner, the velocity of the airstream is adiabatically reduced to zero, and in the absence of work being done, the resulting static temperature of the gas becomes equal to the total temperature of the flowing fluid. This will be true regardless how the "slowing down" process occurs. Therefore, a thermometer fixed with respect to a duct will measure total temperature (neglecting heat transfer effects) because it reduces the velocity of a small portion of the stream to zero.

Although the same final temperature, T_r , is attained whether the slowing down process is reversible or irreversible, the pressure and density finally reached will vary with the degree of irreversibility associated with the slowing down process. For pressure this may be illustrated as follows: in Figure 6-1, imagine the flowing gas at station (1) to be brought to rest adiabatically by means of a duct diverging (dashed lines) to an extremely large area (X) where the flow velocity, in the limit, is zero. If the diverging duct is frictionless, the slowing down process from (1) to (X) is isentropic and is shown as the vertical line from (1) to (2) on the temperature-entropy (T-S) diagram. If the diverging duct is frictional, the slowing down process from (1) to (X) is irreversible but adiabatic (hence, $dS > 0$) and is shown by the line of increasing entropy, (1) to (3), on the T-S diagram.

The final temperature attained at (2) and at (3) is the same; since by the First Law of Thermodynamics written between station (1) and (X) for each of these processes,

$$C_p T_1 + \frac{V^2}{2} = C_p T_2 \text{ (frictionless process)} \quad (6.9)$$

$$C_p T_1 + \frac{V^2}{2} = C_p T_3 \text{ (frictional process)} \quad (6.10)$$

However, when examining the pressure at each state, $P_b < P_c$.

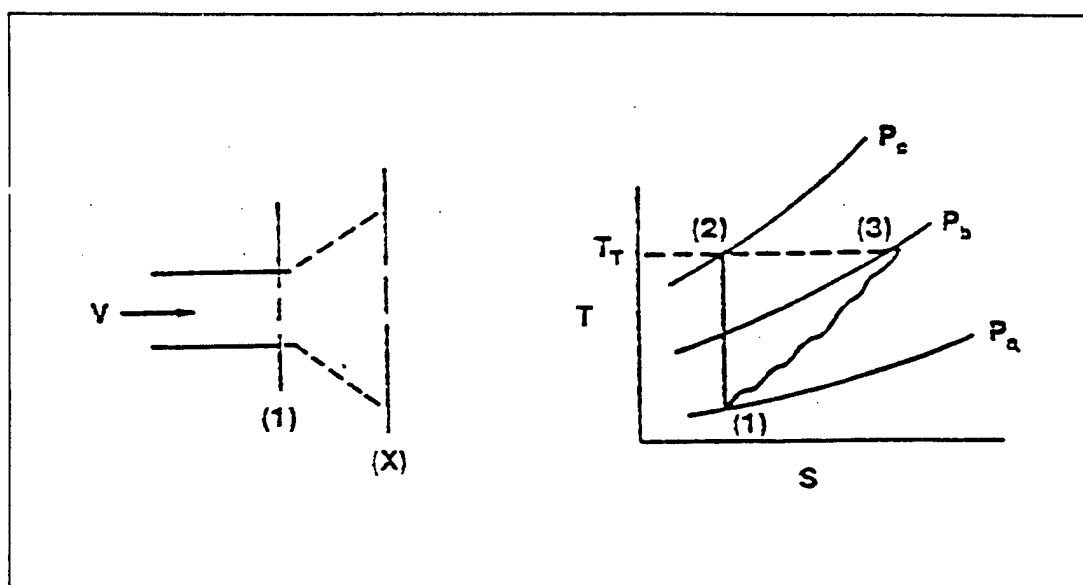


FIGURE 6.1 TOTAL PRESSURE AND DENSITY FOR REVERSIBLE AND IRREVERSIBLE PROCESSES

6.5.2 TOTAL PRESSURE

The total pressure of a flowing gas is defined as the pressure obtained when the gas is brought to rest isentropically. Thus the pressure corresponding to state (2) on the T-S plot in Figure 6.1 is the total pressure of the gas in state (1), hence $P_{(2)} = P_c = P_T$. The pressure measured by a pitot tube placed in subsonic flow corresponds very closely to the total pressure of the gas since the slowing down process preceding the pitot tube is basically isentropic.

6.5.3 TOTAL DENSITY

Total density of a flowing gas is defined similarly to pressure as the density obtained when the gas is brought to rest isentropically.

6.5.4 MATHEMATICAL RELATIONSHIPS FOR TOTAL PROPERTIES

By use of the ideal gas law and the equation of state for an isentropic process

$$P\rho^\gamma = \text{constant.} \quad (6.11)$$

The following relationships between static and total values of pressure, density, and temperature can be developed

$$\frac{P_T}{P} = \left(\frac{T_T}{T} \right)^{\frac{\gamma}{\gamma-1}} \quad (6.12)$$

$$\frac{\rho_T}{\rho} = \left(\frac{T_T}{T} \right)^{\frac{1}{\gamma-1}} \quad (6.13)$$

Since total properties are constant throughout an isentropic flow and are easily measured, they are useful and convenient tools when evaluating the changes in compressible fluid flow. In different texts, the subscripts o, t, or T are used to denote total properties. In this text, "T" is used.

6.6 SPEED OF SOUND

The speed of sound is a fundamental parameter in compressible flow theory and is the speed at which small disturbances (sound waves) propagate through a compressible fluid. The quantity

$$a = \sqrt{\frac{dP}{d\rho}} \quad (6.14)$$

is called the speed of sound or acoustic speed since it is the speed with which sound waves propagate through a fluid. Equation 6.14 is derived for a nonviscous fluid; therefore, it is only valid for small disturbances which do not create any shear forces in the fluid. (Derivation F.1 in Appendix F.)

Sound waves are, by definition, "small"; the criterion being that the velocity gradients in a fluid, dV , due to the pressure disturbances, are so small that they create negligible shear or friction forces, and that the speed of sound is very large;

$$a \gg dV$$

It follows that the motion of a sound wave through a fluid is an isentropic phenomenon, since it does not disturb the "disorder" of the fluid, i.e., the dP , $d\rho$ and dT in the fluid caused by the passage of a sound wave are very small. In reality, the size of an audible sound wave is so small that the entropy increase near the wave is negligible, and Equation 6.14 is quite accurate for computing the speed of sound wave propagation.

Squaring Equation 6.14 ($a^2 = \dots$) gives a pressure-density relationship for a fluid which may be used to eliminate the pressure term in the momentum equation,

$$dP + \rho V dV = 0 \quad (6.3)$$

$$a^2 d\rho + \rho V dV = 0 \quad (6.15)$$

Equation 6.15 is important for later derivation of compressible flow relations, and the inference of isentropic conditions must be remembered when using it.

If pressure is a function of density and entropy state (S),

$$P = P(\rho, S)$$

then by partial differentiation,

$$dP = \frac{\delta P}{\delta S} dS + \frac{\delta P}{\delta \rho} d\rho$$

and the substitution for $d\rho$ in the momentum equation cannot be made as conveniently. However, if the flow conditions are isentropic, $dS = 0$, then

$$\frac{dP}{d\rho} = \frac{\delta P}{\delta \rho}$$

and dP can be eliminated from the momentum equation. Since an isentropic process has been assumed, Equation 6.14 should be correctly written as

$$a = \sqrt{\left(\frac{\delta P}{\delta \rho} \right)_{dS=0}}$$

The speed of sound may be evaluated for a perfect gas from the conservation of energy equation and the equation of state. The relationship between P and ρ , evaluated for an isentropic process, is

$$\frac{P}{\rho^\gamma} = \text{constant}$$

(6.11)

Taking the natural log of this equation and differentiating,

$$\ln P - \gamma \ln \rho = \ln (\text{constant})$$

we have

$$\frac{dP}{P} - \gamma \frac{d\rho}{\rho} = 0$$

or

$$\frac{dP}{d\rho} = \gamma \frac{P}{\rho} \quad (6.16)$$

Substituting

$$\rho = \frac{P}{RT}$$

(Equation of State, 6.5)

$$\frac{dP}{d\rho} = a^2 = \gamma RT$$

$$a = \sqrt{\gamma RT}$$

or

(6.17)

Thus the speed of sound is a function of temperature only.

"Cookbook" equations for the speed of sound, in air, at a local temperature are

$$a[\text{knots}] = 29 \sqrt{T[^\circ R]} \quad (6.18)$$

$$a \text{ [ft/sec]} = 49 \sqrt{T \text{ [}^\circ\text{R}]}$$

or

(6.18a)

6.7 MACH

Mach is the most important parameter in compressible flow theory, since it compares the speed of sound in a fluid (a significant measure of compressibility effects) and the speed at which the fluid is flowing. Mach is defined as the ratio of a flow velocity to a speed of sound.

$$M = \frac{V}{a} \quad (6.19)$$

If Mach is defined in terms of a local speed of sound, it is called local Mach. When local Mach is used, it will be written without a subscript. Mach may be defined in terms of the speed of sound at some given point in the flow, i.e., the ratio of an aircraft velocity to the speed of sound based on the ambient temperature (as opposed to local temperature). For flow in channels, ducts, and nozzles, it is sometimes more convenient to reference the Mach to a specific place in the flow. When this is done, Mach is written with subscripts or superscripts, i.e.,

$$M_T = \frac{V}{a_T} \text{ or } M^* = \frac{V}{a^*}$$

where a_T is the speed of sound at the stagnation temperature, T_T , and a^* is the speed of sound at local sonic conditions. The concept of the local sonic conditions will be discussed later in this chapter.

Rewriting Equation 6.19 in terms of M^2 ,

$$M^2 = \frac{V^2}{a^2} = \frac{V^2}{\gamma RT}$$

it can be seen that V^2 is a measure of the directed or kinetic energy of the fluid flow

and that the temperature term in the denominator is a measure of the internal or random thermal energy of the fluid.

This interpretation brings out two disadvantages of using Mach in flow descriptions:

1. Mach is proportional to the velocity of the flow.
2. Mach tends toward infinity as the temperature decreases.

These limitations will become apparent when working with hypersonic fluid flow or at extreme altitudes where the fluid is no longer a continuous medium.

6.8 CLASSIFICATION OF SPEED RANGES

It is clear, now, that there are at least two basic speed ranges to be considered: subsonic speeds, where the Mach is less than one, and supersonic speeds, where the Mach is greater than one. When describing the aerodynamics of an aircraft, a range, extending from high subsonic speeds to low supersonic speeds, is found which is not described by either the subsonic or supersonic flow equations. This is the transonic speed range. The local flow over an aircraft in transonic flight is part subsonic and part supersonic. The interaction between the two types of flow causes aerodynamic phenomena which have characteristics of neither subsonic nor supersonic flow. These phenomena begin at the critical Mach and continue until the flow on the aircraft is completely supersonic. This range is from about Mach .8 to 1.2. Since the transonic range is difficult (in some cases impossible) to describe mathematically, it will be discussed after more knowledge is gained about supersonic flow. Extremely low velocities ($M < .7$) are studied as incompressible flow. Extremely high velocities typify hypersonic flow, which is of current interest to space scientists concerned with orbital and re-entry velocities. The hypersonic speed range is considered to begin at Mach 5.0, but some hypersonic characteristics appear at speeds as low as Mach 3.5. Hypersonic flow is characterized by high temperatures which cause ionization, gaseous dissociation and recombination, extreme wave angles, boundary layer interaction, and high heat transfer rates.

6.9 TWO-DIMENSIONAL PROPAGATION OF SOUND WAVES

Sound waves are a series of alternate compression and rarefaction pressure pulses such as might be caused by a tuning fork. They are propagated or transmitted in all directions in a fluid at a given speed proportional to the temperature of the fluid. If

the disturbance which is causing sound waves is motionless in the fluid, these waves appear to radiate out from the disturbance in a series of concentric rings like ripples on a pond as in Figure 6.2a.

If the disturbance is moving in the fluid, the wave pattern is quite different since each wave is emitted from a different point in the fluid. For example, if the disturbance is traveling at some speed which is less than the speed of sound in the fluid, the wave pattern is distorted as shown in Figure 6.2b. In this case, the sound wave outruns the disturbance, forming a series of circles one inside the other, but with different centers.

If the disturbance travels at exactly the speed of sound, the wave front and the disturbance travel together, forming the pattern shown in Figure 6.2c. Each successive wave reinforces the next wave, forming a wave front. This is a sound wave front, which is, by definition, isentropic.

If the disturbance travels at greater than sonic velocity, it outruns the wave patterns which radiate out from the point where they were emitted, forming an oblique wavefront trailing behind the disturbance (Figure 6.2d).

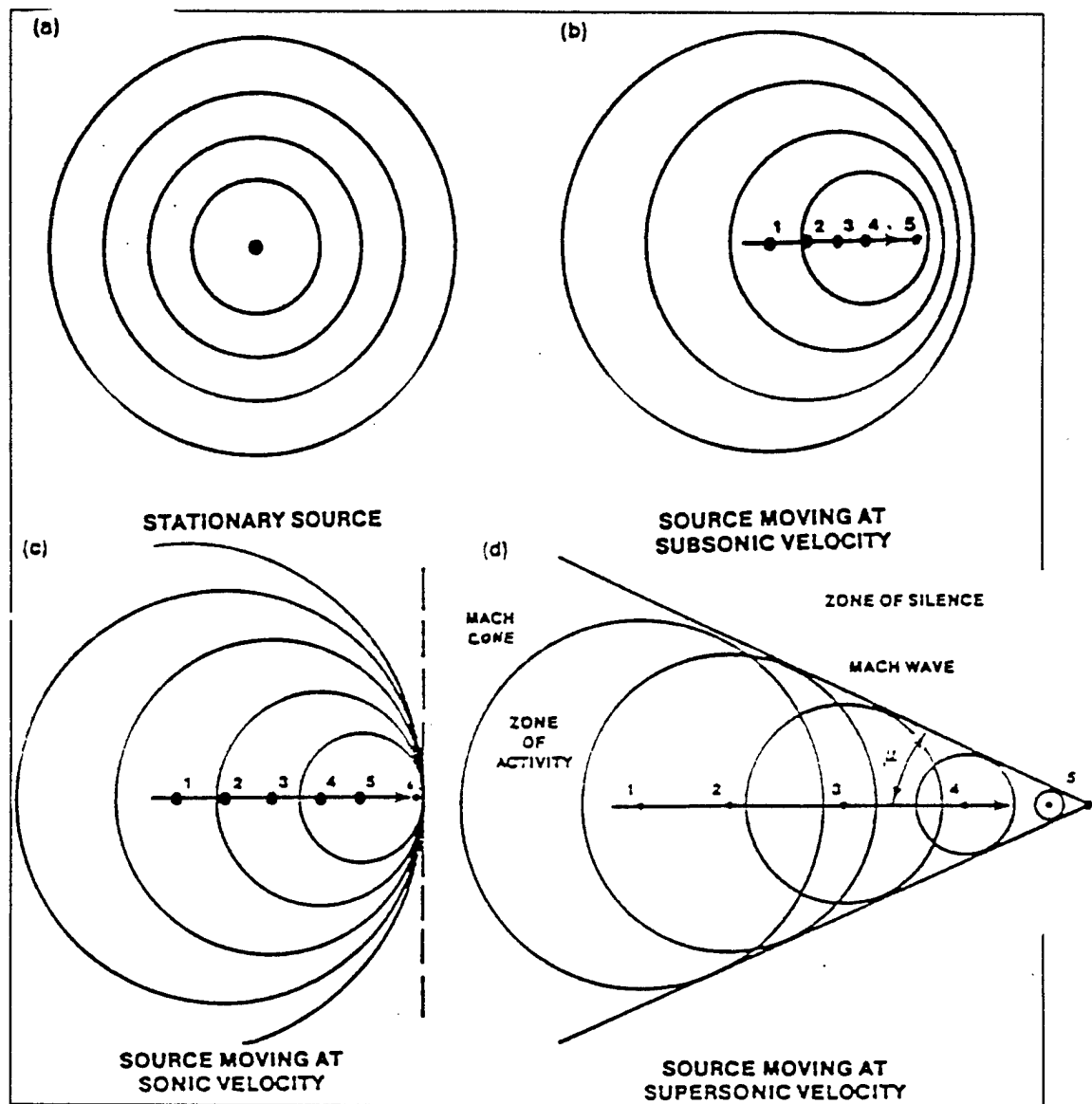


FIGURE 6.2 SOUND WAVE PROPAGATION FROM A POINT SOURCE
(6.1.160)

6.9.1 MACH ANGLES

This isentropic wave front (Figure 6.2d) is analogous to the oblique shock wave, and the angle between the wave front and the direction of the disturbance's motion is called the Mach wave angle or Mach angle, μ . In the paragraph "Oblique Shock Waves," it will be shown that μ is the smallest possible wave angle for any pressure disturbance. It is the angle of a zero strength shock wave (an isentropic shock wave) which is nothing more than a sound wave. The triangle formed by the Mach angle is called the Mach cone, and from the geometry of the Mach cone it can be seen that

$$\sin \mu = a \frac{dt}{V dt} = \frac{a}{V} = \frac{1}{M}$$

where dt is a given time interval, and

$$\text{Mach Angle} = \mu = \sin^{-1} \frac{1}{M} \quad (6.20)$$

6.9.2 ACTIVITY ENVELOPE

The real significance of the propagation of sound waves relative to the speed of the disturbance is the envelope they describe. It can be seen that sound waves or pressure disturbances are not transmitted upstream when the Mach is equal to or greater than one. The pattern of Figure 6.2d illustrates the three rules of supersonic flow given by Von Karman, in 1947, in the Tenth Wright Brothers Lecture. These rules are based on the assumption of small disturbances. They are qualitatively applicable, however, to large disturbances.

- a. The rule of forbidden signals. The effect of pressure changes produced by a body moving at a speed faster than sound cannot reach points ahead of the body.
- b. The zone of activity and zone of silence. All effects produced by a body moving at a supersonic speed are contained within the zone of activity bounded by the Mach cone extending downstream from the body. Conversely, any arbitrary point in a supersonic stream can be affected only by disturbances emanating from source points lying on or within a cone of the vertex angle μ extending upstream from the point considered. The region outside of the zone of activity is called the zone of silence.
- c. The rule of concentrated action. The effects produced by the motion of an object at supersonic speeds are concentrated along the Mach lines. Extrapolating this rule to large disturbances, we can observe its qualitative application in the concentration of effects along a shock wave accompanying a body at supersonic speeds.

6.10 ISENTROPIC FLOW

The isentropic flow process was defined as being both adiabatic and reversible. These conditions are very nearly met in one-dimensional, nonviscous, shock-free flow where both the cross-sectional area of the streamtube and the flow direction are constant or change very slowly. The non-viscous assumption is extremely important when flow in a channel is considered, since, in reality, boundary layer interaction causes

irreversible changes in flow properties, complicating analysis.

The isentropic flow assumptions, while seemingly quite restrictive, are very useful when evaluating one-dimensional flow conditions existing outside of a boundary layer and between shock waves. Special relationships will be derived later in this chapter for evaluating the changes occurring because of shock waves.

Valuable insight into a great number of real aerodynamic and fluid flow problems can be gained from the ability to predict isentropic changes and changes caused by shock waves in supersonic flow. A few of the isentropic flow equations will be derived from the one-dimensional, conservation equations. Many others can be derived when needed or may be found in most texts on supersonic aerodynamics and fluid dynamics.

Since the stagnation properties P_T , ρ_T , and T_T can be experimentally measured or calculated from energy concepts at any place in an isentropic flow, it is useful to obtain relationships between these stagnation properties and the free stream properties of the flow in terms of a function of Mach, that is,

$$\frac{P_T}{P}, \quad \frac{\rho_T}{\rho}, \quad \frac{T_T}{T} = f(M)$$

Using Equation 6.7, which was developed for adiabatic flow,

$$h_T = C_p T + \frac{V^2}{2} \quad (6.7)$$

$$C_p T_T = C_p T + \frac{V^2}{2} \quad (6.21)$$

To write Equation 6.21 in terms of Mach, where $M^2 = V^2 / \gamma RT$, divide the equation by $C_p T$

$$\frac{T_T}{T} = 1 + \frac{V^2}{2 C_p T}$$

$$= 1 + \left[\frac{V^2}{2C_p T} \right] \left[\frac{RC_v}{RC_v} \right]$$

$$= 1 + \left[\frac{R}{2C_v} \right] \left[\frac{V^2}{\gamma RT} \right]$$

but

$$\frac{R}{C_v} = \gamma - 1 \quad \text{since } R = C_p - C_v \text{ and } \gamma = \frac{C_p}{C_v} \text{ therefore,}$$

$$\frac{T_T}{T} = 1 + \frac{\gamma - 1}{2} M^2 \quad (6.22)$$

This is a very important equation, relating stagnation temperature to freestream temperature in terms of flow Mach for an adiabatic flow process. Notice that the flow does not have to be isentropic for this equation to be valid. This equation should be recognized as the one used to determine the ambient air temperature, T_a , from flight test data

$$\frac{T_{ic}}{T_a} = 1 + k_t (\gamma - 1) \frac{M^2}{2} \quad (6.23)$$

where k_t is a recovery factor that describes the efficiency of the adiabatic flow process between the ambient air and the temperature probe. The two equations are identical when the recovery factor, k_t , is equal to one, i.e., the probe is perfectly insulated from the ambient air. In reality, even the worst total temperature probes have a recovery factor greater than 0.98, and most exceed 0.99. In almost all cases the recovery factor values are very predictable and repeatable.

To obtain an expression for PT/P as a function of Mach use Equation 6.12

$$\frac{P_T}{P} = \left[\frac{T_T}{T} \right]^{\frac{\gamma}{\gamma-1}} \quad (6.12)$$

Substituting Equation 6.22 into this equation,

$$\frac{P_T}{P} = \left[1 + \frac{\gamma-1}{2} M^2 \right]^{\frac{\gamma}{\gamma-1}} \quad (6.24)$$

Substituting Equation 6.22 into Equation 6.13,

$$\frac{\rho_T}{\rho} = \left[1 + \frac{\gamma-1}{2} M^2 \right]^{\frac{1}{\gamma-1}} \quad (6.25)$$

It should be noted that it is not necessary for the stagnation properties to actually exist at some point in the flow to write the equations relating them to the free stream pressure, density, and temperature. It is only necessary to assume that the flow at some given point could be slowed isentropically to zero velocity.

It was previously stated that the stagnation properties remained constant throughout an isentropic flow. The proof of this statement begins with the fact that temperature is a direct measure of the internal energy of a flow.

The internal energy of an adiabatic flow is constant since no heat is exchanged with the surroundings. If an adiabatic flow is slowed isentropically to zero velocity, the stagnation temperature measured would be a constant at any point throughout the flow.

If viscous or other irreversible effects were present in the adiabatic flow, the stagnation temperature would still remain constant since no heat is exchanged with the surroundings. The presence of viscous and irreversible effects means that some of the kinetic energy of the flow is converted to thermal energy, but the stagnation temperature of the flow remains constant for reasons stated above.

By integrating the entropy relation, rearranging terms, and evaluating at stagnation conditions

$$S_T = \ln \left[\left(\frac{T_T}{P_T} \right) \frac{\gamma}{\gamma-1} \right] + \ln c$$

It can be seen that P_T is constant in isentropic flow, since S_T and T_T are constant. From the equation of state, $P_T = \rho_T R T_T$, it can be seen that ρ_T is also constant in isentropic flow.

Because P_T , ρ_T , and T_T are all constants in isentropic flow, the ratio of free stream conditions at two different stations in the flow may be obtained by taking a ratio of stagnation properties evaluated at the two stations, i.e.,

$$\frac{P_1/P_{T_1}}{P_2/P_{T_2}} = P_1/P_2$$

Resulting temperature, pressure and density ratios are shown below.

$$\frac{T_1}{T_2} = \frac{1 + \frac{\gamma-1}{2} M_2^2}{1 + \frac{\gamma-1}{2} M_1^2} \quad (6.26)$$

$$\frac{P_1}{P_2} = \left[\frac{1 + \frac{\gamma-1}{2} M_2^2}{1 + \frac{\gamma-1}{2} M_1^2} \right]^{\frac{\gamma}{\gamma-1}} \quad (6.27)$$

$$\frac{\rho_1}{\rho_2} = \left[\frac{1 + \frac{\gamma-1}{2} M_2^2}{1 + \frac{\gamma-1}{2} M_1^2} \right]^{\frac{1}{\gamma-1}} \quad (6.28)$$

Values of P/P_T , ρ/ρ_T , and T/T_T are tabulated versus Mach (at $\gamma = 1.4$ for air) in the appendices of most thermodynamics books. The same quantities are plotted versus Mach in Reference 6.4.

Since Mach is a quantity that can be measured in the flow problem and stagnation properties are constant in isentropic flow, use of these charts and graphs greatly simplifies the work required to calculate P , ρ , and T at a given station in the flow.

6.11 FLOW IN CONVERGENT-DIVERGENT STREAMTUBES

Understanding the characteristics of a compressible fluid flowing through a streamtube is very important in supersonic aerodynamics. If viscous effects are to be neglected in the streamtube, the boundary layer streamline may be used as the streamtube boundary. For this discussion a streamtube is defined as any convergent or divergent section bounded either by physical walls or by streamlines as shown in Figure 6.3. Such a streamtube might be formed by the

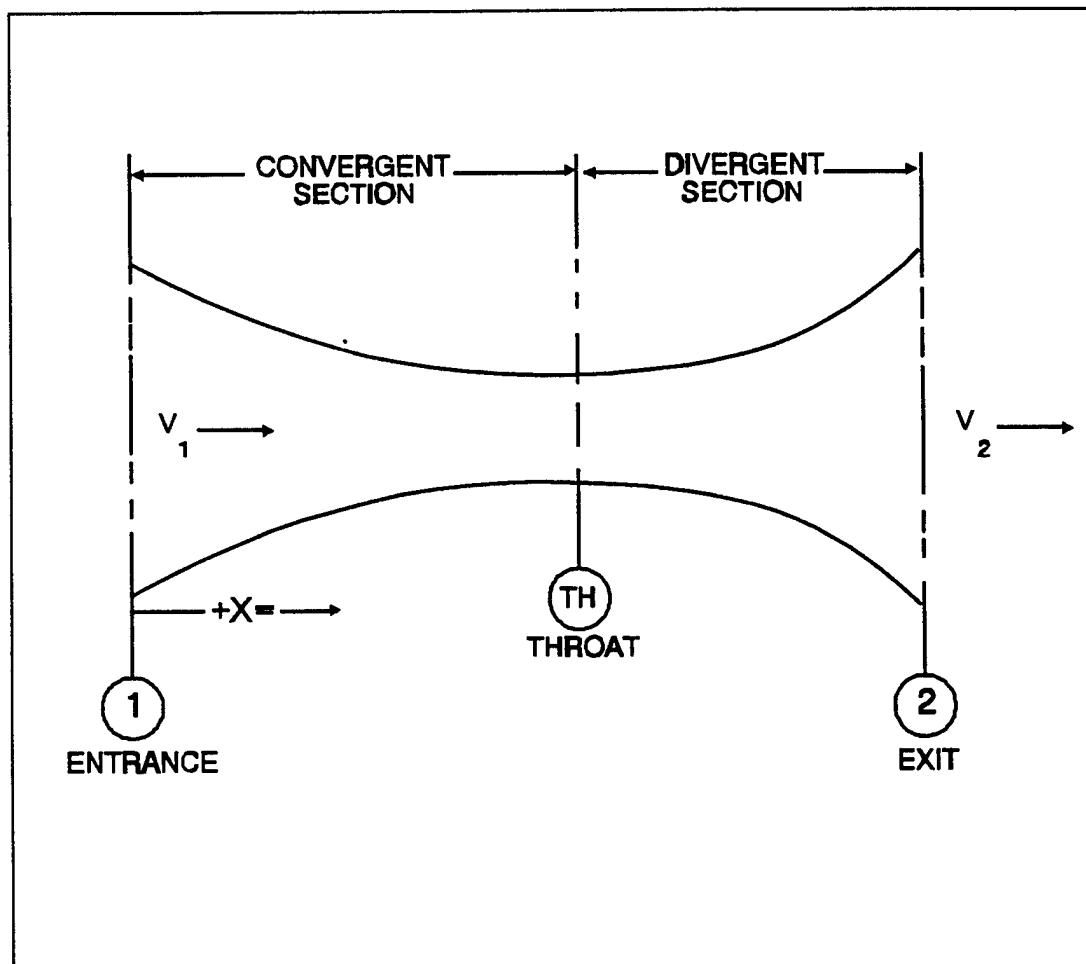


FIGURE 6.3 CONVERGENT DIVERGENT STREAMTUBE

inlet or exhaust duct of a jet aircraft or between converging and diverging streamlines as the air flows over the surface of the aircraft. Also, a supersonic wind tunnel uses convergent-divergent designs to obtain Mach greater than one in the test section.

Compressible flow through a convergent-divergent streamtube is quite different from the classical flow of an incompressible fluid through a venturi. At low velocities, the flow situation is almost identical to the venturi, but at high velocities the change in density causes a complete reversal of the low velocity trends. Consider steady, nonviscous, compressible, isentropic flow in the streamtube shown in Figure 6.3. In steady flow, the mass entering at Station 1 is equal to the mass leaving at Station 2, and the continuity equation may be used to describe the flow conditions

$$\frac{d\rho}{\rho} + \frac{dV}{V} + \frac{dA}{A} = 0 \quad (6.2)$$

Substituting the definition of the speed of sound into the momentum equation as done in Equation 6.15 yields

$$a^2 d\rho + \rho V dV = 0 \quad (6.15)$$

or

$$\frac{d\rho}{\rho} = \frac{V dV}{a^2}$$

Multiplying the right side by $\frac{V}{V}$

$$\frac{d\rho}{\rho} = -M^2 \frac{dV}{V} \quad (6.29)$$

and substituting this into the continuity equation above gives

$$-M^2 \frac{dV}{V} + \frac{dV}{V} + \frac{dA}{A} = 0$$

$$\frac{dA}{A} = (M^2 - 1) \frac{dV}{V} \quad (6.30)$$

Equation 6.30 describes the flow situation caused by compressible fluid flow in streamtubes. Defining a diverging streamtube as having a positive dA , i.e., an increasing area in the direction of the flow, and a converging streamtube as having a negative dA , the following conclusions can be drawn:

1. When the Mach is less than 1, a diverging streamtube causes a decrease in velocity, and a converging streamtube causes an increase in velocity.
2. When the Mach is greater than 1, a diverging nozzle causes an increase in velocity, and a converging nozzle causes a decrease in velocity.
3. When the Mach is 1, dA must be zero.

6.11.1 COMPRESSIBLE STREAMTUBE FLOW

Examining Equation 6.29 may give a physical understanding of what happens to subsonic or supersonic, compressible flow in a streamtube.

$$\frac{d\rho}{\rho} = -M^2 \frac{dV}{V} \quad (6.29)$$

It can be seen that for Mach less than 1, a small change in velocity results in a proportionately smaller change in density.

For air flowing at Mach of .3, .9, 1, and 2, consider the density effects caused by an arbitrary 10% increase in velocity ($dV/V = 10\%$).

At

$$M = .3; \quad \frac{d\rho}{\rho} = -0.9\%$$

$$M = .9; \quad \frac{dp}{\rho} = -8.1\%$$

$$M = 1; \quad \frac{dp}{\rho} = -10\%$$

$$M = 2; \quad \frac{dp}{\rho} = -40\%$$

Notice that for all Mach, an increase in velocity results in a decrease in density. The magnitude of the density change is proportional to the Mach squared; consequently, as the Mach increases, the change in density becomes more pronounced.

It is interesting to note that Equation 6.29 indicates the validity of the incompressible flow assumption. It shows that at low Mach, a change in velocity results in a very small change in density, and as the Mach increases, the assumption becomes poorer, until at Mach 1, the change in velocity is of the same magnitude as the change in density.

6.11.2 AREA CHANGES

To further the analysis, an equation must be obtained relating density change to area change as a function of Mach. If in the derivation of Equation 6.30 the value of dV/V had been substituted instead of dp/ρ , the following relation would have been obtained

$$\frac{dA}{A} = \left[\frac{1}{M^2} - 1 \right] \frac{dp}{\rho}$$

In the preceding discussion, it was found that for subsonic and supersonic Mach the density always decreased for increased velocity. This leads to the question, what shape is required to produce this decrease in density and increase in velocity? From Equation 6.31 it can be seen that for subsonic speed ($M < 1$), a decrease in density (and an increase in velocity) is caused by a converging duct (negative dA). That is, the

factor $\left[\left(\frac{1}{M^2} \right) - 1 \right]$ is positive for subsonic speeds. Supersonic, this factor is negative;

therefore, a diverging duct (positive dA) causes a decrease in density (and a corresponding increase in velocity).

Qualitatively speaking, the decrease in density is a second order effect and can usually be neglected for flow at low Mach because a reduction in area creates only a proportional increase in velocity. At high subsonic speeds, the reduction in density becomes more significant, but the density still is able to decrease fast enough to allow the velocity to increase as the fluid flows into a converging duct. At supersonic speeds, the density does not decrease fast enough in a converging section; therefore the nozzle must diverge to further reduce the density and allow an increase in velocity.

Only the case of accelerating flow has been considered, but it is obvious that the reverse of the described conditions is also true. That is, a subsonic stream is slowed down by a diverging section, and a supersonic stream is slowed down by a converging section. The general conclusions of the convergent-divergent streamtube problem may be summarized as shown in Figure 6.4.

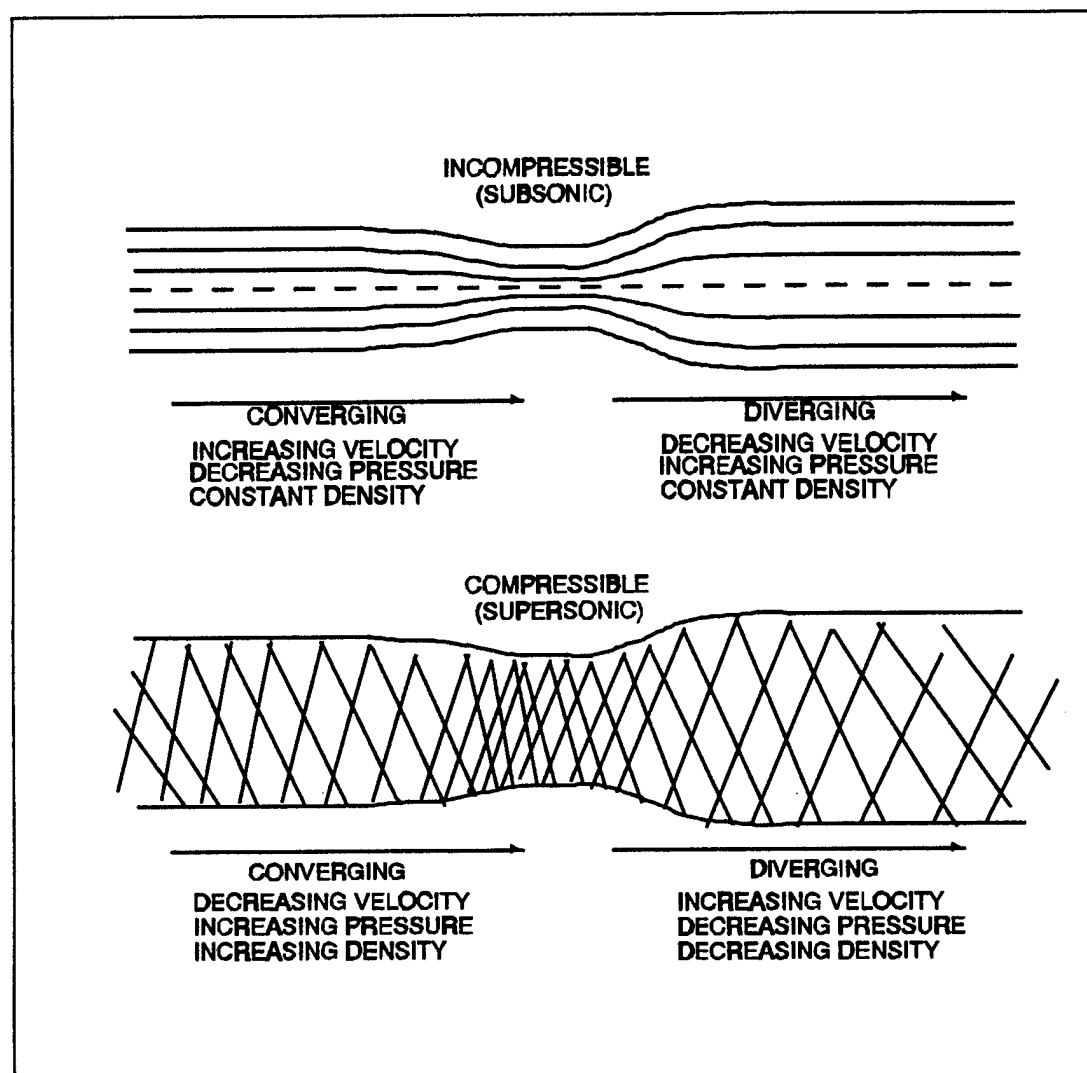


FIGURE 6.4 COMPARISON OF COMPRESSIBLE AND INCOMPRESSIBLE FLOW THROUGH A CLOSED TUBE (6.2:205)

6.11.3 FLOW AT THE THROAT

The flow in a convergent-divergent streamtube has been discussed at some length, but now the specific flow characteristics at the throat of the streamtube must be studied.

The minimum cross-sectional area of a convergent-divergent streamtube is called the throat. At the throat the area change per length of travel along the streamtube stops decreasing and starts increasing. At this section, the derivative $dA/dx = 0$, or $dA = 0$. Two conditions can exist at the throat since dA is zero. Either dV and/or $(M^2 - 1)$ must equal zero to satisfy Equation 6.30.

The first condition, $dV = 0$, is characteristic of flow in a subsonic streamtube in which the fluid accelerates to a maximum subsonic speed at the throat and then decelerates

again in the divergent section. It is also characteristic of supersonic flow which decelerates in the converging section, reaching a lower supersonic or exactly sonic velocity at the throat and then accelerates again in the divergent section.

The second condition, $(M^2 - 1) = 0$, is characteristic of what is called choked flow. It occurs when $M = 1$ at the throat. This condition exists whenever the flow is accelerated from subsonic to supersonic speeds by a nozzle or when flow is decelerated from supersonic to subsonic speeds by a diffuser. By definition, a nozzle accelerates flow, while a diffuser decelerates flow, although each is similar in appearance.

Flow through a streamtube is caused by a pressure differential between the inlet and exit. Increasing the inlet pressure or lowering the exit pressure causes an increase in the flow velocity and the mass flow rate. Since the maximum subsonic velocity occurs at the throat, sonic velocity ($M=1$) is attained first at the throat, and further reduction in exit pressure will not increase the velocity at the throat. This may be seen by considering the mechanism which causes a change in the mass flow rate and the flow velocity in the convergent-divergent streamtube (Figure 6.5).

If the exit pressure is exactly equal to the inlet pressure, no flow will occur. There are three critical values of exit pressure for a given inlet pressure. Between pressure equilibrium and first critical pressure, the flow will accelerate in the convergent portion of the streamtube and then decelerate through the diverging portion, remaining subsonic throughout. This is called the venturi regime. If the pressure is reduced to the first critical pressure at the exit, the flow will accelerate through the convergent

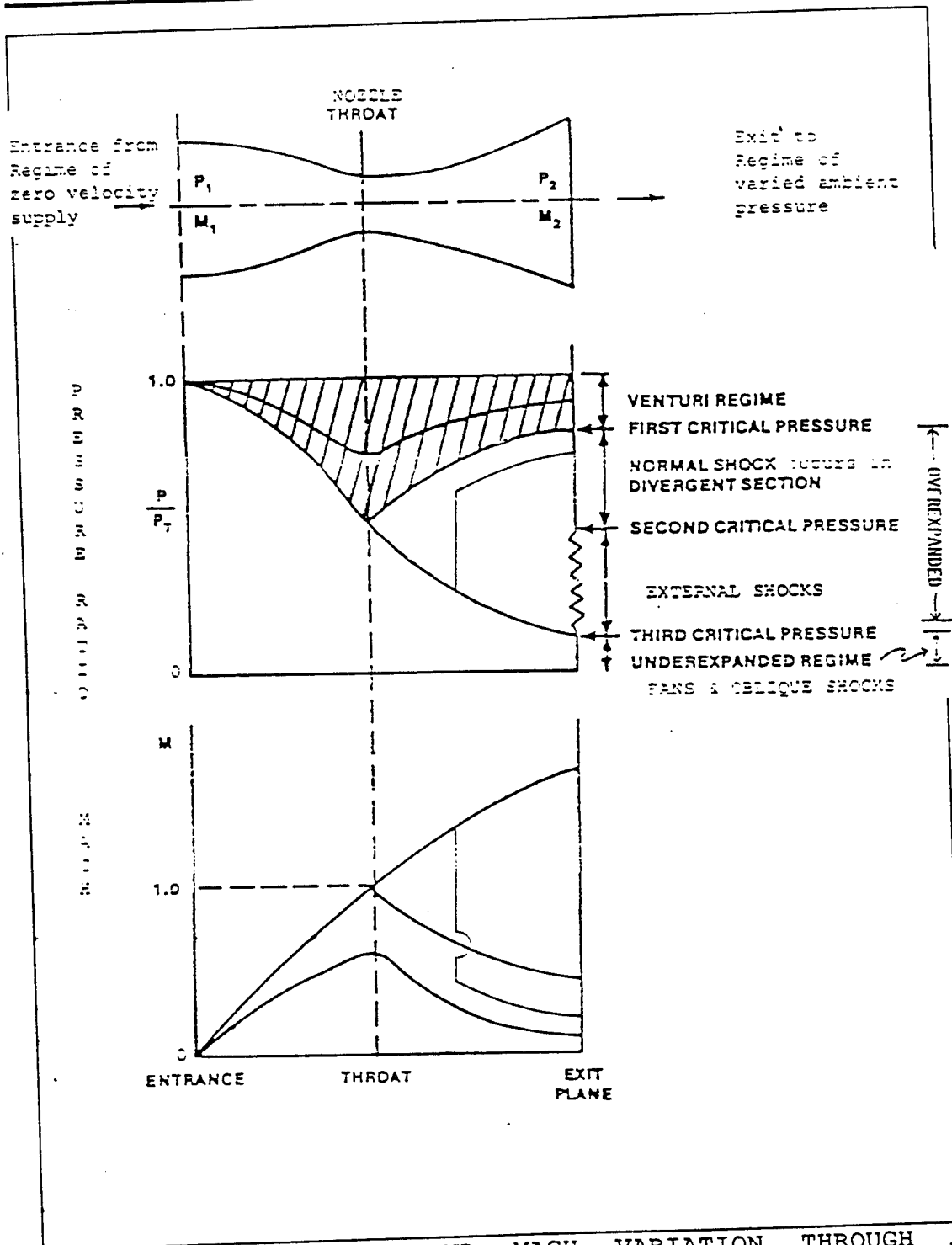


FIGURE 6.5 PRESSURE AND MACH VARIATION THROUGH A CONVERGING-DIVERGING STREAMTUBE (6.3:157)

portion, reach sonic velocity at the throat, and then decelerate back to a subsonic value. Once sonic conditions have been attained at the throat, further reductions in

exit pressure will not affect what happens upstream of the throat. The maximum mass flow rate has been achieved for that inlet pressure, and the streamtube is said to be choked. Further reduction in exit pressure beyond the first critical point will produce a normal shock somewhere in the divergent portion of the streamtube until the second critical pressure is reached. At the second critical pressure, a normal shock stands at the exit plane. Further reduction in exit pressure beyond the second critical value will produce oblique shocks or a combination oblique-normal shock outside the streamtube as shown in Figure 6.6a. This is called the overexpanded condition, indicating that the streamtube is too long, and will occur until reaching the third critical pressure. The third critical value is the only pressure for which no shocks occur anywhere in the streamtube flow field, and supersonic flow is maintained downstream of the throat. This is the on-design condition. Further reduction in pressure below the third critical value is an underexpanded condition, indicating the streamtube is too short, and expansion fans will form outside the streamtube as illustrated in Figure 6.6b.

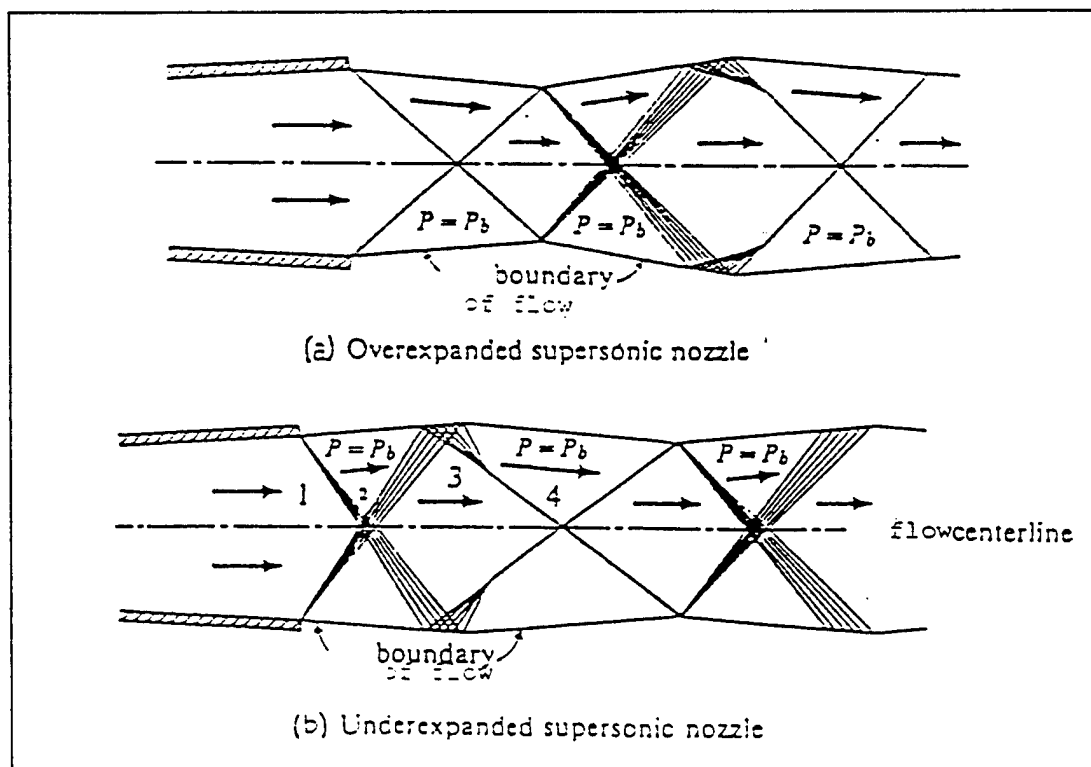


FIGURE 6.6 PRESSURE ADJUSTMENT OUTSIDE A NOZZLE OR STREAMTUBE (6.3:219, 220)

6.11.4 MASS FLOW IN A CHOKED STREAMTUBE

The mass flow rate of a gas ($\dot{m} = \rho Va$) increases with increasing pressure differential

between the entrance and exit of a subsonic, converging-diverging streamtube until sonic velocity is attained in the throat. When sonic velocity is reached, it has been shown that the velocity and density at the throat are fixed; consequently the mass flow rate, \dot{m} , is fixed or the streamtube is choked. Sonic velocity is the maximum velocity that can occur in the throat; therefore it fixes the maximum mass flow through the streamtube for given entrance conditions.

This should not be interpreted to mean that a choked streamtube is passing the maximum mass flow for the streamtube; it is passing the maximum mass flow for given entrance conditions. Since the streamtube was assumed isentropic, this is the same as saying a choked streamtube is passing the maximum mass flow for given stagnation conditions.

A choked streamtube makes an excellent metering device for gaseous fluids. By adjusting the stagnation or entrance conditions, the exact mass flow can be measured and calculated. In reality, a well designed metering streamtube passes within 2 - 3% of the mass flow calculated for an isentropic streamtube.

An equation for the mass flow rate through an isentropic streamtube can be derived

by substituting appropriate values into $\dot{m} = \rho VA$:

$$\dot{m} = \frac{P_r}{\sqrt{T_r}} A \frac{\sqrt{\gamma}}{R} \left[\frac{M}{\left(1 + \frac{\gamma-1}{2} M^2\right)^{\frac{\gamma+1}{2(\gamma-1)}}} \right] \quad (6.32)$$

If the streamline is choked, $M = 1$ and $A = A_{throat} = A^*$:

$$\dot{m} = \frac{P_r}{\sqrt{T_r}} A_{throat} \sqrt{\frac{\gamma}{R}} \left(1 + \frac{\gamma-1}{2}\right)^{-\frac{\gamma+1}{2(\gamma-1)}} \quad (6.33)$$

6.11.5 LOCAL SONIC CONDITIONS

When a streamline is choked, specific values for P , ρ , T , A , etc., are determined at the throat. These unique values are designated with a superscript, $*$, and are written P^* , ρ^* , T^* , A^* , etc. The concept of the local sonic area, A^* , where $M = 1$, is similar to the stagnation condition concept. Both refer to flow conditions at some specific Mach, i.e., $M = 1$ for local sonic conditions and $M = 0$ for stagnation conditions.

It is not necessary for the flow to be actually at Mach 1 to define the local sonic values. To determine local sonic conditions at some point in a flow, it has to be assumed that the area of the channel could be varied to the value A^* . When this is done, the prevailing conditions at the section with area A^* are local sonic conditions.

For instance, in an isentropic flow, A^* can be imagined at any point, that is, the channel can be reduced in area to that which would reduce a supersonic stream to Mach 1 or increase a subsonic stream to Mach 1.

Properties at local sonic conditions in an isentropic flow may be conveniently evaluated in terms of stagnation conditions, which are usually known or easily measured. The general procedure is to evaluate the identities

$$P^* = \frac{P_r}{P^*} ; \quad \rho^* = \frac{\rho_r}{\rho^*} ; \quad T^* = \frac{T_r}{T^*}$$

using Equation 6.24

$$\frac{P_r}{P} = \left[1 + \frac{\gamma-1}{2} M^2 \right]^{\frac{\gamma}{\gamma-1}} \quad (6.24)$$

and that local sonic conditions are defined where $M = 1$, gives

$$P_r = \left[1 + \frac{\gamma-1}{2} \right]^{\frac{\gamma}{\gamma-1}}$$

and

$$P^* = \frac{P_r}{\left[1 + \frac{\gamma-1}{2} \right]^{\frac{\gamma}{\gamma-1}}} \quad (6.34)$$

The P^* and T^* can be easily derived, and for air, $\gamma = 1.4$, the local sonic properties as a function of stagnation properties are

$$P^* = P_T (.528) \quad (6.35)$$

$$\rho^* = \rho_T (.634) \quad (6.36)$$

$$T^* = T_T (.833) \quad (6.37)$$

6.11.6 M*

The concept of local sonic conditions allows a dimensionless parameter, M^* , to be defined. Mach, M , is a very convenient parameter but has the disadvantages listed in the paragraph, "Mach."

Often it is convenient to work with the parameter M^* , which is the flow velocity V , divided by a^* , the speed of sound at local sonic conditions.

$$M^* = \frac{V}{a^*} \quad (6.38)$$

It should be noted immediately that M^* does not mean Mach at a place where $M = 1$ like all other starred quantities but is defined by Equation 6.38.

Unique relations between M and M^* can be derived for adiabatic flow using the definition of M^* and the energy equation for a perfect gas (refer to Appendix F, Derivation F.5)

$$M^{*2} = \frac{\frac{\gamma+1}{2} M^2}{1 + \frac{\gamma-1}{2} M^2} \quad (6.39)$$

$$M^2 = \frac{\frac{2}{\gamma+1} M^{*2}}{1 - \frac{\gamma-1}{\gamma+1} M^{*2}} \quad (6.4)$$

0)

From these two equations it can be seen that M^* is a simple index of when the flow is subsonic and when the flow is supersonic, i.e.:
when

$$M < 1; \quad M^* < 1$$

$$M > 1; \quad M^* > 1$$

$$M = 1; \quad M^* = 1$$

$$M = 0; \quad M^* = 0$$

$$M = \infty \quad M^* = \sqrt{\frac{\gamma+1}{\gamma-1}} = \sqrt{6} \text{ (for air)}$$

Equation 6.39 is tabulated in Reference 6.4, and if M^* is known, then M can be found or vice versa. Using M^* will greatly simplify the normal shock equations.

6.11.7 AREA RATIO

Just as it is convenient to work with dimensionless parameters P/P_T , etc., it is convenient to use a dimensionless area ratio, A/A^* . Equating Equation 6.32 and 6.33, this parameter is found to be

$$\frac{A}{A^*} = \frac{1}{M} \left[\frac{2}{\gamma+1} \right] \left(1 + \frac{\gamma-1}{2} M^2 \right)^{\frac{\gamma+1}{2(\gamma-1)}} \quad (6.41)$$

and is always greater than one. For a given value of A/A^* , there are always two values of M , one for subsonic flow and the other for supersonic flow.

6.12 NORMAL SHOCK WAVES

Shock waves are observed as a discontinuity between supersonic and subsonic flow. The flow passes from supersonic to subsonic speeds in an extremely short distance which is of the order of magnitude of the mean free path of the molecules in the flow. The kinetic energy of the supersonic, upstream molecules is instantaneously converted to pressure-volume (pv) and thermal energy.

Experimental studies of normal shocks in supersonic wind tunnels show fivefold pressure increases and threefold velocity decreases behind the shock. These changes occur in a distance too small to be measured on a photographic plate, but theoretical calculations and experimental measurements indicate a distance of the order of 10^{-5} inches.

Because changes due to a normal shock occur in such a short distance, the changes are highly irreversible, and a shock wave is not isentropic. Two valid assumptions made when studying normal shocks are that:

1. The flow through a shock is adiabatic.
2. The shock is very thin and has a constant cross-sectional area between the front and rear face.

With these two assumptions and the conservation equations (see "One-Dimensional Flow Approximation"), the changes in flow properties caused by a shock can be derived as functions of M_1 , i.e., P_2/P_1 , ρ_2/ρ_1 , T_2/T_1 , M_2 . These derivations are conceptually simple but involve lengthy mathematical equation juggling which is carried out in most textbooks on compressible flow; therefore only the results of the derivations will be listed (refer to Appendix F, Derivation F.6).

A pictorial representation of a normal shock and the change in flow properties across the shock is shown in Figure 6.7.

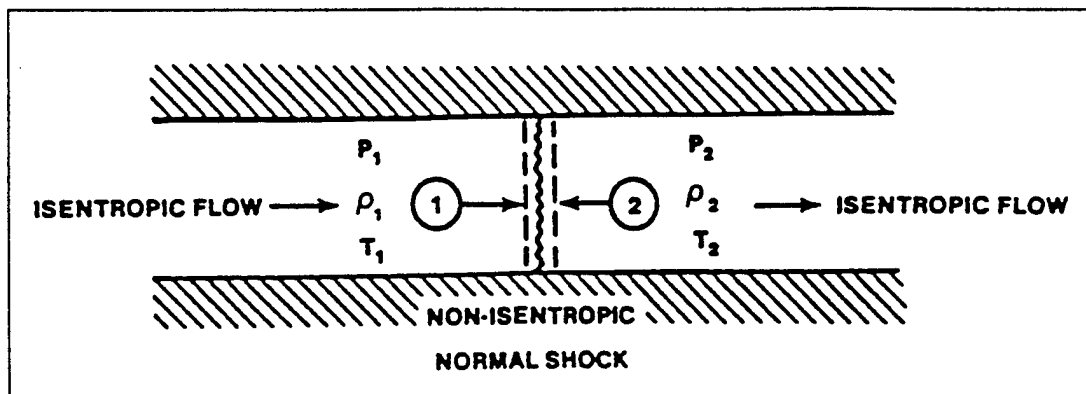


FIGURE 6.7 FLOW PROPERTIES IN THE VICINITY OF A NORMAL SHOCK

6.12.1 NORMAL SHOCK EQUATIONS

The notation used to describe the flow situation must be established before listing the normal shock equations. For these relations, the following assumptions were made:

1. All property changes occur in a constant area
2. Flow across the shock is adiabatic
3. Flow upstream and downstream of the shock is isentropic

$$\frac{P_2}{P_1} = \frac{1 - \gamma + 2 \gamma M_1^2}{1 + \gamma} \quad (6.42)$$

$$\frac{\rho_2}{\rho_1} = \left[\frac{2 + (\gamma - 1) M_1^2}{(\gamma + 1) M_1^2} \right]^{\frac{1}{\gamma}} \quad (6.43)$$

$$\frac{T_2}{T_1} = \left[\frac{1 - \gamma + 2\gamma M_1^2}{1 + \gamma} \right]$$

$$\left[\frac{2 + (\gamma - 1) M_1^2}{(1 + \gamma) M_1^2} \right] \quad (6.44)$$

$$M_2^2 = \frac{M_1^2 + \frac{2}{\gamma - 1}}{\left(\frac{2\gamma}{\gamma - 1} M_1^2 \right) - 1}$$

Values of P_2/P_1 , ρ_2/ρ_1 , T_2/T_1 , and M_2 are tabulated versus Mach, M_1 , (at $\gamma = 1.4$ for air) in the appendices of most thermodynamic books. The same quantities are plotted versus Mach in Reference 6.4.

6.12.2 NORMAL SHOCK SUMMARY

A shock wave is an extremely thin discontinuity which forms between supersonic and subsonic flow. The shock wave is an adiabatic process with no stagnation temperature loss across it, but as can be shown by entropy considerations, there is an accompanying stagnation pressure loss.

Supersonic flow always exists upstream of a shock wave, and the upstream stagnation pressure is greater than the downstream stagnation pressure.

General flow properties can be compared and tabulated as

$$V_1 > V_2 \quad S_1 < S_2$$

$$T_{r1} = T_{r2} \quad \rho_1 < \rho_2$$

$$P_{r_1} > P_{r_2} \quad M_1 > M_2$$

$$\rho_{r_1} > \rho_{r_2} \quad a_1 < a_2$$

$$T_1 < T_2 \quad a^*_1 = a^*_2$$

$$P_1 < P_2 \quad M^*_1 > M^*_2$$

$$A^*_1 < A^*_2 \quad T^*_1 = T^*_2$$

$$P^*_1 \geq P^*_2 \quad \rho^*_1 \geq \rho^*_2$$

6.13 SUPERSONIC PITOT TUBE

The loss in stagnation pressure across a normal shock affects the stagnation pressures sensed by aircraft pitot static systems (Figure 6.8).

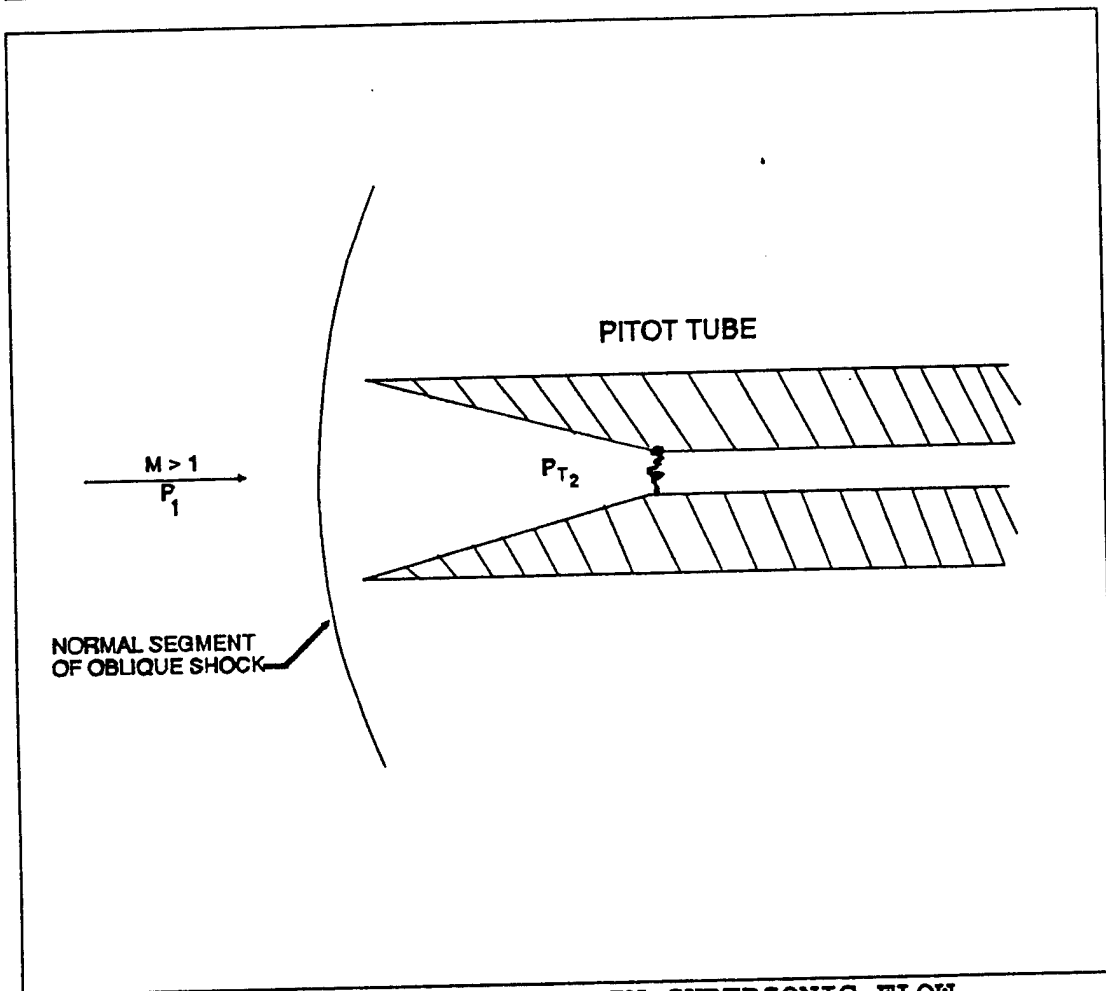


FIGURE 6.8 PITOT TUBE IN SUPERSONIC FLOW

To determine Mach from free stream static pressure and stagnation pressure behind a normal shock standing in front of a pitot tube, the Rayleigh Pitot Relation is often used

$$\frac{P_{T_2}}{P_1} = \frac{\left(\frac{\gamma+1}{2} M_1^2 \right)^{\frac{\gamma}{\gamma-1}}}{\left(\frac{2\gamma}{\gamma+1} M_1^2 - \frac{\gamma-1}{\gamma+1} \right)^{\frac{1}{\gamma-1}}} \quad (6.46)$$

By measuring P_1 and P_{T_2} , M_1 can be determined, and in many compressible flow textbooks, these values are plotted versus M_1 for $\gamma_{\text{air}} = 1.4$.

When using Equation 6.46, the free stream static pressure must be measured in front of the shock wave. This is a very difficult procedure for an aircraft in supersonic flight. Experiments have proven that if the static source is approximately ten pitot

tube diameters behind the shock wave, the static pressure measured is quite close to free stream static pressure.

On the pitot booms of supersonic aircraft, static pressure measuring holes will be found at varying distances from the end of the boom. The location of these holes usually has been determined experimentally to produce the closest approximation of free stream static pressure in supersonic flight.

6.14 OBLIQUE SHOCK WAVES

In the last paragraph on normal shocks, shock wave theory was presented, and the thermodynamic and kinematic changes that occurred when the flow traversed a normal shock were studied. Next, the changes that occur when flow passes through an oblique shock must be considered.

A normal shock is a special form of a pressure discontinuity in a fluid. In general, the discontinuities observed experimentally are inclined to the free stream velocity and are called oblique shocks.

Oblique shocks occur in supersonic flow because continuous compression waves caused by a concave, curved surface in the flow tend to merge, forming an oblique discontinuity at a finite distance from the surface.

When flow is forced to change direction suddenly at a sharp concave corner, an attached, oblique shock forms at the corner. Oblique shocks occur in almost all supersonic flow situations of practical interest, but the mere existence of supersonic flow does not imply that there must be shock waves somewhere in the flow.

Developing the relations between the fluid properties on the two sides of an oblique shock is not as formidable a task as it might seem, because many of the normal shock equations with a slight modification apply equally well to oblique shocks.

Suppose a stationary observer sees the flow at Station 1 suddenly decelerate and compress to the conditions at Station 2 because it has traversed a normal shock wave (Figure 6.9).

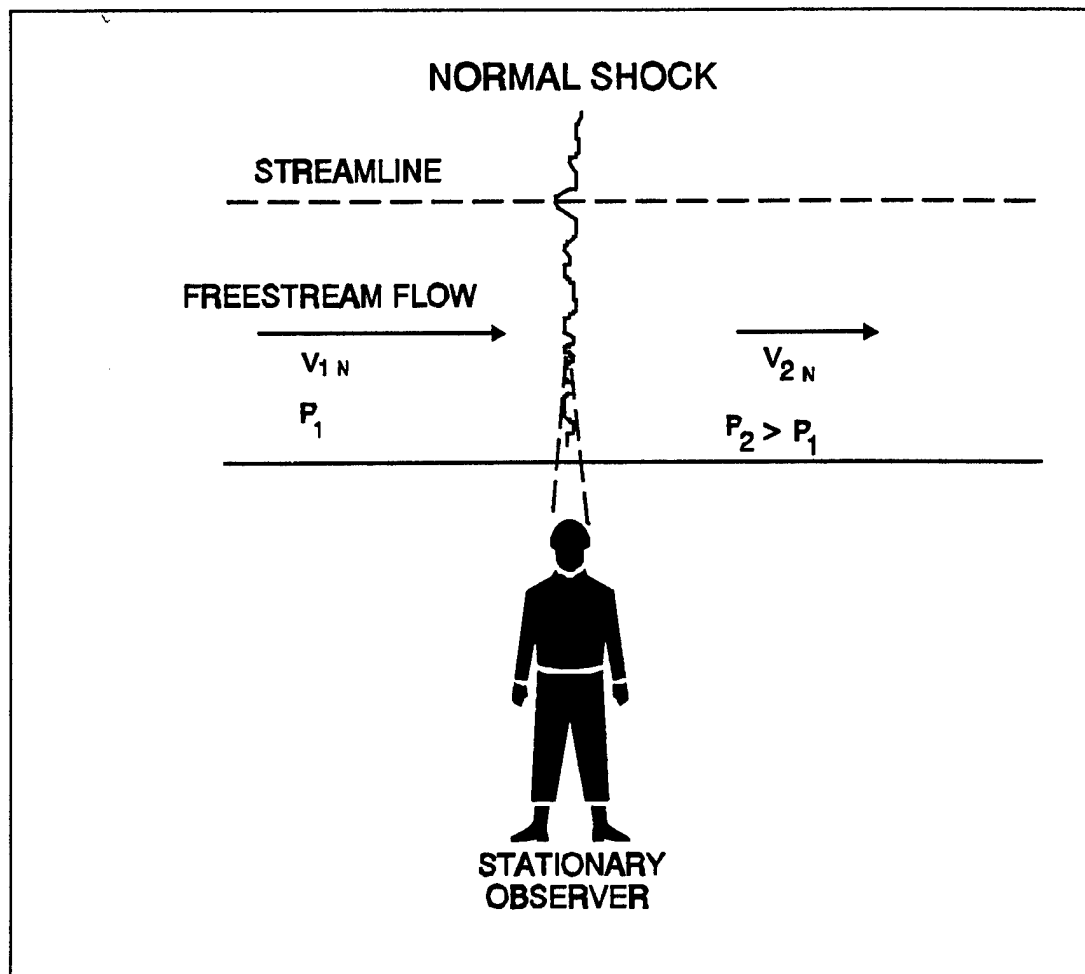


FIGURE 6.9 SHOCK PROCESS AS SEEN BY STATIONARY OBSERVER

Next, imagine that the observer moves along the shock wave with a velocity V_t . The moving observer would see a flow situation in which the shock is inclined to the free stream flow and in which the flow undergoes a sudden change in direction when it crosses the shock (Figure 6.10).

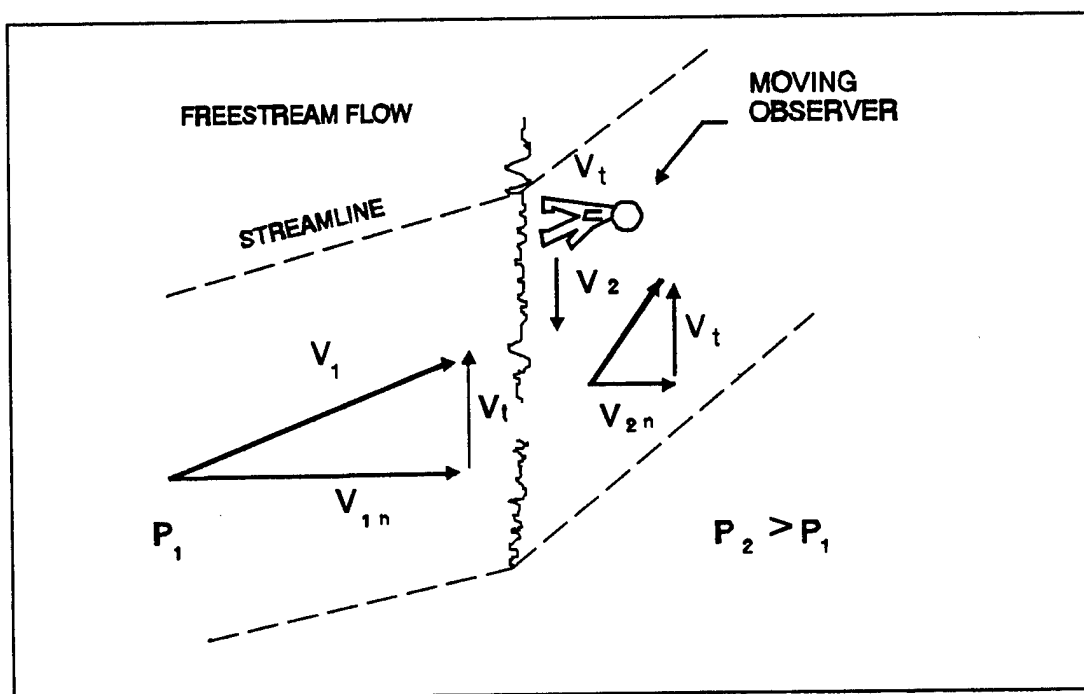


FIGURE 6.10 SHOCK PROCESS AS SEEN BY MOVING OBSERVER

The oblique flow pattern constructed in this manner has equal tangential velocity components, V_t , on both sides of the shock. By placing a solid wall along one of the streamlines in Figure 6.10 and rotating the picture so that incoming velocity, V_1 , is horizontal, the supersonic flow situation in the neighborhood of a concave corner is described (Figure 6.11).

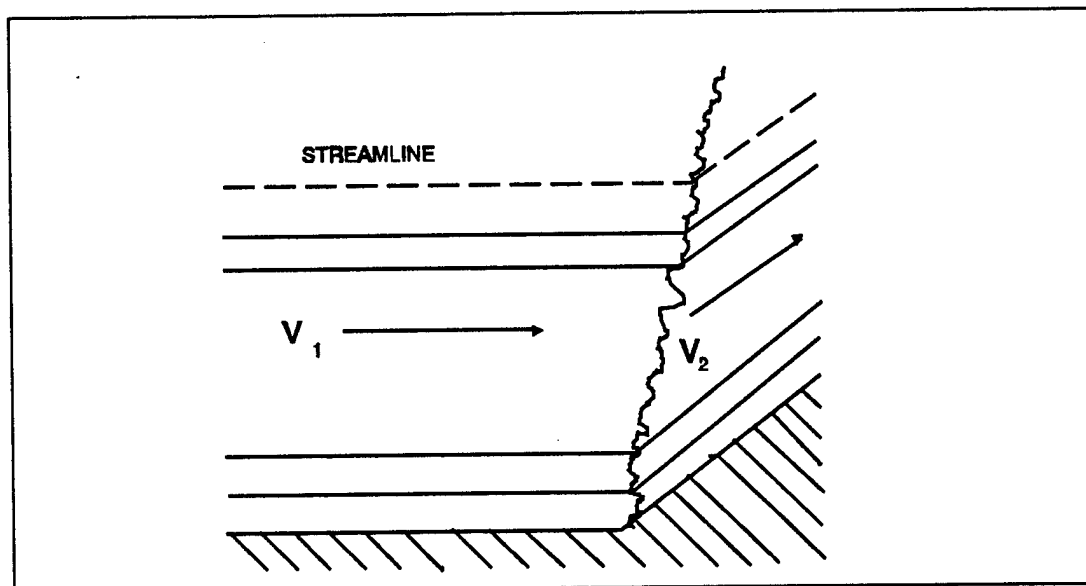


FIGURE 6.11 SUPERSONIC FLOW INTO A CORNER

By imparting a uniform velocity to the flow field along any shock, a straight segment of an oblique shock may be transformed into a normal shock. To fix this concept, consider the falling rain in Figure 6.12.

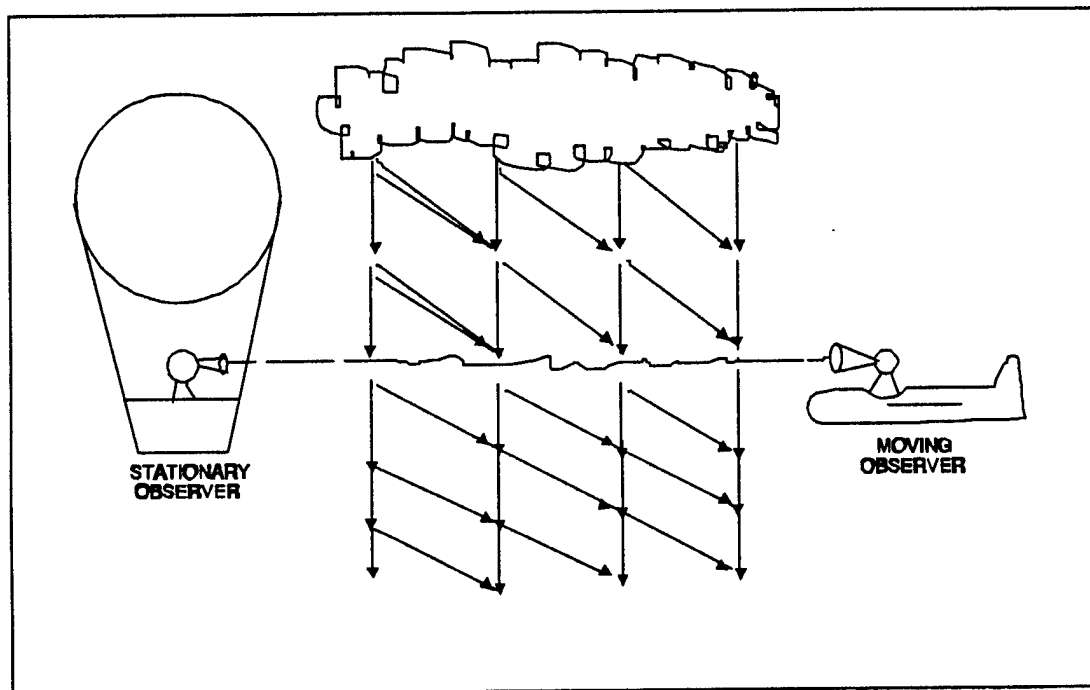


FIGURE 6.12 ANALOGY TO AID UNDERSTANDING OF OBLIQUE SHOCKS

Relative to an observer at rest, the rain is falling vertically. Relative to an observer moving perpendicular to the rainfall, the rain is descending at an angle.

Let the rain be slowed down instantaneously at some altitude. An observer in a balloon at this altitude sees the rain falling vertically and slowing down at this level as shown by the single lines in Figure 6.12. The pilot of an aircraft traveling with a horizontal velocity V_t at this altitude sees the path of the raindrops as though they were being deflected as they pass through this level (double lines in Figure 6.12). The pilot's observation is also correct, for relative to the aircraft the drops are being deflected. Essentially, the velocity of the aircraft has been superimposed upon the changing velocity of the raindrops.

A careful comparison of Figures 6.9 and 6.10 will show that the thermodynamic properties of P , ρ , T , a , and S are unchanged by the motion of the observer. On the other hand, V_1 , M_1 , P_T , and T_T are altered when the observer's motion V_t is superimposed on the normal shock flow situation.

The magnitude of V_t is arbitrary and depends upon the angle the oblique shock makes with the horizontal streamline in front of the shock and the velocity of the approaching flow. This presents an additional degree of freedom in the oblique shock relations.

An additional degree of freedom means that although only one independent parameter, i.e., approach Mach, M_1 , is required for normal shock relations, two independent parameters are required for oblique shock relations, i.e., M_1 and wave angle, θ .

6.14.1 OBLIQUE SHOCK RELATIONS

Since a shock appears to be normal or oblique depending upon the relative motion of the observer, the differences between normal and oblique shocks can be explained in geometric terms.

The flow orientation, flow notation, and angle descriptions used when modifying the normal shock equations are shown in Figure 6.13.

The number of degrees the flow must turn due to the concave corner is called the turning angle or wedge angle, δ . The angle the oblique shock makes with the incoming (upstream) streamlines is called the shock wave angle, θ . Conditions upstream of the oblique shock have the subscript 1, and conditions downstream have the subscript 2.

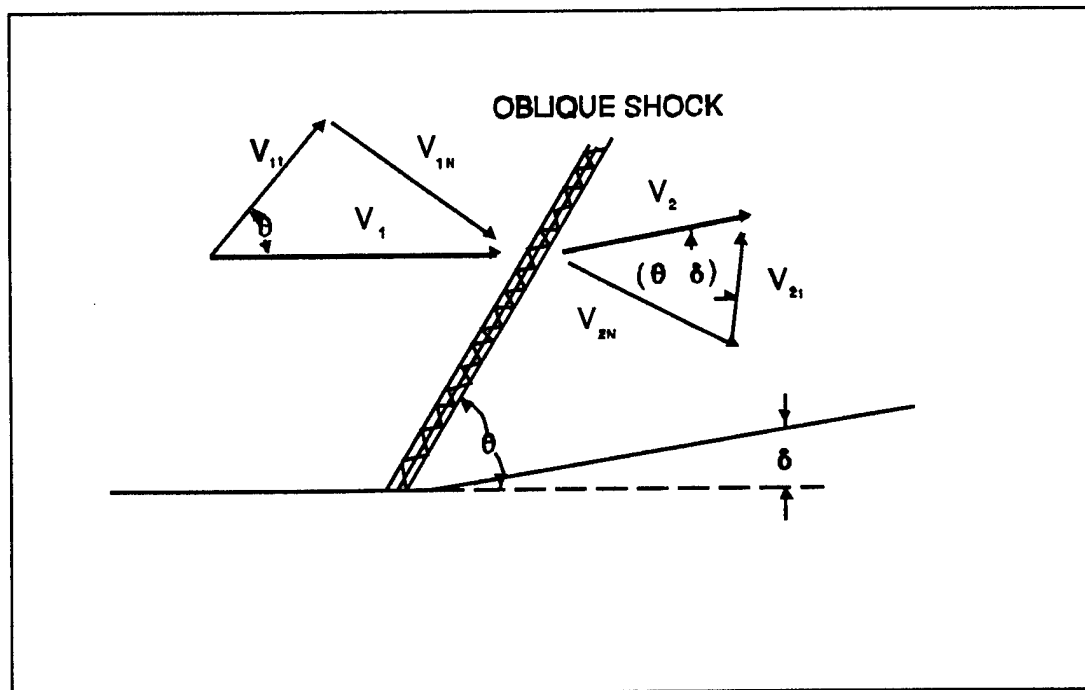


FIGURE 6.13 ANALYSIS OF VELOCITY COMPONENTS ACROSS AN OBLIQUE SHOCK

From this figure, it can be seen

$$M_{1N} = M_1 \sin \theta \quad (6.47)$$

where

M_1 = Flow Mach in front of an oblique shock

M_{1N} = Flow Mach in front of a normal shock

Consequently, all of the normal shock equations except those relating to total properties, can be modified to apply to oblique shocks by substituting $M_1 \sin \theta$ everywhere M_1 appears. The oblique shock equations are

$$\frac{P_2}{P_1} = \frac{1 - \gamma + 2\gamma M_1^2 \sin^2 \theta}{1 + \gamma} \quad (6.48)$$

$$\frac{P_2}{P_1} = \left[\frac{2 + (\gamma - 1) M_1^2 \sin^2 \theta}{(\gamma + 1) M_1^2 \sin^2 \theta} \right]^{\frac{1}{\gamma}} \quad (6.49)$$

$$\frac{T_2}{T_1} = \left[\frac{2\gamma M_1^2 \sin^2 \theta - \frac{\gamma - 1}{\gamma + 1}}{\frac{\gamma - 1}{\gamma + 1}} \right] \left[\frac{\gamma - 1}{\gamma + 1} + \frac{2}{(\gamma + 1) M_1^2 \sin^2 \theta} \right] \quad (6.50)$$

$$M_2^2 \sin^2(\theta - \delta) = \frac{M_1^2 \sin^2 \theta + \frac{2}{\gamma - 1}}{\frac{2\gamma M_1^2 \sin^2 \theta - 1}{\gamma - 1}} \quad (6.51)$$

$$\frac{P_{r_2}}{P_{r_1}} = \left[\frac{1}{\left[\frac{\gamma - 1}{\gamma + 1} + \frac{2}{(\gamma + 1) M_1^2 \sin^2 \theta} \right] \left[\frac{2\gamma M_1^2 \sin^2 \theta - \frac{\gamma - 1}{\gamma + 1}}{\gamma - 1} \right]} \right]^{\frac{1}{\gamma - 1}} \quad (6.52)$$

6.14.2 MINIMUM AND MAXIMUM WAVE ANGLES

In the normal shock analysis, it was found that a shock can only occur when the free stream Mach is greater than one. The same is true for oblique shocks; the free stream Mach component normal to the shock must be greater than one.

The minimum wave angle for a given free stream Mach of $M_1 > 1$ can be found from Equation 6.47

$$M_{1N} = M_1 \sin \theta = 1$$

or

$$\theta_{(Min)} = \sin^{-1} \frac{1}{M_1} \quad (6.53)$$

Notice that the minimum oblique shock wave angle, $\theta_{(Min)}$, for the given free stream Mach, M_1 , is the same as the Mach angle, μ , (Equation 6.20) formed by an isentropic pressure disturbance traveling at $M_1 > 1$.

This shows that an oblique shock wave at minimum wave angle to the free stream flow is a zero strength or isentropic shock. This lends additional credence to our one-dimensional flow assumption, for gentle turns.

The maximum oblique shock wave angle for a given free stream Mach is 90° . This is the limiting case and is a normal shock.

6.14.3 RELATION BETWEEN θ AND δ

From Figure 6.13

$$\tan \theta = \frac{V_{1N}}{V_{1t}}$$

Eliminating V_{1t} from these equations, (since $V_{1t} = V_{1t}$) then using the continuity equation, Equation 6.49, and a great amount of algebraic and trigonometric manipulation:

$$\frac{\tan(\theta - \delta)}{\tan \theta} = \frac{(\gamma - 1)M_1^2 \sin^2 \theta + 2}{(\gamma + 1)M_1^2 \sin^2 \theta} \quad (6.54)$$

For a given M_1 , Equation 6.54 is an implicit relation between θ and δ . It may be rewritten to show the dependence of δ explicitly (after much trigonometric manipulation).

$$\tan \delta = 2 \cot \theta \frac{M_1^2 \sin^2 \theta - 1}{M_1^2 (\gamma + \cos 2 \theta) + 2} \quad (6.55)$$

This equation may be solved for various combinations of Mach, M_1 , and wave angle,

θ , and plotted as in Figure 6.14.

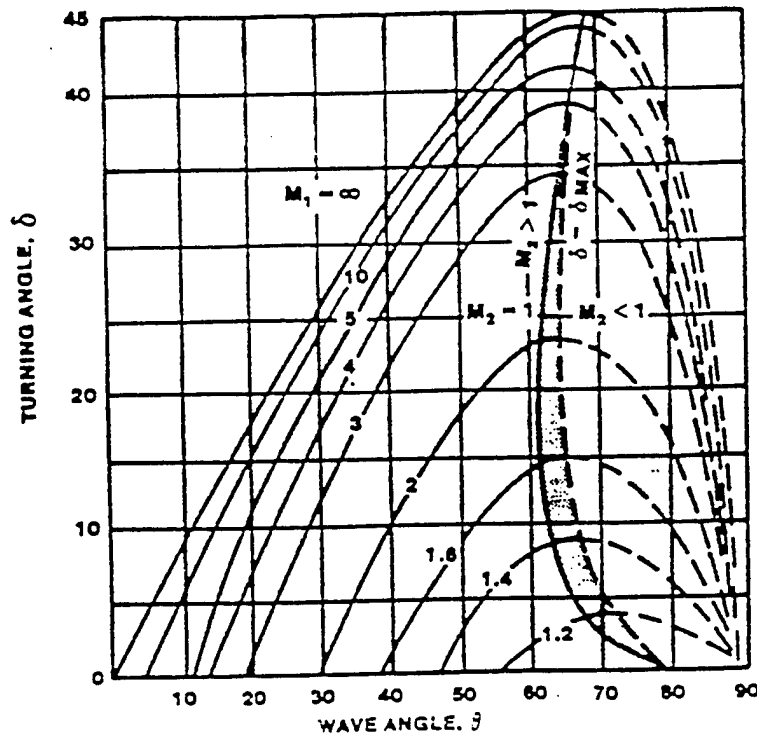


FIGURE 6.14 TURNING ANGLE AS A FUNCTION OF WAVE ANGLE FOR FLOW THROUGH AN OBLIQUE SHOCK

Careful study of this figure will reveal several points of great interest when analyzing the flow through an oblique shock wave.

The existence of a maximum and minimum wave angle is verified by the fact that

Equation 6.55 becomes zero at $\theta = \pi/2$ and at $\theta = \sin^{-1} 1/M_1$.

The turning angle, δ , has a maximum value for a given value of M_1 . Turning angles larger than this maximum angle cause the oblique shock to detach from the surface at the concave corner. If δ is less than δ_{\max} , an attached oblique shock will form.

There are two possible oblique shock solutions for a given turning angle, δ , and a given M_1 . The weak shock solution is represented by the solid lines in Figure 6.14, and the strong shock solution by the dotted lines.

The strong shock solution (the oblique shock with the greater wave angle) is characterized by subsonic flow downstream of the shock and by large energy losses in the shock. As a general rule, systems in nature tend to minimize their losses; therefore the weak shock occurs more frequently. However, there is no known mathematical law which predicts the type of shock that will occur for a given free stream Mach and a given turning angle. The locus of points for which the Mach behind the shock, M_2 is equal to one is also plotted. It can be seen that the Mach downstream of a weak shock is usually supersonic, but in a small region (cross-hatched) near δ_{\max} for a given free stream Mach, the Mach downstream of a weak shock can be subsonic.

The wave angle, θ , is generally the unknown quantity in analytical work and is conventionally plotted versus M_1 for different turning angles, (Figure 6.15).

From this figure, three important points can be noted:

1. There is a minimum allowable flow Mach for a given turning angle, below which the oblique shock will detach from the surface.
2. The wave angle of a weak shock decreases with increased free stream Mach, while the wave angle of a strong shock increases (approaching 90 degrees) with increasing Mach.
3. For a given free stream Mach, the wave angle θ approaches the mach angle as δ is decreased.

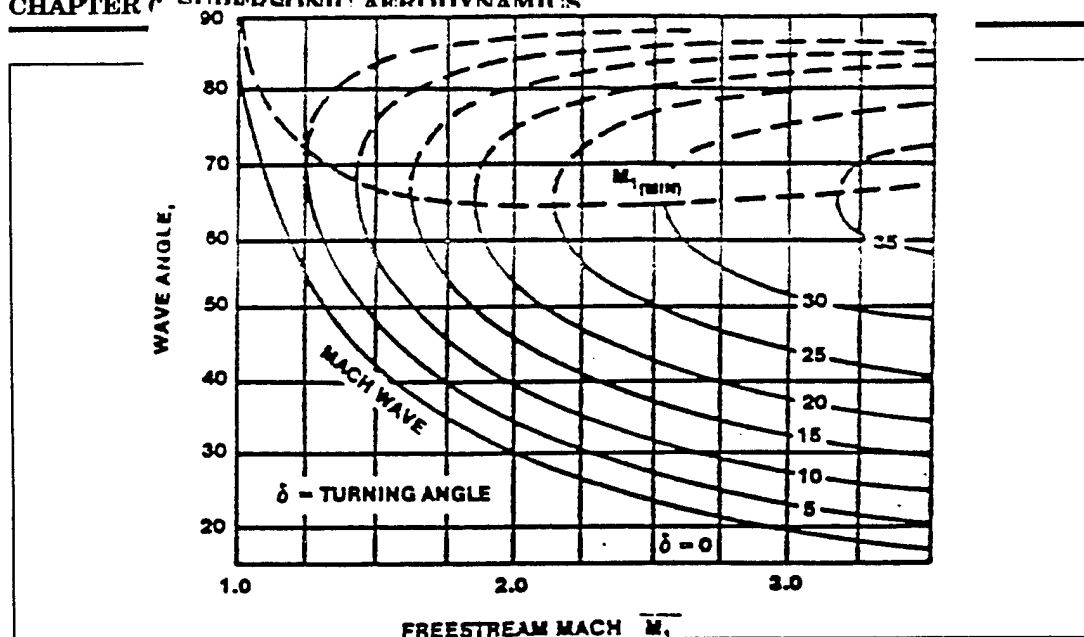


FIGURE 6.15 WAVE ANGLE AS A FUNCTION OF MACH FOR FLOW THROUGH AN OBLIQUE SHOCK

Because of the complexity of the equations for normal and oblique shock waves, it is common practice to use tables or charts of their solutions when solving a compressible flow problem. An excellent set of charts is in reference 6.4.

6.14.4 MACH LINES

Considering that portion of figure 6.14 where $M_2 > 1$, a decrease in turning angle δ corresponds to a decrease in wave angle θ . When δ becomes zero, θ reaches the limiting value given by equation 6.53 which was previously shown to be the Mach angle μ (equation 6.20).

$$\theta_{\min} = \sin^{-1} \frac{1}{M_1} = \mu \quad (6.53)$$

Analyzing the strength of the oblique shock formed at zero turning angle, with the oblique shock relations, Equations 6.48 through 6.52, it can be seen that the so-called "shock" has zero strength, or that no physical discontinuity in the supersonic flow exists.

For any point in a supersonic flow, there is a characteristic angle associated with the Mach of the flow at that point. This angle is the Mach angle μ . Lines drawn at an inclination of μ at a point in the flow are called Mach lines or sometimes Mach waves.

6.15 ISENTROPIC COMPRESSION

A shock wave compresses supersonic flow by increasing the pressure and density of the fluid in a very short but finite distance. A simple method to compress supersonic flow is to deflect the flow boundary into the flow through an angle, thereby creating an oblique shock wave through which the flow must pass.

By dividing the total boundary deflection into several small segments of $\Delta\delta$, the compression can be visualized as occurring through several successive oblique shocks which divide the flow field near the boundary into segments of uniform flow (Figure 6.16).

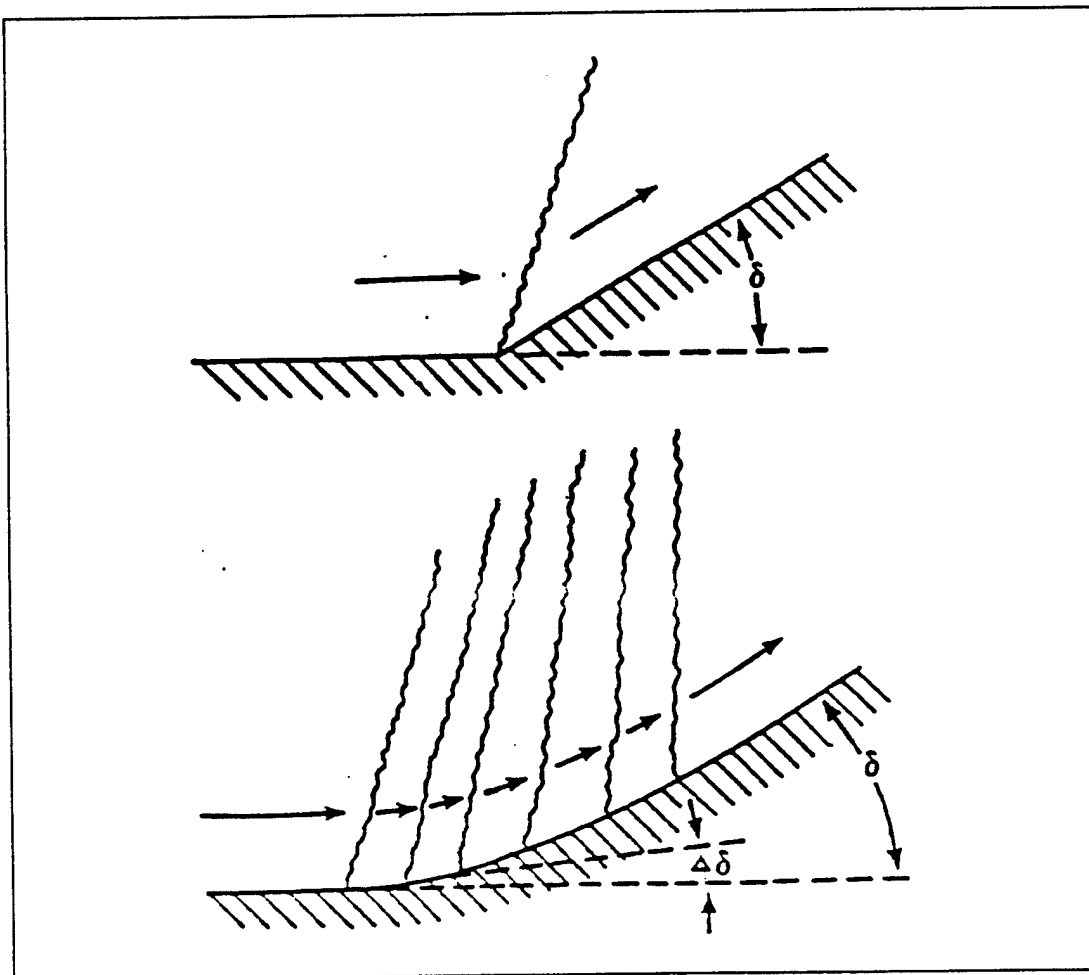


FIGURE 6.16 ISENTROPIC COMPRESSION

In each region between oblique shocks, the supersonic flow is independent of the regions upstream and downstream, making it possible to analyze the flow field region by region. Using the approximate equation for weak shocks to compare the one shock

compression to the multi-shock compression, it can be shown that for each wave

$$\Delta P \approx \Delta \delta$$

$$\Delta S \approx (\Delta \delta)^3$$

If there are n segments being considered in the complete turning angle then

$$\delta = n\Delta\delta$$

and

$$\Delta P_{TOTAL} \approx n\Delta\delta \approx \delta$$

$$\Delta S_{TOTAL} \approx n(\Delta\delta)^3 \approx n\Delta\delta(\Delta\delta)^2 \approx \delta(\Delta\delta)^2$$

Thus, if a large number of weak waves cause the compression, the entropy increase is reduced drastically compared to a one shock compression for the same total turning angle.

By making $\Delta\delta$ smaller and smaller, a smooth turn with $\Delta\delta \rightarrow 0$ is created in the limit, the entropy increase becomes zero, and the compression can be considered isentropic.

This limiting process produces the following results:

1. The oblique shocks approach zero strength and become straight Mach lines.
2. Each region of uniform flow approaches the width of a Mach line; thus on each Mach line the flow inclination and Mach are constant.

3. The flow upstream of each Mach line is not affected by downstream changes in the wall.

4. The approximate equations for changes in properties across weak waves may be written in differential form, i.e., ΔP becomes dP .

The above discussion considers flow near the boundary of the supersonic flow field. Farther away from the wall, due to the convergence of Mach lines, the flow is no longer isentropic, and the Mach lines converge, forming an oblique shock wave.

6.16 ISENTROPIC COMPRESSION

When the boundary of a supersonic flow is deflected into the flow, the flow is compressed. If the deflection is abrupt, an oblique shock wave forms in the corner. If the deflection is smooth, an isentropic analysis of the compression may be performed.

What happens when the boundary is deflected away from the supersonic flow? If a single oblique shock wave formed and the flow expanded through it, this would require that the normal component of velocity after the shock be greater than the normal component of velocity ahead of this shock, i.e., an increase in velocity through the shock (Figure 6.17). This is in direct violation of the second law of thermodynamics because it demands a decrease in entropy (refer to Appendix F, Derivation F.7), even though the equations of motion are satisfied.

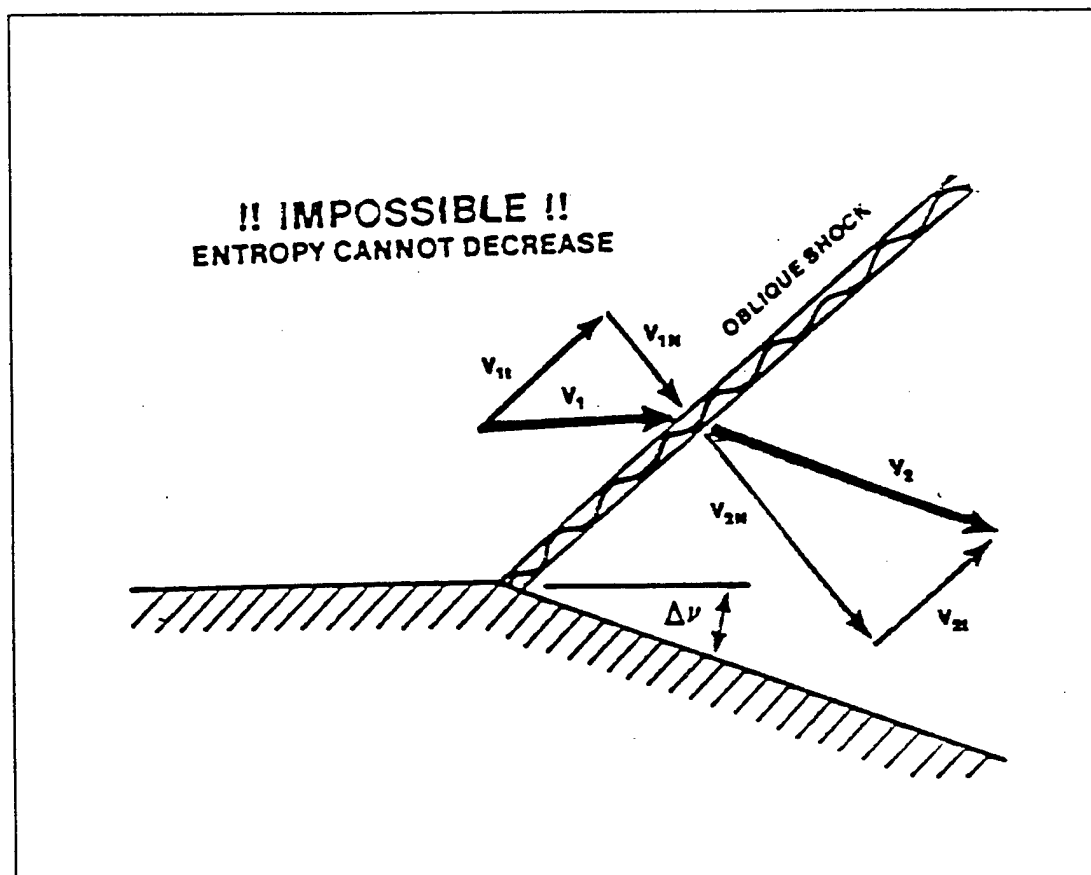


**FIGURE 6.17 IMPOSSIBILITY OF SHOCK FORMATION FLOW
TURNING AWAY FROM ITSELF**

Actually, the same nonlinear effect that makes Mach lines converge in a compression makes the Mach lines diverge in an expansion, and the supersonic expansion is an isentropic phenomenon throughout.

Consider the expansion of supersonic flow caused by the boundary deflection $\Delta\delta$ in Figure 6.18a.

If P_2 is less than P_1 , the disturbances from the lower pressure will be transmitted out into the stream.

The pressure P_2 will not be transmitted upstream since the flow is supersonic, and it will only be felt as far upstream as the Mach line extending out from the corner into the flow.

When the flow passes this Mach line, it will sense the lower pressure and will tend to turn and accelerate because of the pressure differential. Associated with the flow

velocity increase is a pressure decrease which changes the flow properties immediately following the Mach line and consequently defines a new Mach line upstream of which the influence of P_2 cannot be felt. Hence, the flow gradually increases velocity and changes direction through an infinite number of these Mach lines, forming a fan shaped array referred to as a "Prandtl-Meyer expansion fan" as shown in Figure 6.18b.

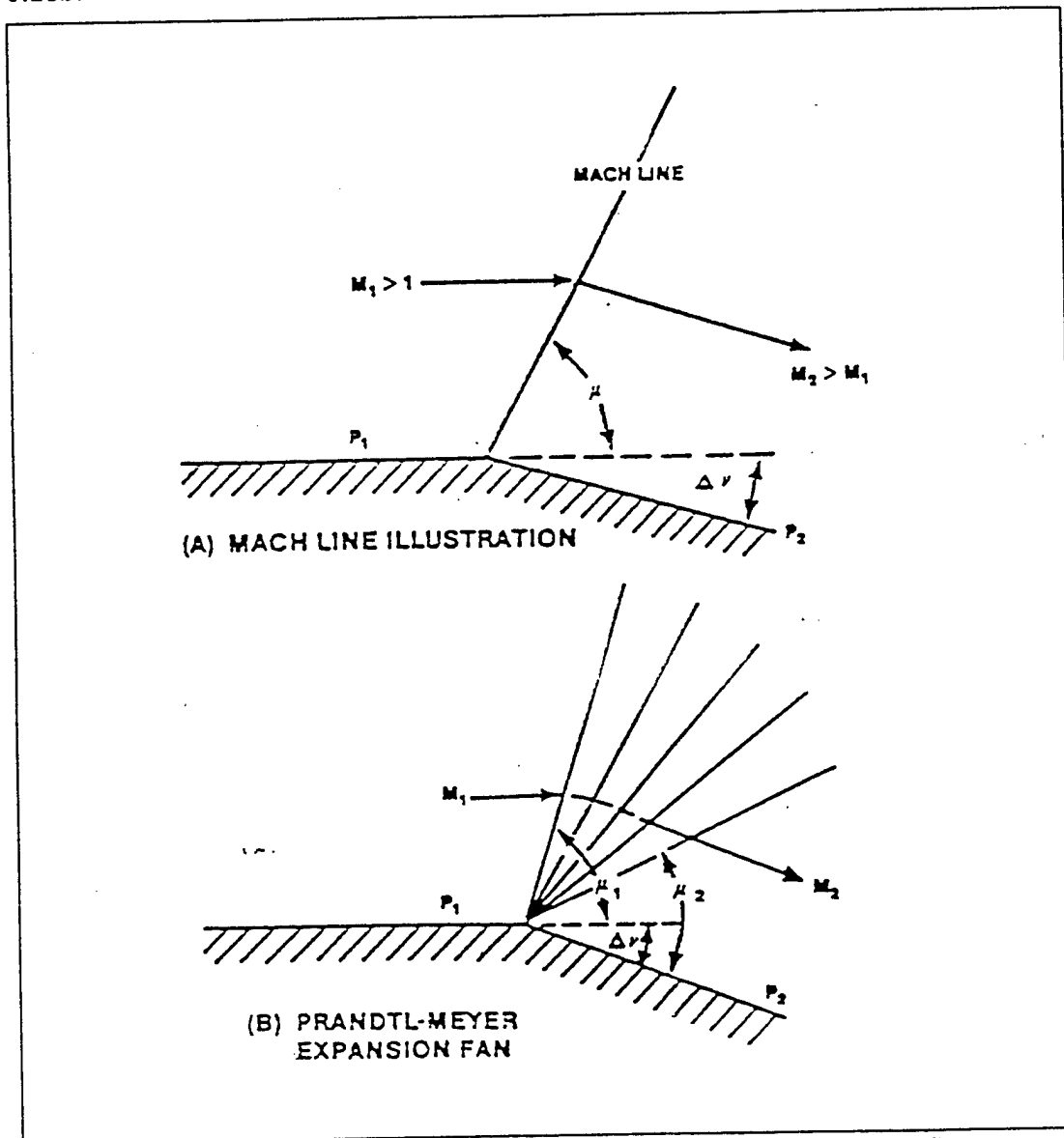


FIGURE 6.18 SUPERSONIC FLOW AROUND A CORNER

As the Mach increases through the first line and the pressure decreases, the approach of subsequent pressure signals is altered slightly by the increased Mach, thus causing the next Mach wave to be more inclined to the free stream. The Mach angle

calculated for the last Mach line is that calculated from the final Mach, M_2 , after the turn.

Supersonic expansion occurs not only at abrupt corners but also on smooth surfaces. In this case, the fan is distributed over the entire curve as shown in Figure 6.19.

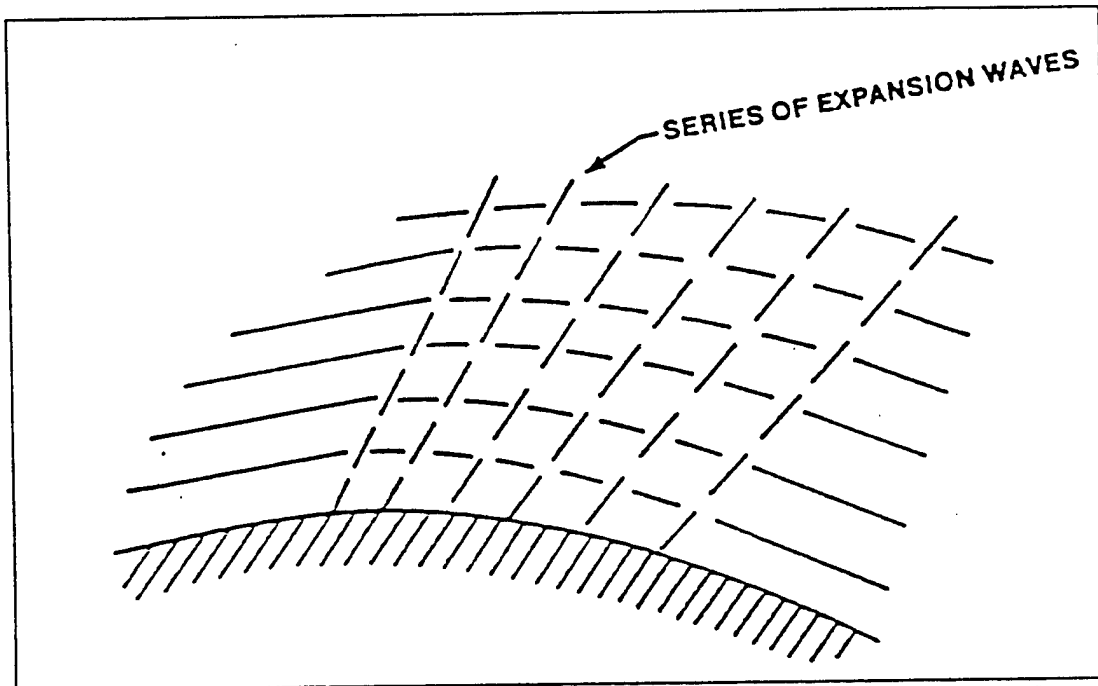


FIGURE 6.19 SUPERSONIC FLOW AROUND A SMOOTH CORNER
(6.2:212)

Further insight into the reason for the finite distance required to accelerate the flow around the corner might be gained from a physical interpretation of the acceleration itself. An instantaneous change in velocity and direction around the corner would mean that there was an infinite acceleration for a given mass of fluid. But from Newton's law, $F = ma$, an infinite acceleration requires an infinite force or pressure gradient, and no such source of energy is present; therefore the acceleration cannot be instantaneous. The equation

$$\frac{\Delta V}{V} = + \frac{\Delta v}{\sqrt{M_1^2 - 1}}$$

is an approximate expression relating the velocity change through an isentropic Mach wave to incoming Mach, M_1 , and expansion angle, Δv . Derivation of this equation is tedious and will be omitted. It may be found in many aerodynamic textbooks on

supersonic flow.

For small values of Δv and ΔV , Equation 6.56 may be written in differential form

$$+dv = \sqrt{M^2 - 1} \frac{dV}{V}$$

and integrated

$$+v + \text{const} = \int \sqrt{M^2 - 1} \frac{dV}{V} = v(M)$$

To evaluate the integral and thus find an explicit form of $v(M)$, V must be rewritten in terms of M using the following relationships

$$V = aM$$

$$\frac{a_1^2}{a^2} = \frac{\gamma R T_T}{\gamma R T} = \frac{T_T}{T} = T = 1 + \frac{\gamma - 1}{2} M^2$$

from which

$$\frac{dV}{V} = \frac{dM}{M} + \frac{da}{a} = \frac{dM}{M} \left[\frac{1}{1 + \frac{\gamma - 1}{2} M^2} \right]$$

therefore

$$v(M) = \int_{M_{\text{initial}}}^{M_{\text{final}}} \frac{\sqrt{M^2 - 1}}{\left(1 + \frac{\gamma - 1}{2} M^2\right) M} dM = v_{\text{final}} - v_{\text{initial}}$$

This integral may be evaluated between two Mach numbers and is called the Prandtl-Meyer function

$$v(M) = \sqrt{\frac{\gamma+1}{\gamma-1}} \tan^{-1} \sqrt{\frac{\gamma-1}{\gamma+1} (M^2-1)} - \tan^{-1} \sqrt{M^2-1}$$

To simplify analysis the constant of integration was chosen such that $v_{\text{init}} = 0$ when $M_{\text{init}} = 1$. Thus, for every supersonic Mach there is a corresponding angle v which represents the angle through which a flow that is initially at Mach 1 must turn to achieve that supersonic Mach.

6.16.1 SUPERSONIC INITIAL CONDITIONS

If M_1 prior to turning is greater than Mach 1, the associated v_1 is greater than zero. To find the Mach following a turn through an angle Δv , it is necessary to add Δv to the v corresponding to M_1 and find the final Mach, M_2 , corresponding to v . In equation form, this may be written

$$v_2 = v_1 + |\Delta v| \quad (6.58)$$

where Δv is the turning angle shown in Figure 6.18a. Absolute values of Δv are used to avoid any confusion associated with the sign of the turning angle.

Tables for solving two-dimensional isentropic expansion problems may be found in Reference 6.4 and Figure 6.20 outlines the method to be used. Once the Mach after expansion is known, all of the supersonic flow properties may be calculated from isentropic relations.

Consider the problem of $M_1 = 2$ flow expanding through an angle of 24° . What is the Mach after the turn? Enter Figure 6.20 with $M_1 = 2$ and find $v_1 = 26^\circ$. This is the angle $M_1 = 1$ flow must turn through to reach a value of Mach two. Adding $v_1 + \Delta v$ and reentering the figure at this value of 50° , M_2 can be found to have a value of Mach three.

6.16.2 MAXIMUM TURNING ANGLE

If the Mach in Equation 6.57 goes to infinity, which corresponds to expanding supersonic flow to zero pressure, the maximum turning angle is obtained

$$v_{\max} = \frac{\pi}{2} \left[\sqrt{\frac{\gamma+1}{\gamma-1}} - 1 \right] \quad (6.59)$$

Thus a flow that is initially at Mach 1 can turn 130.5° . But a stream that is initially at 2.5 Mach can turn only 90° . The higher the initial Mach, the lower the turning capability. Using Equations 6.58 and 6.59, an expression for the turning capability, v_{tc} , of the flow can be obtained.

$$v_{tc} = v_{\max} - v_1$$

Attention is called to the fact that these are the theoretical angles at which the flow will leave the surface for any initial Mach and that very high deflection angles are indicated at all Mach. In practice, real fluid effects such as boundary layer and viscosity will greatly reduce the angle at which the flow will leave the surface.

Table 6.1 summarizes the characteristics of the three wave forms encountered in supersonic flow.

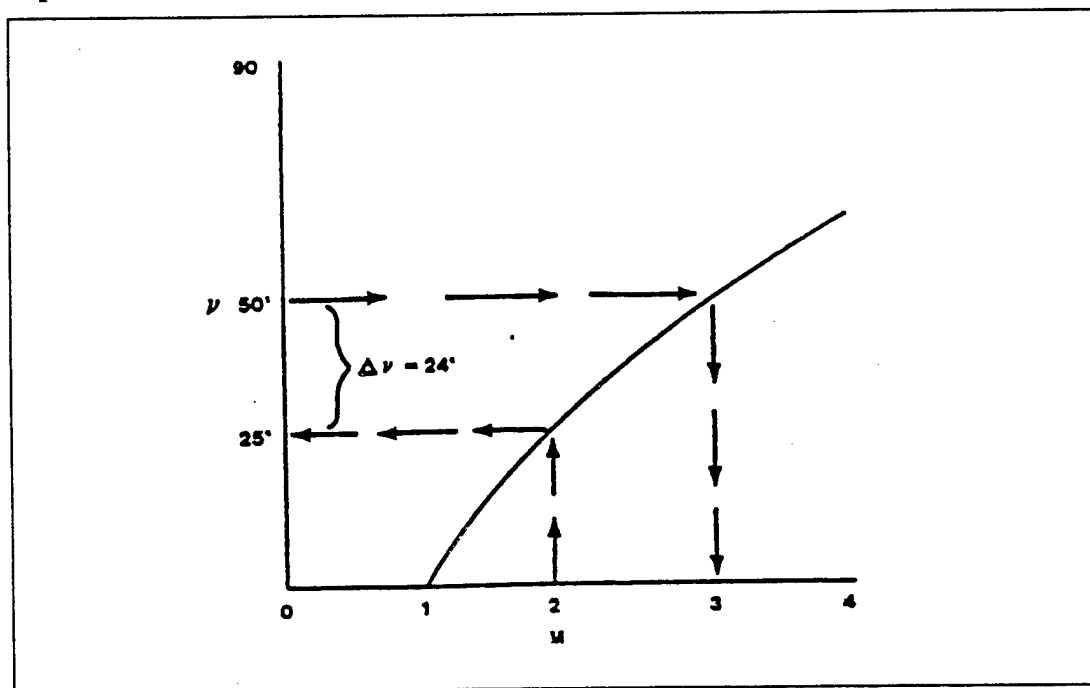


FIGURE 6.20 TURNING ANGLE AS A FUNCTION OF MACH FOR PRANDTL-MEYER FLOW

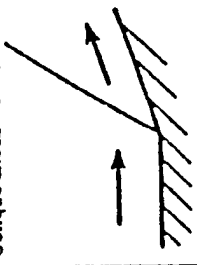
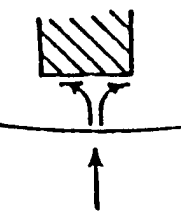
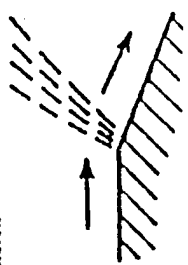
Type of wave formation	Oblique shock wave	Normal shock wave	Expansion wave
			
Flow direction change	"Flow into a corner," turned into preceding flow.	No change	"Flow around a corner," turned away from pre- ceding flow.
Effect on velocity and Mach.	Decreased but still super- sonic	Decreased to subsonic	Increased to higher super- sonic
Effect on static pressure and density.	Increase	Great increase	Decrease
Effect on total pressure.	Decrease	Great decrease	No change (no shock).

TABLE 6.1 SUPERSONIC WAVE CHARACTERISTICS (6.2:213)

6.17 INTERACTION OF WAVE FORMS

Successive oblique wave forms may interfere with one another. Four cases are possible:

1. Expansion followed by expansion
2. Compression followed by compression
3. Compression followed by expansion
4. Expansion followed by compression

This discussion is limited to two-dimensional analysis.

Case one is most easily analyzed because there are no interference effects. This can be seen with reference to Figure 6.21. The final effect is equivalent to flow over a rounded corner with the same total deflection angle.

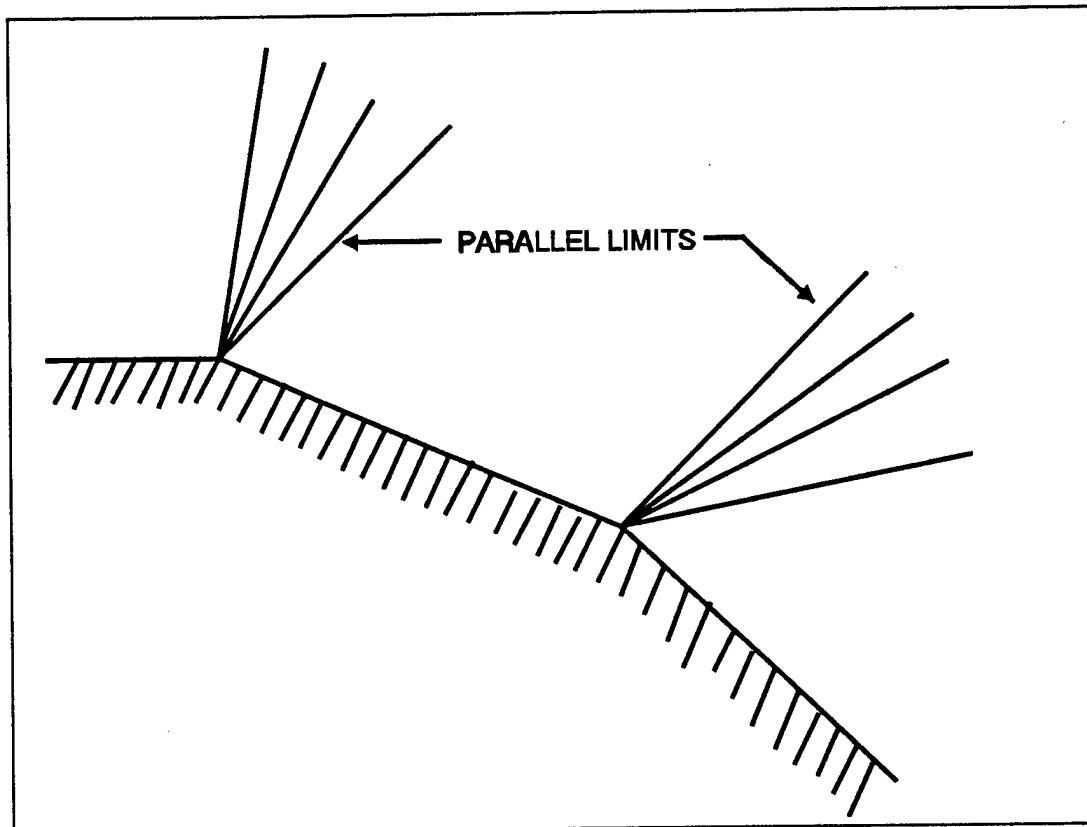


FIGURE 6.21 TWO EXPANSIONS (6.5.132)

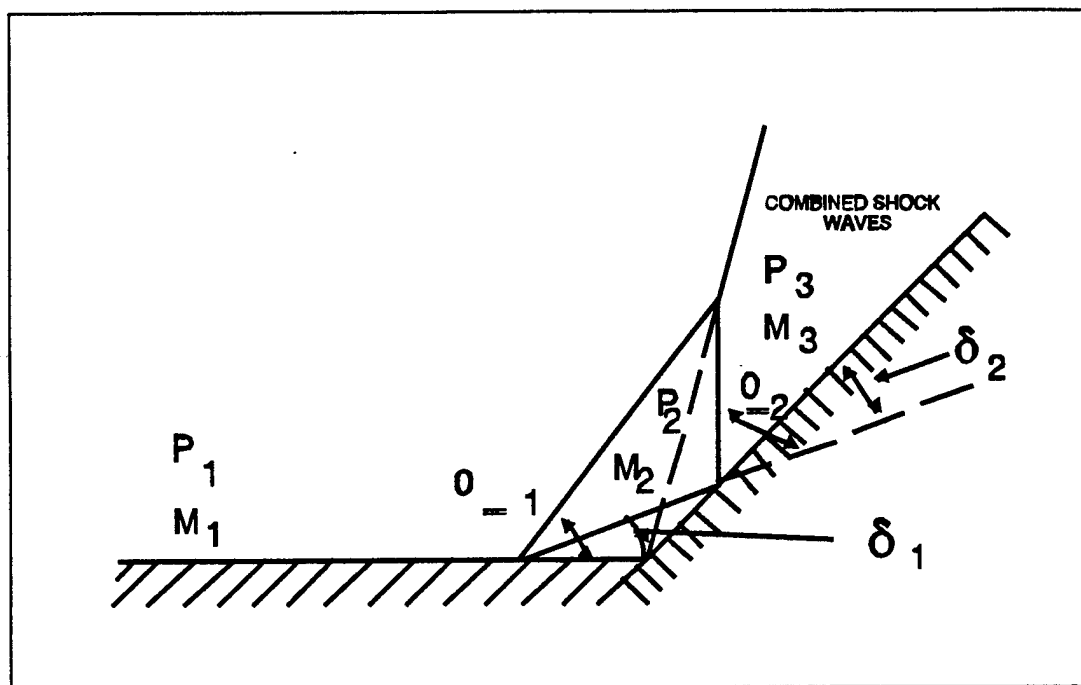
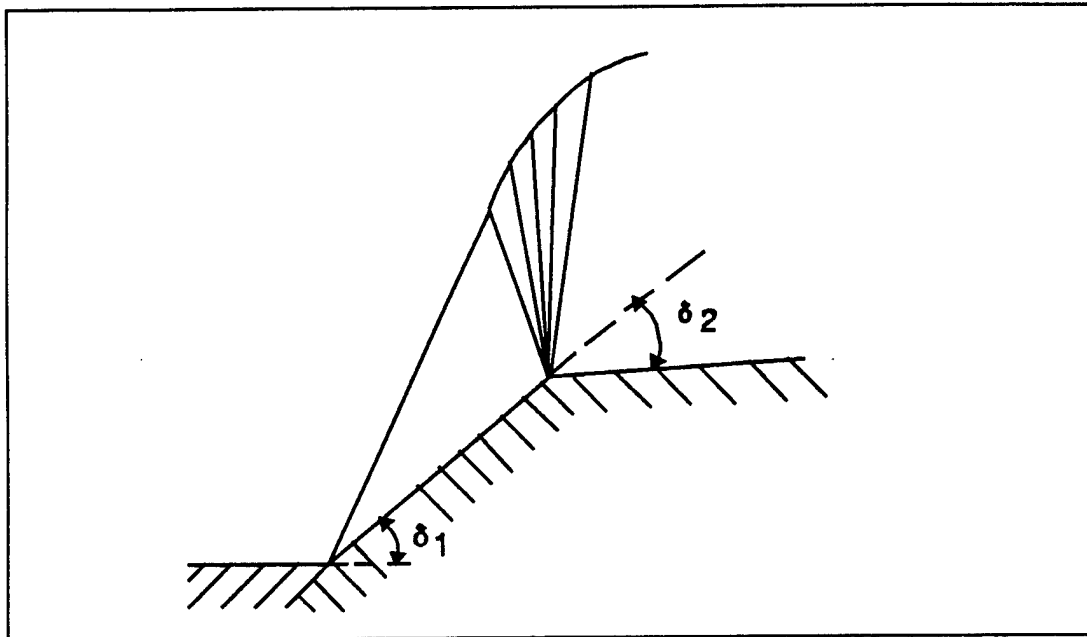


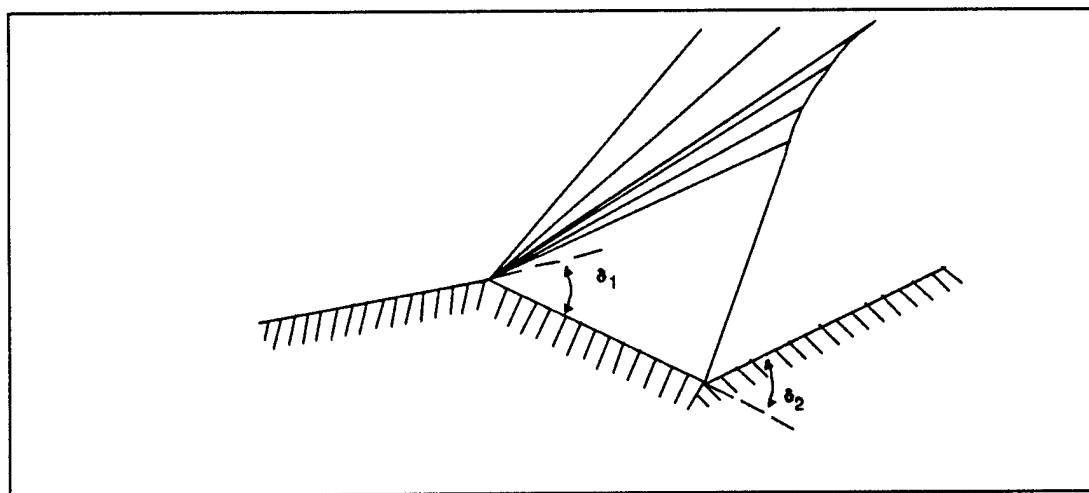
FIGURE 6.22 TWO COMPRESSIONS (6.5.133)

When one oblique shock is followed by another, as in Figure 6.22, interaction must occur and results in a single shock of increased intensity at some distance away from the wall. Recall that the Mach after an oblique shock is always decreased and the flow is bent toward the wave. A second oblique shock generated behind the first with a subsequent second change in flow direction increases the shock wave angle because of the reduction in stream velocity, and the wave will be tilted toward the first oblique shock due to the initial deflection. Therefore, the two shock lines must intersect. The intersection of the two separate waves must form a wave which has the same angle as that applying to a wave formed by a single intersection of the initial and final surfaces. The wave formed by the combination is therefore stronger than either one alone.

If we have an oblique shock followed by an expansion, we must also have an intersection. Because of the nature of expansion waves, the intersection will be a diffuse effect which tends to weaken the shock at points away from the surface. Because the velocity of the wave is dependent upon its intensity, the weakening effect in the regions away from the surface will reduce the propagation velocity and cause the oblique shock wave front to bend as illustrated in Figure 6.23.

**FIGURE 6.23 SHOCK FOLLOWED BY EXPANSION (6.5:134)**

The case of expansion followed by compression is very similar to the case just discussed. Intersection with a weakening of the shock wave must occur. The details of the intersection are different because the intersection occurs on the free stream side of the shock instead of in the reduced velocity region behind the shock. Intersection cannot be avoided because the shock wave stands at a higher angle with respect to the expanded flow lines than do some or all of the local Mach lines at the expansion corner. This case is illustrated in Figure 6.24 (6.5.132-136).

**FIGURE 6.24 EXPANSION FOLLOWED BY SHOCK (6.5:135)**

6.18 TWO-DIMENSIONAL SUPERSONIC AIRFOILS

In order to appreciate the effect of these various wave forms upon aerodynamic characteristics in supersonic flow, refer to Figure 6.25. Parts a and b show the wave pattern and resulting pressure distribution for a thin flat plate at a positive angle of attack. The airstream moving over the upper surface passes through an expansion wave at the leading edge and an oblique shock at the trailing edge. Therefore, a uniform suction pressure exists over the upper surface. The airstream moving underneath the flat plate passes through an oblique shock wave at the leading edge and an expansion wave at the trailing edge. Therefore, a uniform positive pressure exists on the underside of the section (shock losses). This pressure distribution produces a net lift and also a drag due to lift. The drag is analogous to induced drag in subsonic flow but is not a function of downwash as is the case in subsonic flow. Remember that pressure disturbances cannot be transmitted ahead of an object in supersonic flow, so the fluid is not aware of the approaching object.

The flat plate, although aerodynamically quite efficient at supersonic speeds, is not structurally satisfactory. It is difficult to give it enough strength to withstand the loads imposed on the airfoil during high speed flight.

Parts c and d of Figure 6.25 show the wave pattern and pressure distribution for a double wedge airfoil at zero lift. The resulting pressure distribution on the surfaces of the double wedge produces no net lift, but the increased pressure on the forward half along with the decreased pressure on the rear half of the section produces wave drag. This wave drag is a result of the components of the pressure forces which are parallel to the free stream direction, and can be a large portion of the total drag at high supersonic speeds.

Parts e and f of Figure 6.25 illustrate the wave pattern and resulting pressure distribution for the double wedge airfoil at a small positive angle of attack. The net pressure distribution produces drag due to lift in addition to the wave drag at zero lift. Similarly, parts g and h show the wave pattern and pressure distribution for a circular arc airfoil (also called a bi-convex airfoil) at a small angle of attack.

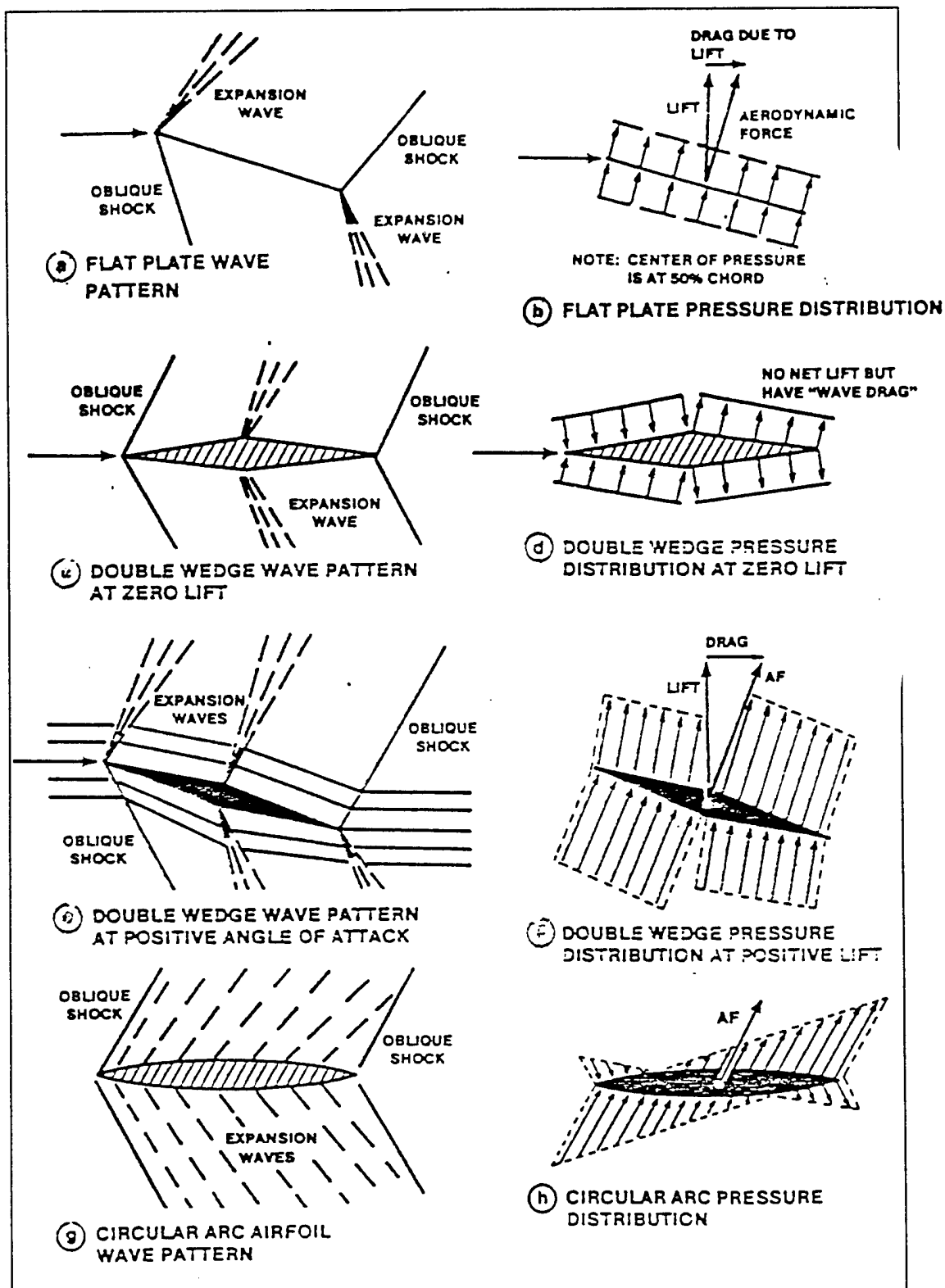


FIGURE 6.25 SUPERSONIC FLOW PATTERN AND DISTRIBUTION OF PRESSURE (6.1:163, 165; 6.2:214)

6.19 PRESSURE COEFFICIENT FOR TWO-DIMENSIONAL SUPERSONIC AIRFOILS AND INFINITE WINGS

The preceding paragraphs on the different supersonic waveforms have developed all of the mathematical tools required to compute the lift and drag on a simple two-dimensional supersonic airfoil. Consider the double wedge or diamond airfoil shown in Figure 6.26.

If the flight Mach, M_∞ , remote ambient pressure, P_∞ , angle of attack, α , and the geometry of the wing are known, pressures in areas 2, 3, 5, and 6 can be computed. Oblique shock relationships can be used to determine P_2 and P_5 from P_∞ , and Prandtl-Meyer relations can be used to determine P_3 and P_6 from P_2 and P_5 . Once these pressures are known, lift and drag can be readily determined from geometric relationships.

This problem can be attacked in a more systematic manner by recalling the definition of pressure coefficient

$$C_p \equiv \frac{P - P_\infty}{q_\infty}$$

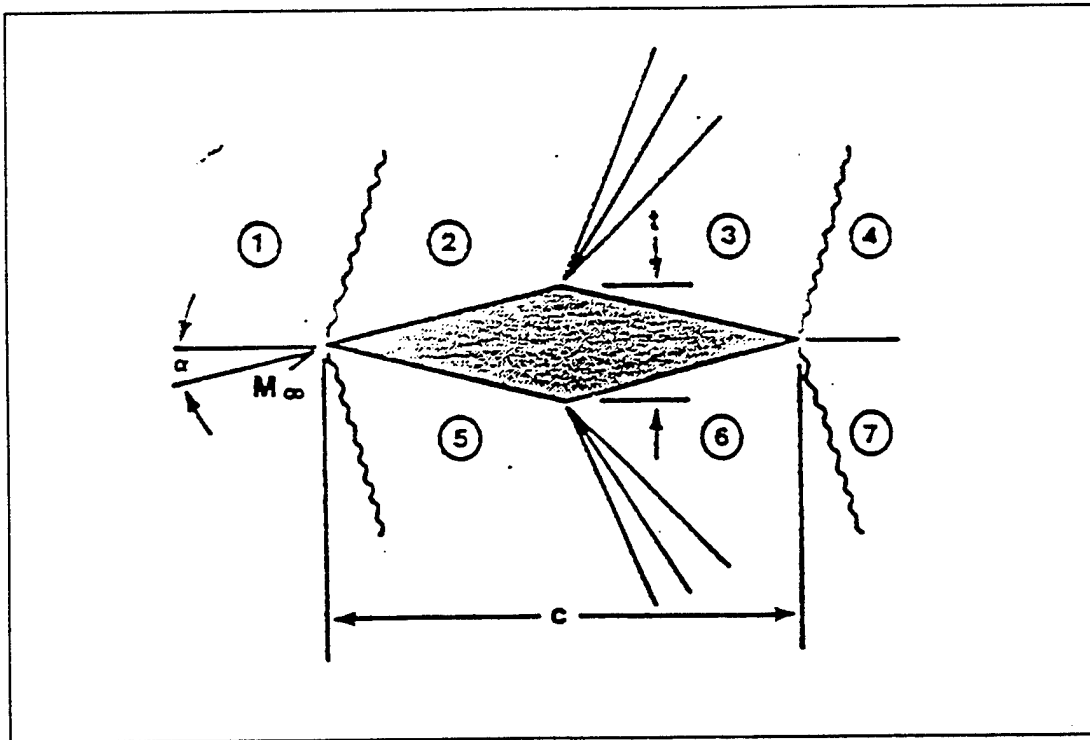


FIGURE 6.25 DOUBLE WEDGE AIRFOIL IN SUPERSONIC FLOW

For an example of the diamond airfoil, the local pressure coefficient can be expressed as

$$C_{P_x} = \frac{P_x - P_\infty}{q_\infty} \quad (6.61)$$

when $x = 2, 3, 5,$ or 6 , depending on the area of the airfoil under consideration.

In terms of remote Mach, M_∞ , Equation 6.61 can be rewritten as

$$C_{P_x} \equiv \frac{2}{M_\infty^2 \gamma} \left[\frac{P_x}{P_\infty} - 1 \right] \quad (6.62)$$

Given α , the geometry of the airfoil, M_∞ , and $\gamma = 1.4$, C_{P_2} and C_{P_6} can be determined directly from Reference 6.4 and use of Equation 6.62.

The evaluation of Equation 6.62 for C_{P_3} and C_{P_6} can also be easily made. In determining C_{P_3} , for example,

$$\frac{P_3}{P_\infty} = \left[\frac{P_2}{P_\infty} \right] \left[\frac{P_{r_2}}{P_2} \right] \left[\frac{P_3}{P_{r_3}} \right] \quad (6.63)$$

All of the ratios on the right side of Equation 6.63 are found in Reference 6.4 tables after M_2 and M_3 are determined. After C_{p_2} , C_{p_3} , C_{p_5} , and C_{p_6} are determined, the forces normal to each surface can be calculated, since

$$F_x = (C_p)_x q_\infty S$$

when F_x is the force normal to the surface, and again $x = 2, 3, 5$, or 6 , depending upon the area of the airfoil under consideration. Once all the F_x 's are known, they can be resolved into components perpendicular to and parallel with the relative wind to determine lift and drag on the airfoil at the given angle of attack.

6.20 THIN WING THEORY

Although an analytic determination of lift and drag forces acting on even a simple two-dimensional supersonic airfoil is a somewhat lengthy problem (as shown in the paragraph on two-dimensional wings), an approximate determination is readily accomplished.

Probably the most widely accepted of the approximate (or thin wing) supersonic theories is the one due to Ackeret which is either called the linear theory or simply the Ackeret theory. For thin airfoils set at relatively small angles of attack, the Ackeret theory agrees well with experimental data from Mach of about 1.2 to 5.0, and therefore the assumptions made in its development are empirically justified.

A pressure coefficient is developed (Derivation F.8 Appendix F) such that

$$C_p = \frac{\Delta P}{q} = \pm \frac{2\delta}{\sqrt{M^2 - 1}}$$

where the minus sign holds for an expansion and the plus sign holds for a compression.

For the double wedge, Ackeret Theory predicts that

$$C_L = \frac{4\alpha}{\sqrt{M^2-1}} \quad (6.64)$$

$$C_D = \frac{4\alpha^2}{\sqrt{M^2-1}} + \frac{4}{\sqrt{M^2-1}} \left(\frac{t}{c} \right)^2 \quad (6.65)$$

Where t is the thickness and c is the chord.

We can write the drag coefficient of the double wedge in the same form we had for subsonic flow,

$$C_{D_{tot}} = C_{D_i} + C_{D_p} \quad (6.66)$$

Comparing the terms in Equation 6.66 with Ackeret theory gives

$$C_{D_p} = \frac{4 \left(\frac{t}{c} \right)^2}{\sqrt{M^2-1}} \quad (6.67)$$

$$C_{D_i} = \frac{4\alpha^2}{\sqrt{M^2-1}} \quad (6.68)$$

As in subsonic flow, C_{D_p} is not a function of α . It is often defined as the wave drag coefficient when $\alpha = 0$. This term is due to the profile shape and is similar to the profile (parasite) drag term of a subsonic wing section, although it does not depend on viscosity. C_{D_p} is a function of Mach and the thickness ratio (t/c) defined in Figure 6.26.

The second term, C_{D_i} , can be defined as drag coefficient due to lift and is a direct function of α^2

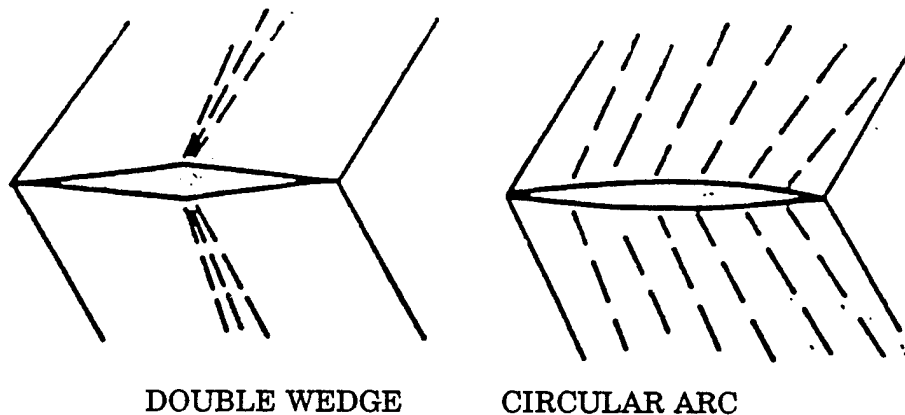
By allowing t to equal zero, Equation 6.65 immediately simplifies to the coefficient of drag equation for a flat plate, Equation 6.69.

$$C_{D_{tot}} = \frac{4\alpha^2}{\sqrt{M^2-1}} \quad (6.69)$$

From Ackeret theory the equation for lift coefficient for both the flat plate and for the double wedge turns out to be

$$C_L = \frac{4\alpha}{\sqrt{M^2-1}} \quad (6.70)$$

The Ackeret theory presented here may be extended to other airfoil shapes, and in all cases, the form of the equations is similar. Figure 6.27 summarizes the lift and drag coefficient relationships for the double wedge and circular arc airfoils, the two types most commonly used for supersonic flight vehicles.



WAVE DRAG COEFFICIENT:

$$C_{D_P} = \frac{4\left(\frac{t}{c}\right)^2}{\sqrt{M^2-1}} \quad C_{D_P} = \frac{5.33\left(\frac{t}{c}\right)^2}{\sqrt{M^2-1}}$$

LIFT COEFFICIENT:

$$C_L = \frac{4\alpha}{\sqrt{M^2-1}} \quad C_L = \frac{4\alpha}{\sqrt{M^2-1}}$$

DRAW DUE TO LIFT:

$$C_{D_L} = \frac{4\alpha^2}{\sqrt{M^2-1}} \quad C_{D_i} = \frac{4\alpha^2}{\sqrt{M^2-1}}$$

LIFT CURVE SLOPE:

$$C_{L_\alpha} = \frac{4}{\sqrt{M^2-1}} \quad C_{L_\alpha} = \frac{4}{\sqrt{M^2-1}}$$

Where

(t/c) = AIRFOIL THICKNESS RATIO

α = ANGLE OF ATTACK (IN RADIANS)

M = MACH

FIGURE 6.27 APPROXIMATE EQUATIONS FOR SUPERSONIC SECTION CHARACTERISTICS (6.2:225)

6.21 SUPERSONIC FLOW IN THREE DIMENSIONS

In supersonic three-dimensional flow we must consider the fact that the stream lines do not turn immediately as they do in the two-dimensional case. Therefore, the shock wave for a typical three-dimensional shape, i.e., a cone, will be weaker for a given velocity. The stream lines approach the object's surface in a rather asymptotic fashion. This is seen from the fact that at all points off the apex of the cone, the section presented to the flow is a hyperbolic section rather than a sharp point. Because of this fact, we have the gradual transition shown in Figure 6.28.

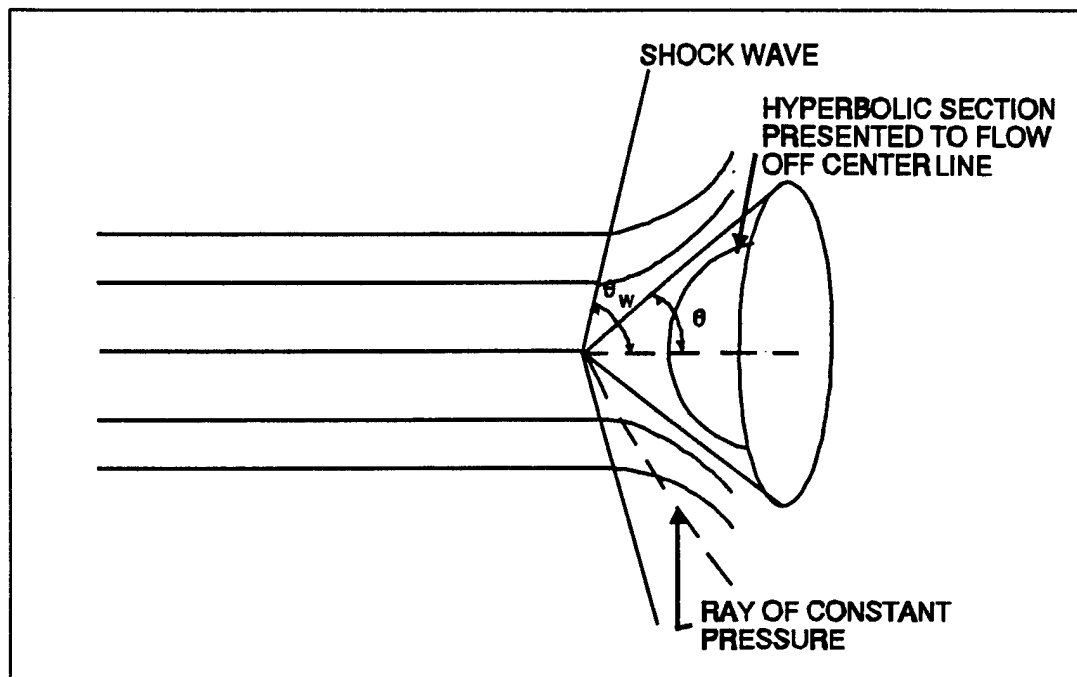
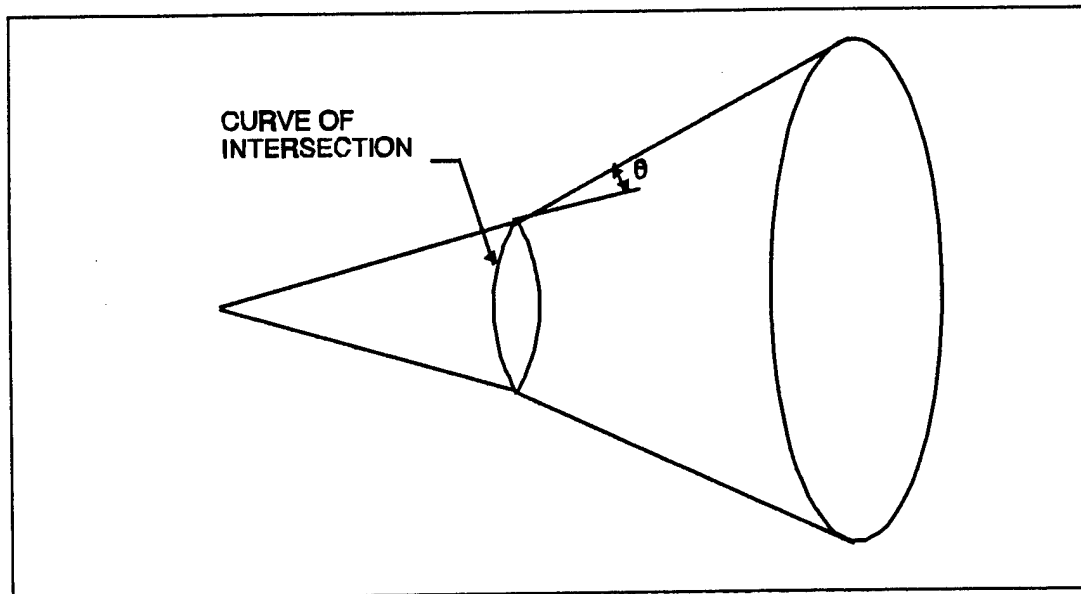


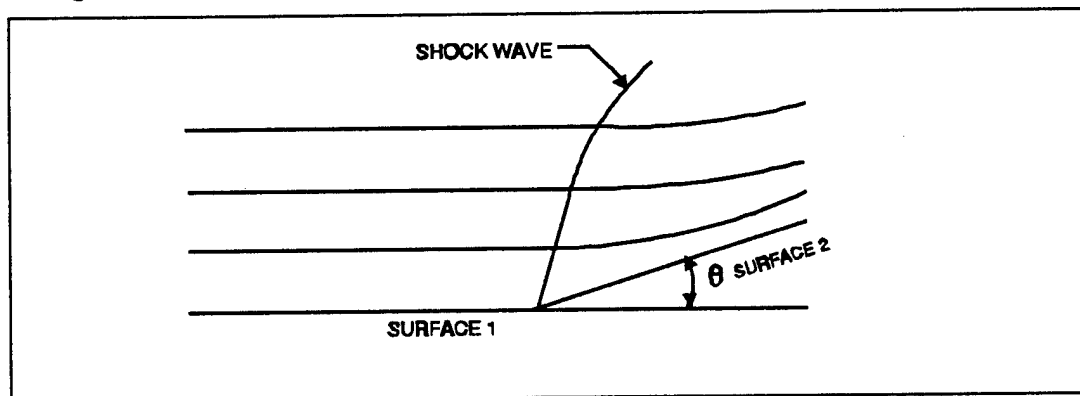
FIGURE 6.28 STREAM LINES ABOUT A CONE (6.5:123)

As would be expected, the pressure, density, temperature, velocity, and Mach all vary between the shock wave and the surface. After increasing through the shock wave, the static pressure and density would continue to increase along a stream line, and the velocity and Mach would therefore continue to decrease. However, the pressure along any ray from the apex of the cone is constant. Since the surface of the cone is essentially the limiting ray from the apex, the surface pressure is constant. Because of the nature of the flow, this pressure is considerably lower than that found at the surface of an infinite wedge of the same apex angle. For a given vertex angle and free stream flow, the pressure change for a cone is about one-third that for a wedge.

If the cone we have been discussing is suddenly flared out at a new angle, we will have a condition in which the surface is formed by the intersection of two coaxial cones. This situation is illustrated in Figure 6.29.

**FIGURE 6.29 THE FLARED CONE (6.5:123)**

The curve of intersection of the two surfaces is a circle as shown. If this circle is of large radius, we shall have the approximation of two-dimensional flow at the corner as the air is forced to turn through the angle θ . The effect of the rounded shape, however, acts to relieve the severity of the shock and modify the details of the flow. Because of this action, the line of the shock wave will be a curve rather than a straight line. This is illustrated in Figure 6.30.

**FIGURE 6.30 FLOW IN A ROUND CORNER (6.5:124)**

As shown, the stream lines change direction at the shock wave. However, they continue to change gradually to approach the condition of parallel flow as we expect on the surface of a cone. The bending of the shock line is related to the surface curvature (6.5:122-124).

Practical application of the three-dimensional effects discussed above could be applied to the juncture of canopy and nose on an aircraft or to conical plugs found in engine inlets such as those on the SR-71.

6.22 THREE-DIMENSIONAL SUPERSONIC WINGS

To this point we have considered only the infinite wing in two-dimensional flow. If we have a finite planform such as that given in Figure 6.31, we can expect the apex to generate a Mach cone as indicated. This will be true in any practical case of an aircraft in flight because of the nose section ahead of the wing. The nose will generate a cone of disturbance in which at least a portion of the wing will fly.

As the velocity of flight, V_∞ increases, the cone narrows as indicated in Figure 6.31b.

When the leading edge of the wing is behind the Mach cone angle as shown in Figure 6.31a, the normal Mach is subsonic, and no shock wave is created at the leading edge. The pressure distribution and the forces resulting will be equivalent to those found in an airfoil normal to the stream at the corresponding subsonic Mach. In this case, it is advantageous to use a subsonic airfoil section rather than a supersonic section if the wing will always be below the effective Mach of unity.

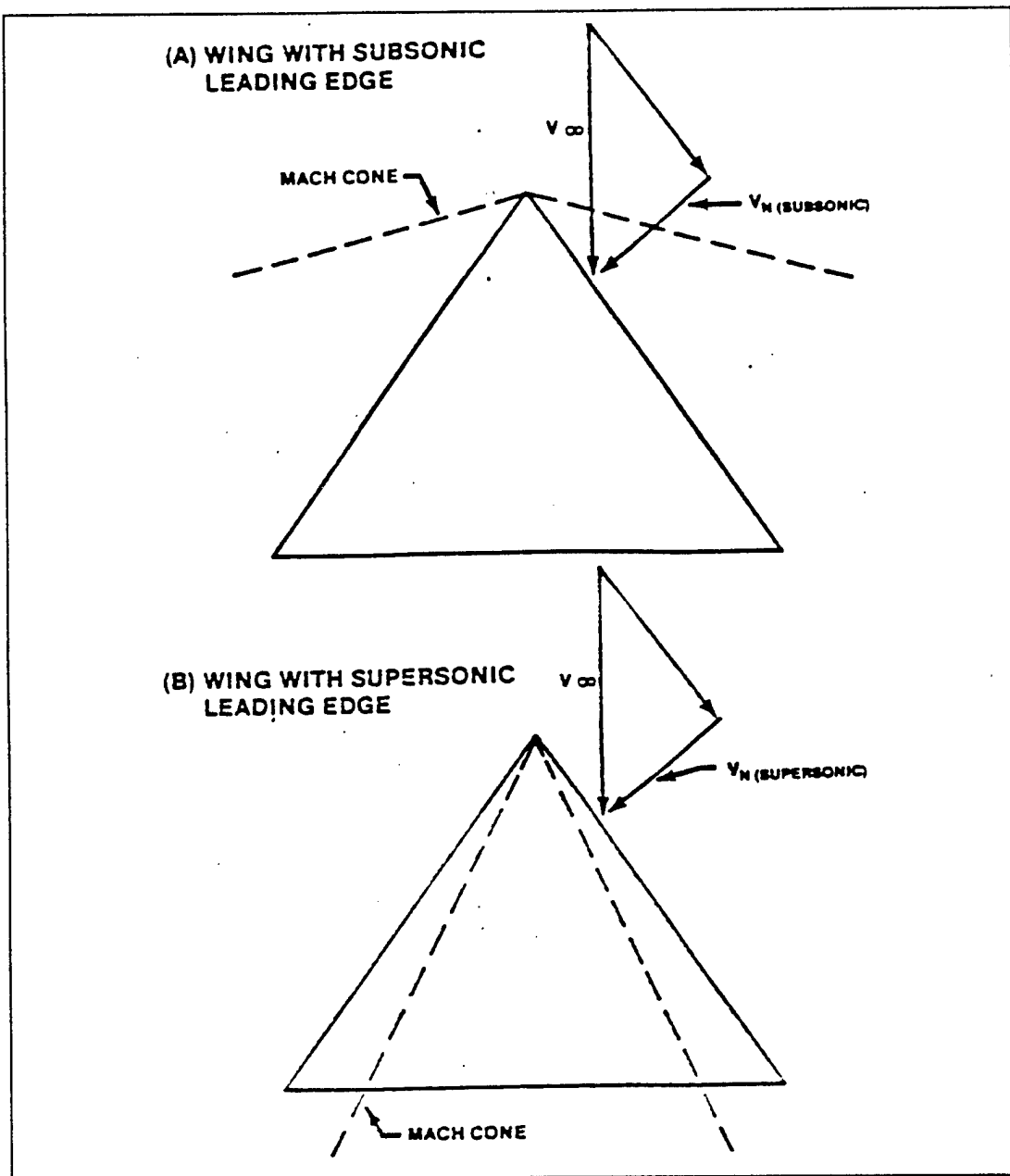


FIGURE 6.31 MACH CONE LIMITS

If the Mach cone falls behind the leading edge as shown in Figure 6.31b, the effective flow on the wing is supersonic at the leading edge. However, it is quite possible that the effective flow may be supersonic at the leading edge but subsonic at the trailing edge. This would certainly happen behind a shock cone. The pressure distribution is modified by the transition from supersonic to subsonic flow. These effects are also involved in the analysis of tip losses. Each point on the leading edge generates a pressure differential inside its own Mach cone. This pressure distribution is

essentially conical. These are essentially additive until reaching the tip. The area in a cone behind the tip has a reduced pressure gradient; therefore, less lift. Let us consider a flat plate wing of finite aspect ratio as shown in Figure 6.32.

Since the tip losses are confined to the region within the tip cones, the tips could be cut off at an angle slightly greater than the Mach angle so that none of the wing is contained within the Mach cone. Then there are no induced effects, and the wing acts as in two-dimensional flow, and Equations 6.65 and 6.70 apply.

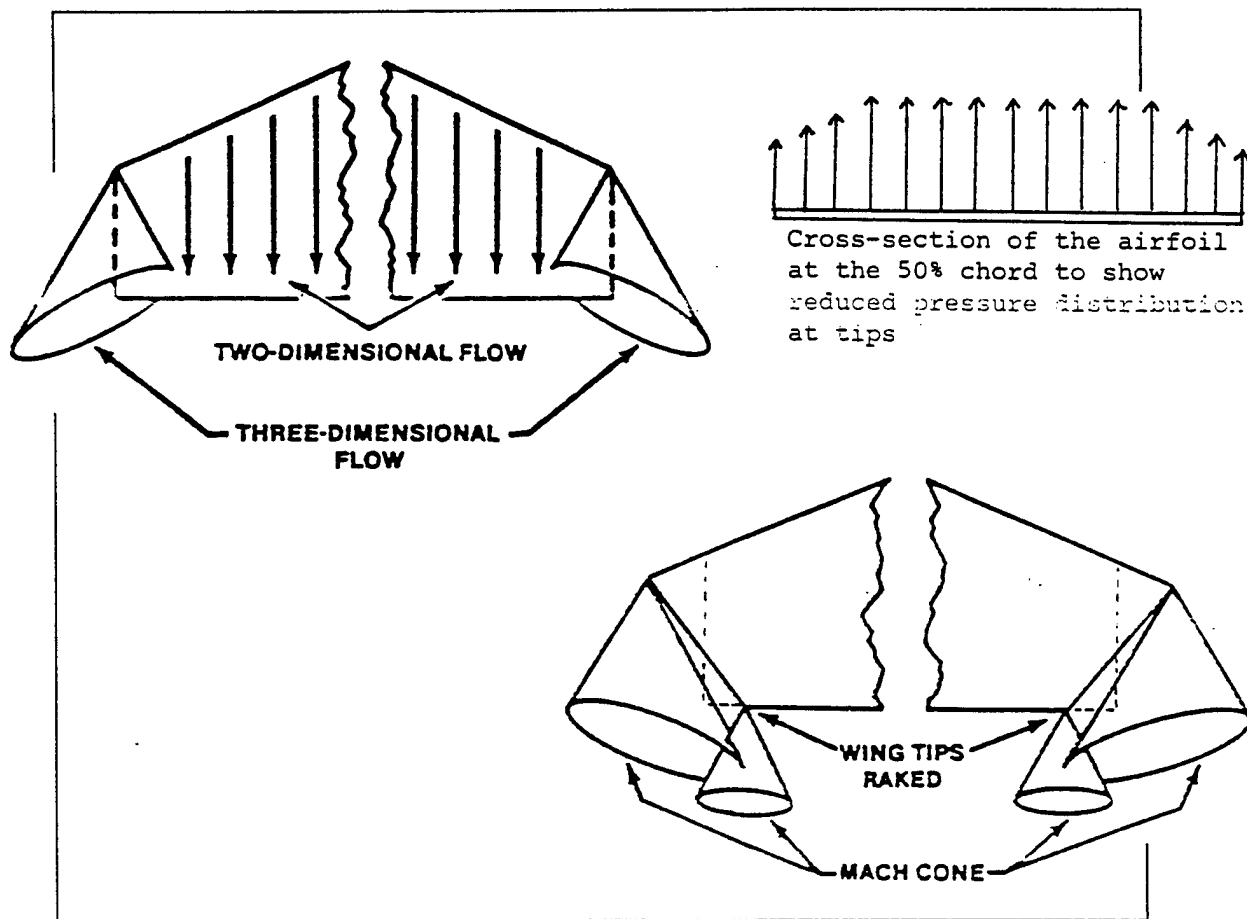


FIGURE 6.32 SUPERSONIC TIP EFFECTS (6.1:166)

6.23 TRANSONIC FLOW REGIME

In the previous paragraphs, the subject of transonic aerodynamics has been judiciously avoided. It can be seen from Ackeret thin wing theory (Equations 6.67 - 6.70) that lift and drag tend to become infinite in the vicinity of Mach 1. A similar result is also found from subsonic theory proposed by Prandtl and Glauert, shown in Figure 6.33.

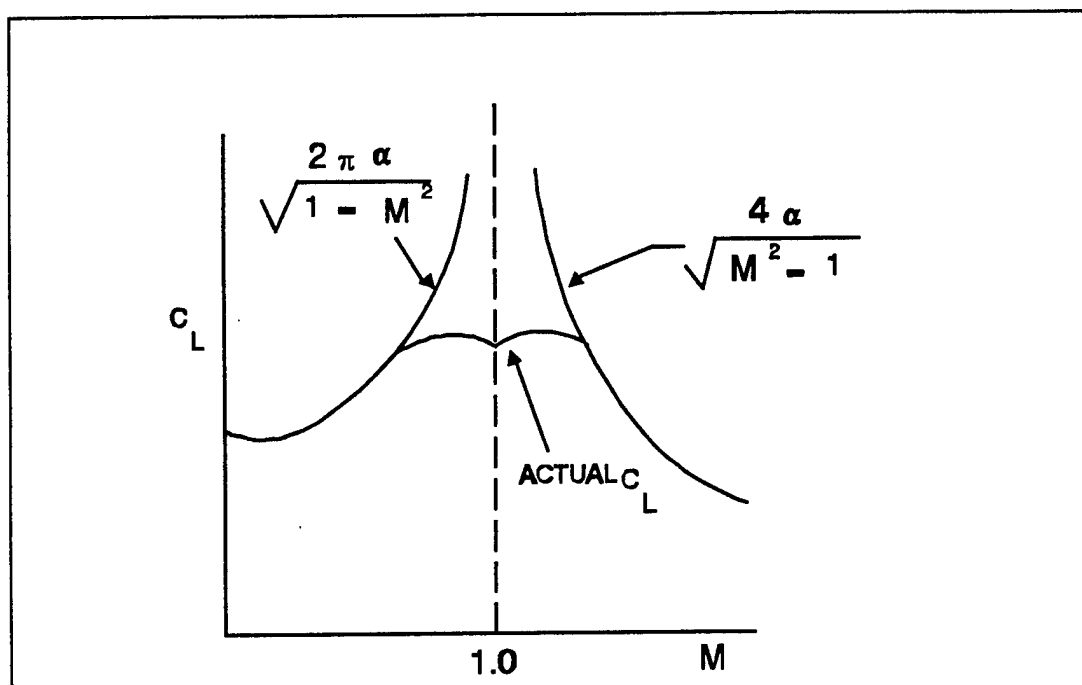


FIGURE 6.33 TRANSONIC LIFT COEFFICIENT CHARACTERISTICS

From this figure comes the concept of the mythical sonic barrier. In the actual case, the lift coefficient follows a trend more like that indicated by the dotted line.

Transonic flow over a body is complicated by the fact that both subsonic and supersonic flows exist simultaneously on the surface of the aircraft. The interaction between these two types of flow plus the viscous effects in the boundary layer create a condition that defies direct mathematical analysis.

Even experimental results in the wind tunnel are difficult to obtain because of the tunnel choking effects caused when a model is placed in the nearly sonic throat of the tunnel. The approach in this chapter will be to extrapolate the concepts of viscous, subsonic flow and nonviscous supersonic flow into this region of mixed flow conditions resulting in a qualitative look at the transonic speed range.

The transonic speed range begins when sonic flow first occurs over the surface of the vehicle and ends when the flow is supersonic over the entire surface (with the possible exception of a small insignificant subsonic region at the leading edge).

From Bernoulli's theorem, it has been shown that the velocity increases and the pressure decreases as air flows subsonically over the surface of an airfoil. As the Mach of the vehicle is increased, the flow near the thickest portion of the airfoil

approaches Mach 1 as in Figure 6.34a.

This is the critical Mach of the airfoil and is always less than 1. When the vehicle velocity exceeds the critical Mach, regions of subsonic and supersonic flow are created on the airfoil as shown in Figure 6.34, parts b and c.

A shock always exists at the trailing edge of the supersonic region, and as the vehicle velocity is increased above the critical Mach, the supersonic region grows fore and aft of the point of maximum thickness until it reaches the trailing edge and is very nearly attached to the leading edge as in Figure 6.34e.

When the bow shock attaches to the leading edge, the airfoil has left the transonic speed regime and has entered the supersonic regime.

6.23.1 THICKNESS

As speed increases from subsonic to transonic, thick, unswept, straight-tapered wings show increases in lift-curve slope up to Mach slightly beyond the critical. The slope then drops to a lower value followed by a rise starting near Mach 1 to a value almost as high as the value at the critical Mach. This type of behavior is illustrated in Figure 6.33.

Reducing either the aspect ratio, the wing thickness ratio, or both reduces the magnitude of these effects. For very thin wings and for wings of very low aspect ratio, these transonic nonlinearities do not exist, and the C_L - M curve resembles Figure 6.35.

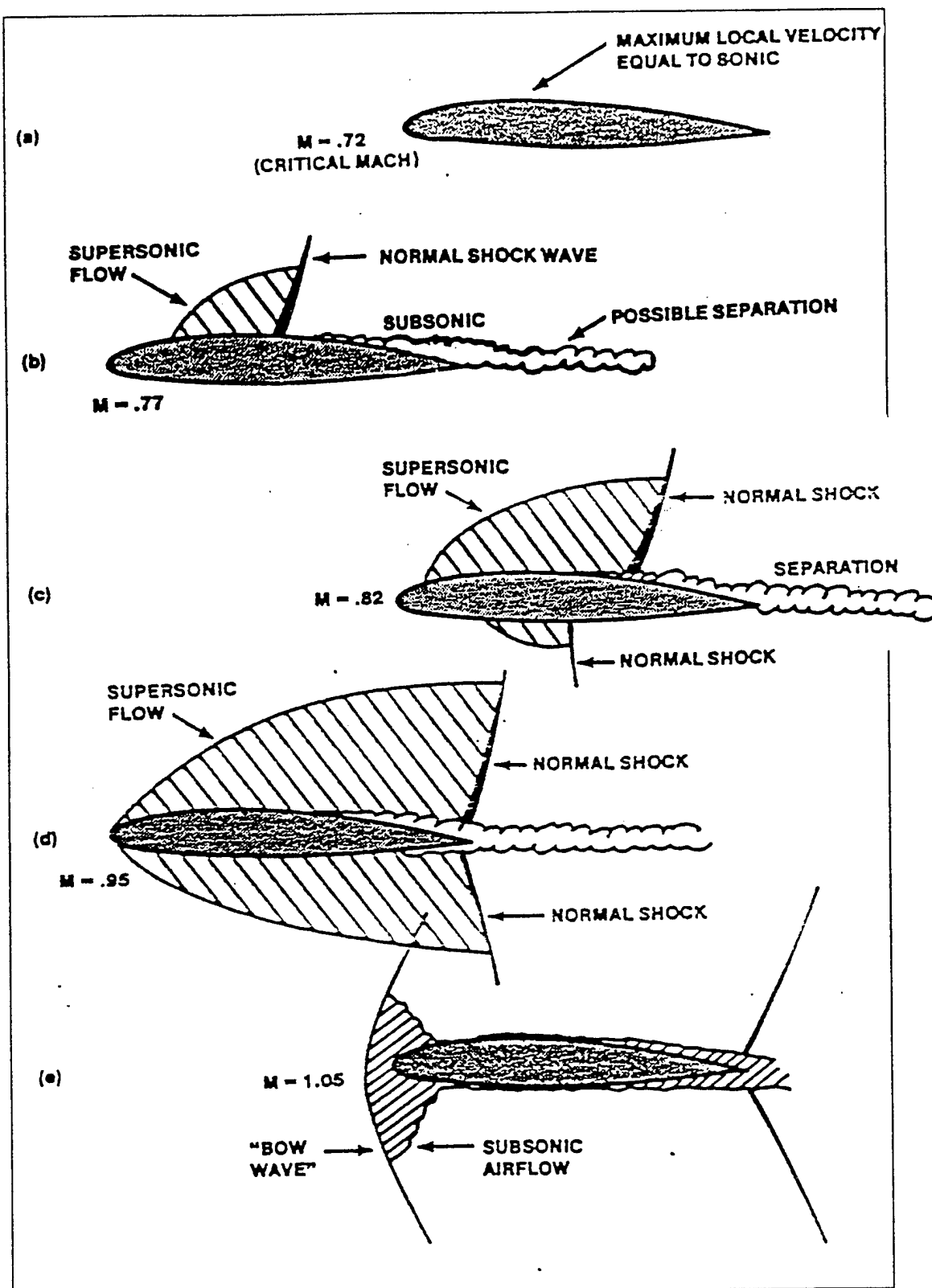
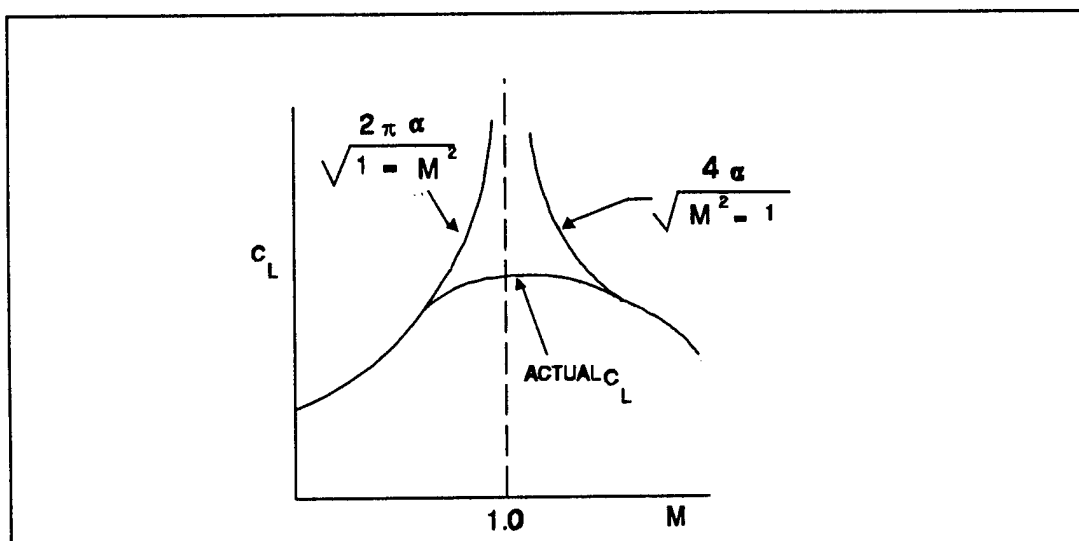


FIGURE 6.34 TRANSONIC FLOW PATTERNS (6.2:216)

**FIGURE 6.35 THIN WING TRANSONIC LIFT COEFFICIENT**

Further evidence of the benefits of reducing airfoil thickness for the transonic flight regime is shown in Figure 6.36, where pressure coefficient as a function of critical Mach is shown for various thicknesses of airfoils.

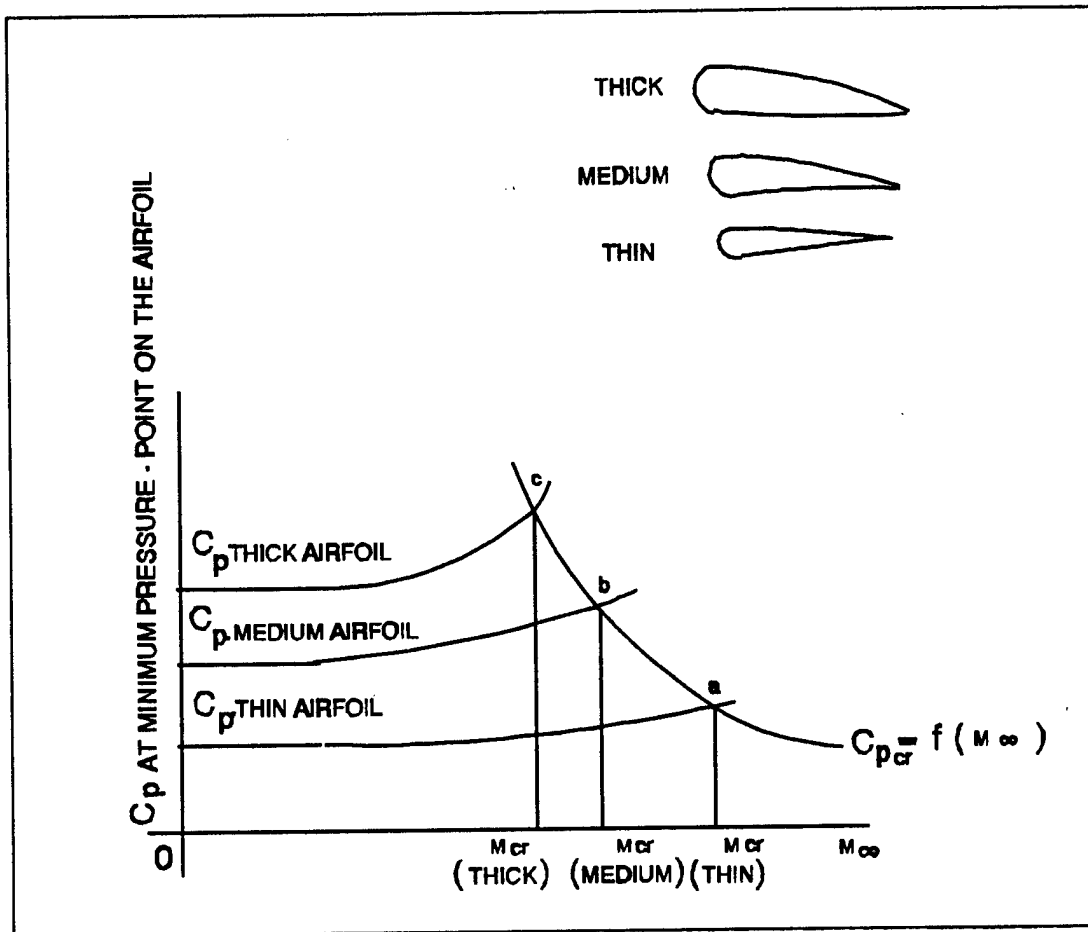


FIGURE 6.36 CRITICAL PRESSURE COEFFICIENT AND CRITICAL MACH FOR AIRFOILS OF DIFFERENT THICKNESS (6.6:167)

6.23.2 SUPERCRITICAL AIRFOILS

Another method which can be utilized to increase critical Mach and delay the transonic drag rise is to use a supercritical airfoil. Such an airfoil is depicted in Figure 6.37. The supercritical airfoil is thicker than the conventional airfoil; this results in greater rigidity and internal volume. At the same time, the recovery shock wave on top of the wing is weaker and is moved much further aft than on conventional airfoils. The supercritical airfoil causes less boundary layer separation, resulting in a delay in the drag rise which occurs on a conventional airfoil section at the critical Mach. The result is that the drag rise associated with passage through critical Mach is delayed.

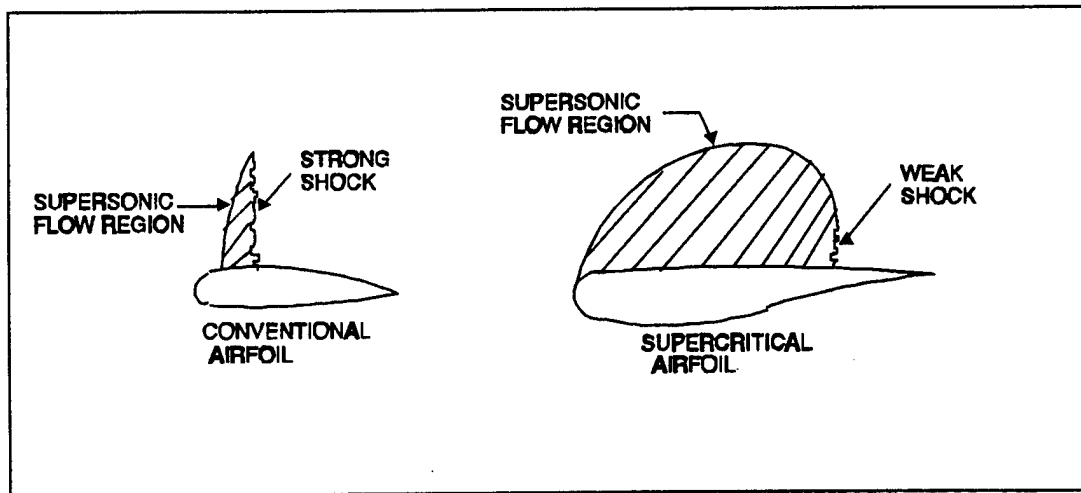


FIGURE 6.37 COMPARISON OF DRAG RISE PHENOMENA AT CRITICAL MACH

6.23.3 WING SWEEP

The final method to be discussed for delaying critical Mach to higher values is wing sweep. To the airstream, the velocity (or Mach) that is important is the component that is perpendicular to the leading edge of the wing. By referring to Figure 6.38a, it is seen that the component of velocity perpendicular to the leading edge of the wing is less than the free stream value by the cosine of the sweep angle Λ . Therefore, the critical Mach is increased, and the transonic drag rise is delayed. Reduction in drag coefficient as a function of Mach for several values of wing sweep is illustrated in Figure 6.38b.

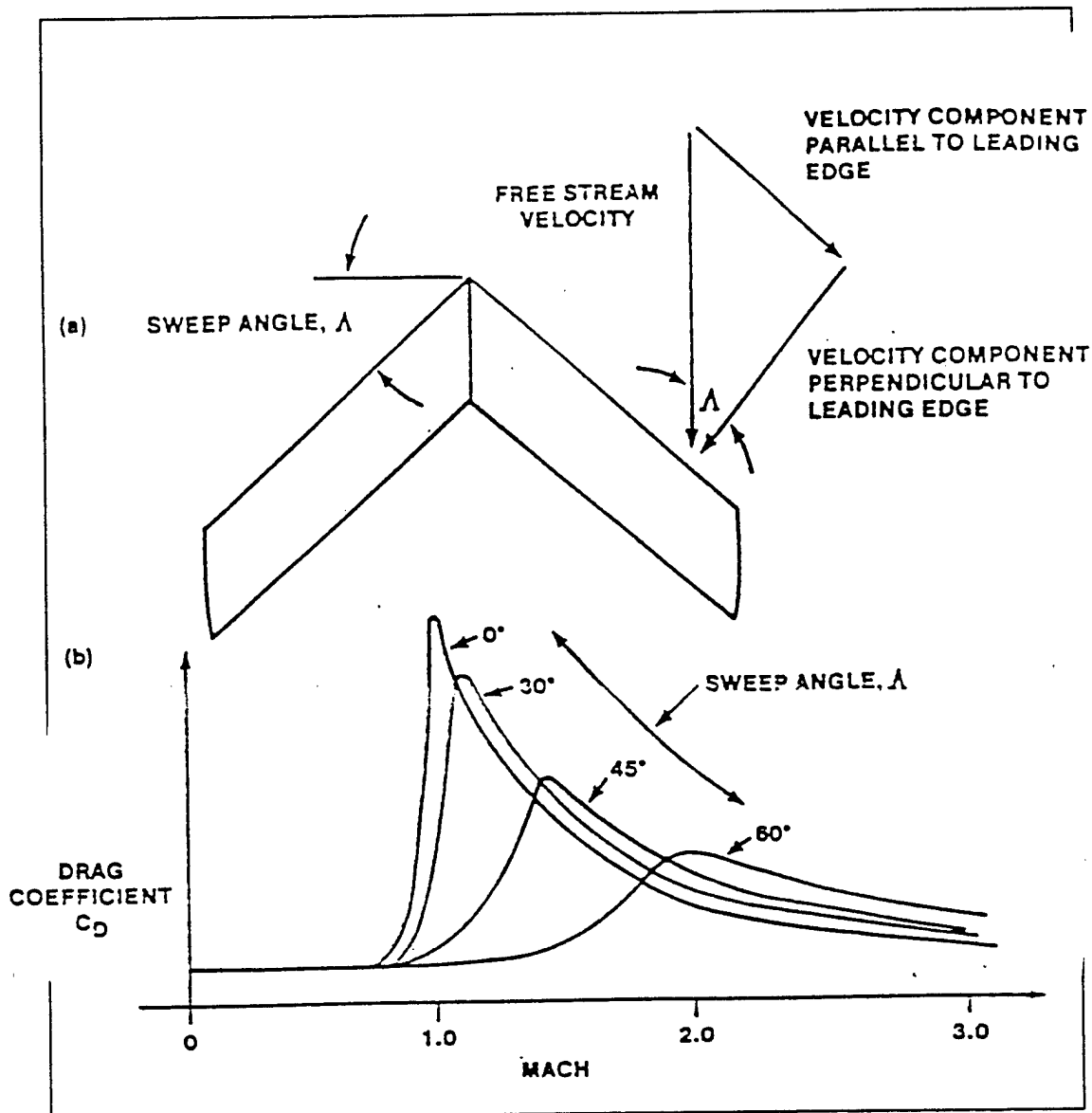


FIGURE 6.38 GENERAL EFFECTS OF SWEEPBACK (6.2:227)

Spanwise flow tends to develop from the root toward the tip as depicted in Figure 6.39. This spanwise flow contributes to the strength of wing tip vortices, thereby increasing induced drag at high angles of attack. The swept back wing also tends to separate and stall first at the wing tip. This is, of course, undesirable from a control point of view as ailerons are normally located toward the wing tip. These stall characteristics are also depicted in Figure 6.39. The tendency can be decreased by twisting and/or tapering the wing, but again a penalty arises due to the structural complications caused by bending toward the wing tips; this twists the wing and imposes torsional loading.

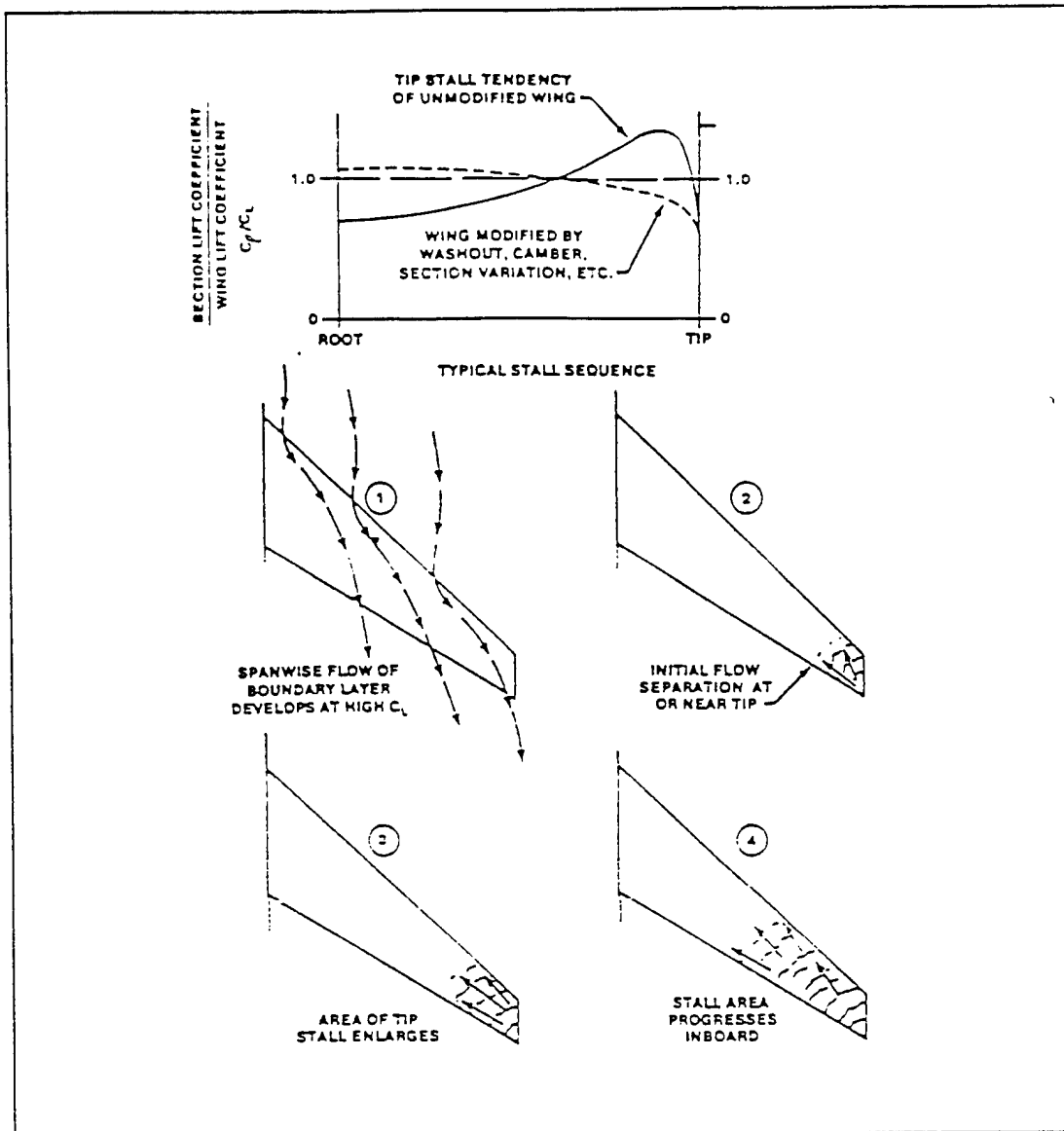


FIGURE 6.39 STALL CHARACTERISTICS OF TAPERED SWEEP WING (6.2:232)

A further disadvantage of wing sweep is illustrated in Figure 6.40. Note that for the same angle of attack, a straight wing is capable of producing a much higher lift coefficient than a swept wing.

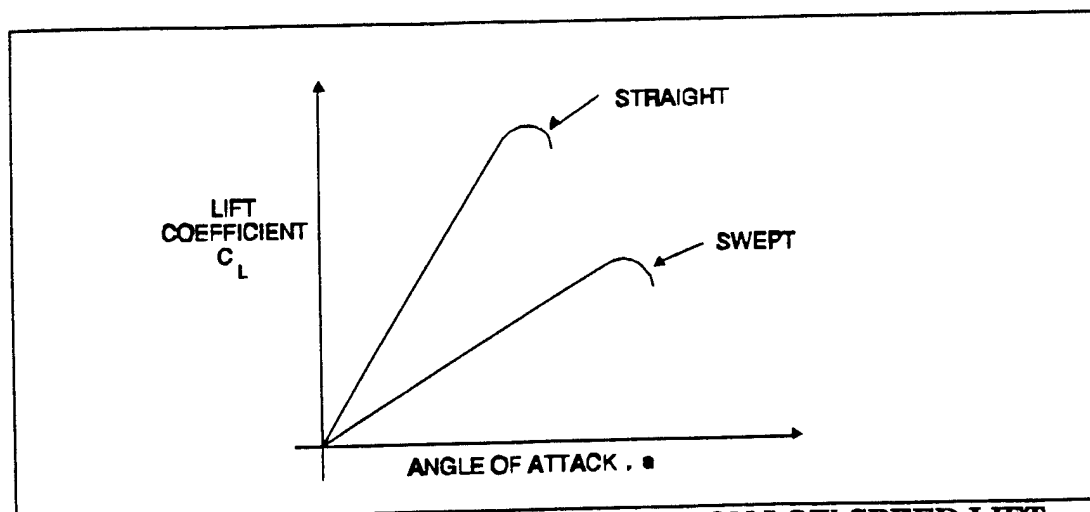


FIGURE 6.40 EFFECT OF SWEEPBACK ON LOW SPEED LIFT CURVE (6.2:228)

Aerodynamically, the effect of wing sweep with regard to delaying critical Mach applies to forward sweep as well as sweep back. The spanwise flow on a forward swept wing, however, is from the tip toward the root and tends to be beneficial. The major reason forward swept wings have not been widely used in the past is because of aeroelastic divergence problems. The present day improvement in composite materials has provided us with a material that has the stiffness needed to combat such problems.

Despite many disadvantages, rearward wing sweep has been for many years the primary method used to delay transonic drag rise. Reference to Figure 6.38b, however, shows that at higher supersonic Mach, a straight wing becomes superior from a drag standpoint.

6.23.4 FUSELAGE SHAPE AND AREA RULE

The onset of shock formation is also accompanied by a very severe drag rise. For an aircraft the best fuselage shape and the best wing fuselage combination that will delay the drag rise and/or tend to limit the severity of its effect is of major interest.

As a matter of both calculation and testing, it is found that a body of revolution with high fineness ratio (ratio of length to diameter) gives the least drag. The nose section should not be a cone. The best shape for the nose resembles that shown in Figure 6.41.

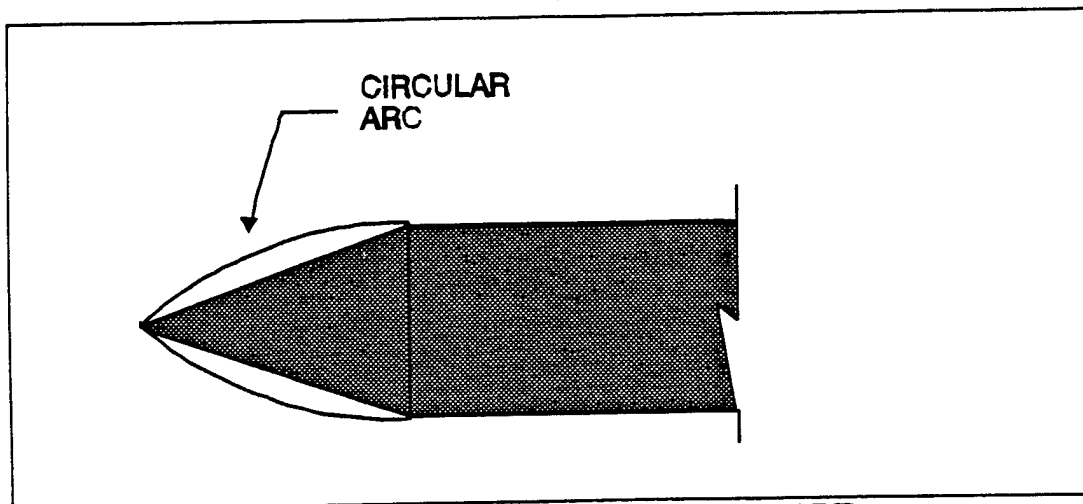


FIGURE 6.41 OPTIMUM NOSE SHAPE

Unfortunately, a true body of revolution is not found in actual vehicles. As an example, the canopy will form a bulge in the fuselage. The wings, when attached, will further modify the shape. However, without the necessity of preserving the exact form of the aircraft, the equivalent effect of wings and canopy can be preserved by making an equivalent body of revolution with the proper bulges located in the appropriate regions. This is shown in Figure 6.42.

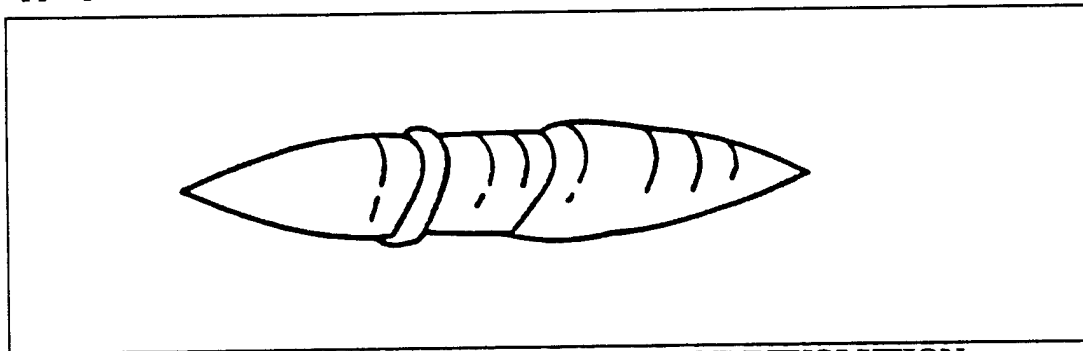


FIGURE 6.42 EQUIVALENT BODY OF REVOLUTION

The abrupt offsets in the surface will cause an increase in drag above that for the ideal body of revolution. To minimize drag it will be necessary to remove material from the region of the bulges. Because the wings must be present, the contour of the fuselage is changed in this region to compensate for them. The same thing can be done in the region of the canopy. In some instances, it may be necessary to introduce bulges in the fuselage behind or ahead of the wing to introduce the equivalent effect of the smooth aerodynamic contour. A striking example of this effect is the extending of the "cab" of the Boeing 747. Wind tunnel data show that the Mach at which drag

rise shows a significant increase is delayed by smoothing the area distribution by fairing the fuselage-cab juncture. The drag effect of the fairing is insignificant until M_{cr} is reached for the unfaired juncture; then the fairing delays the Mach at which waves are generated. As shown in Figure 6.43, the fairing causes an increase in M_{cr} for M_{cr} for $.3 < C_L < .5$.

The application of the transonic area rule will delay the drag rise, but in any event shock formation cannot be avoided if the flight Mach is sufficiently increased. The contour of the fuselage that will be effective at Mach 1 is not as effective at Mach 1.2. In fact, the conditions which provided an advantage in the transonic region may become a disadvantage at higher Mach. It is generally considered that area rule application is pointless above Mach 1.5. Further illustrations of the effects of area ruling are shown in Figure 6.44.

Transonic flow also produces important changes in the aerodynamic pitching moment characteristics of wing sections. The aerodynamic center of airfoils in subsonic flow is located at about the 25% chord point. As the airfoil is subjected to supersonic flow, the aerodynamic center changes to about the 50% chord point. Thus, the aircraft in transonic flight can experience large changes in longitudinal stability because of the large changes in the position of the aerodynamic center. If an aircraft stabilizes in the transonic region, the aerodynamic center may oscillate between the 25% chord point and the 50% chord point, often at very high frequency; this further aggravates longitudinal stability problems.

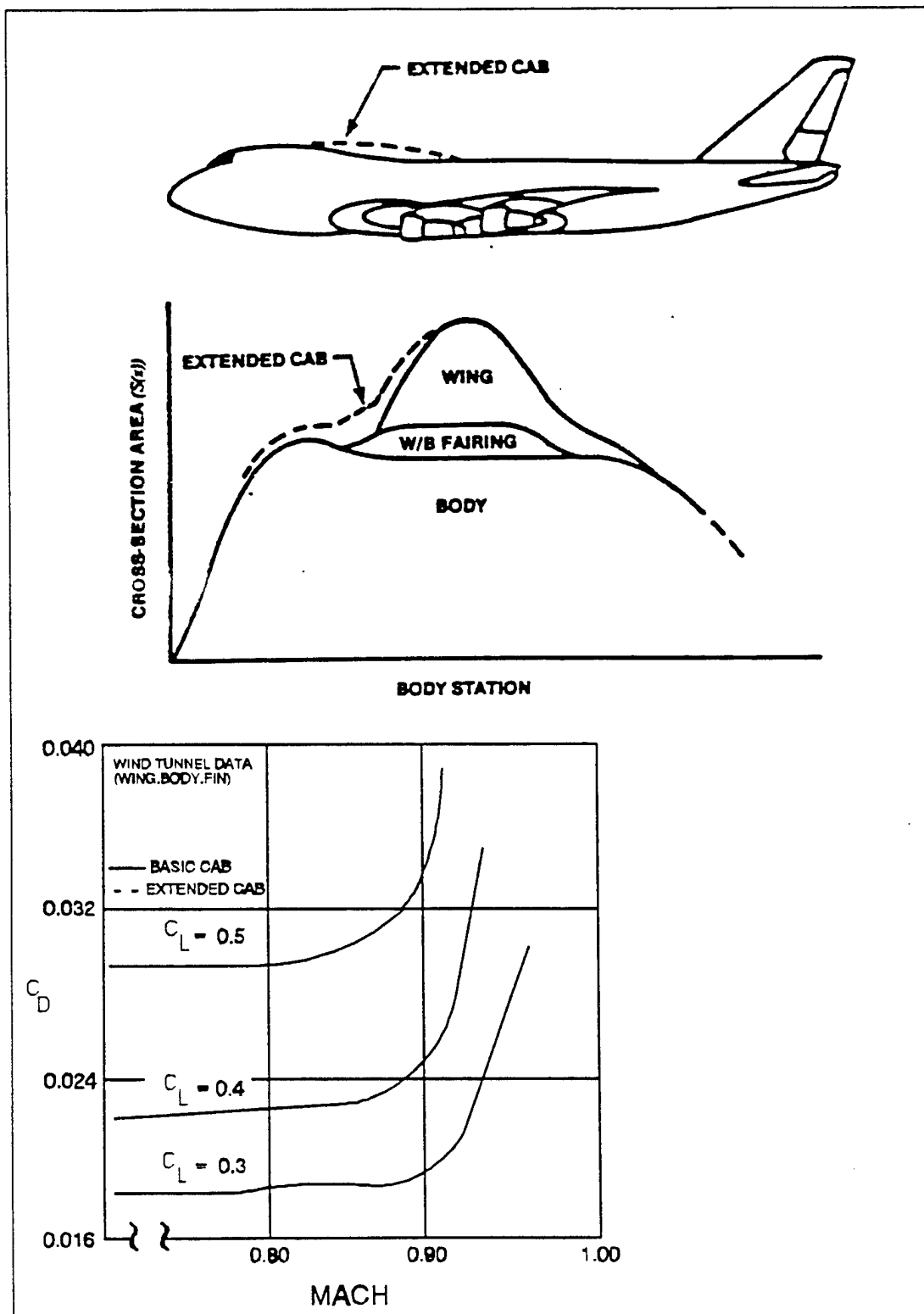


FIGURE 6.43 BENEFITS OF AREA RULE APPLICATION

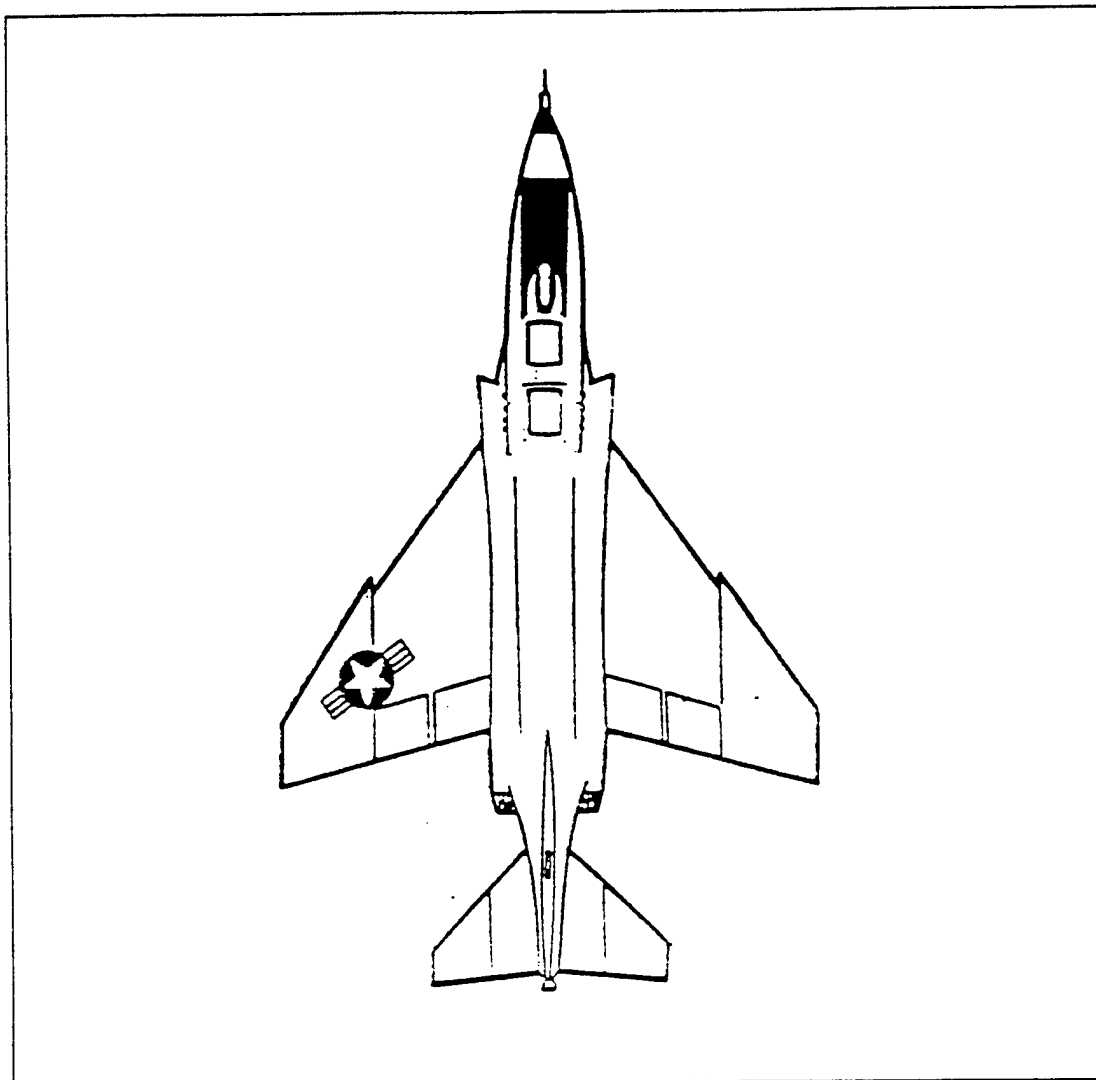


FIGURE 6.44 "COKE BOTTLE" FUSELAGE (6.1:166)

6.23.5 TRANSONIC AND SUPERSONIC CONTROL SURFACES

The design of control surfaces for transonic and supersonic flight involves many important considerations. This fact is illustrated by the typical transonic and supersonic flow patterns of Figure 6.45. Trailing edge control surfaces can be affected adversely by the shock waves formed in flight above the critical Mach. If the airflow is separated by the shock wave, the resulting buffet of the control surface can be very objectionable. In addition to the buffet of the surface, the change in the pressure distribution due to separation and the shock wave location can create very large changes in control surface hinge moments. Such large changes in hinge moments create very undesirable control forces and present the need for an "irreversible" control system. An irreversible control system would employ powerful hydraulic or

electric actuators to move the surfaces upon control by the pilot, and the airloads developed on the surface could not feed back to the pilot. Of course, suitable control forces would be synthesized by bungees, "q" springs, bob-weights, etc.

Transonic and supersonic flight can cause a noticeable reduction in the effectiveness of trailing edge control surfaces. The deflection of a trailing edge control surface at low subsonic speeds alters the pressure distribution on the fixed portion as well as the movable portion of the surface. This is true to the extent that a 1° deflection of a 40% chord elevator produces a lift change very nearly the equivalent of a 1-degree change in stabilizer setting. However, if supersonic flow exists on the surface, a deflection of the trailing edge control surface cannot influence the pressure distribution in the supersonic area ahead of the movable control surface. This is especially true in high supersonic flight where supersonic flow exists over the entire chord and the change in pressure distribution is limited to the area of the control surface. The reduction in effectiveness of the trailing edge control surface at transonic and supersonic speeds necessitates the use of an all movable surface. Application of the all movable control surface to the horizontal tail is most usual since the increase in longitudinal stability in supersonic flight requires a high degree of control effectiveness to achieve required controllability for supersonic maneuvering (6.2:236, 238).

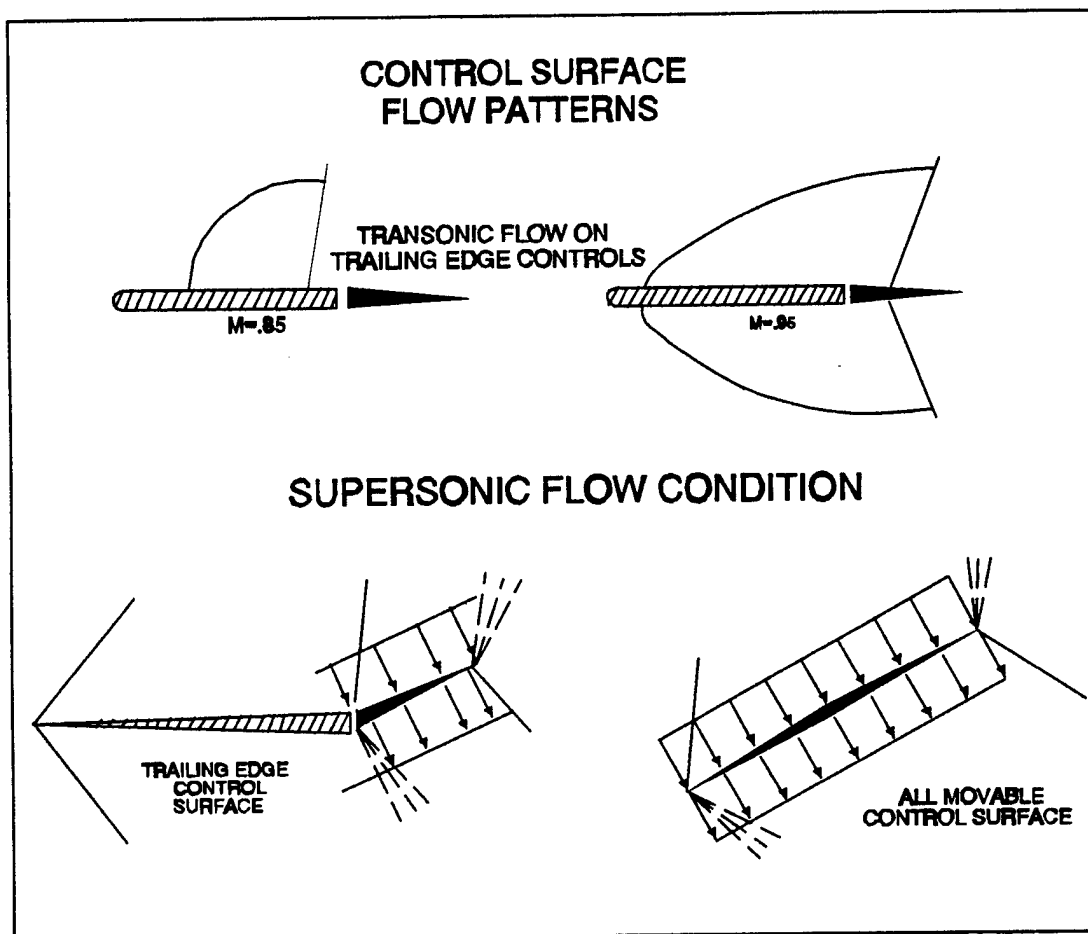


FIGURE 6.45 PLANFORM EFFECTS AND CONTROL SURFACES
(6.2:237)

6.24 SUMMARY

In this chapter we have studied the theory of supersonic and transonic flow. Emphasis was placed on the practical application of the theory to realistic two and three dimensional flow problems about aerodynamic shapes. Understanding and application of supersonic theory will be necessary in Chapter 7 on Propulsion.

Present day supersonic aircraft and space shuttle operations necessitate a thorough understanding of this material by the flight test pilot and flight test engineer.

- 6.1 Aerodynamics for Pilots, ATC Pamphlet 51-3, July 1979.
- 6.2 Hurt, H.H., Jr., Aerodynamics for Naval Aviators, NAVWEPS 00-80T-80, Office of the Chief of Naval Operations Aviation Training Division, U.S. Navy, 1960.
- 6.3 Zucker, R.D., Fundamentals of Gas Dynamics. Champaign, IL: Matrix Publishers, Inc., 1977.
- 6.4 NACA Report 1135, Equations, Tables and Charts for Compressible Flow, Ames Research Staff, Ames Aeronautical Laboratory, Moffett Field, CA.
- 6.5 Carroll, R.L. The Aerodynamics of Powered Flight. New York: John Wiley & Sons, 1960.
- 6.6 Anderson, J.D., Jr., Introduction to Flight. New York: McGraw-Hill Inc., 1978.
- 6.7 John, J.E.A., Gas Dynamics. Boston, Mass: Allyn and Bacon, 1969.